The p66ShcA Adaptor Protein Regulates GPNMB Expression in Response to Oxidative Stress by Modulating the TFE3/TFEB Transcriptional Network

By

Clark James Thomson

Department of Biochemistry

Faculty of Medicine

McGill University

Montreal, Quebec, Canada

March 2022

A thesis submitted to McGill University in partial fulfillment of the requirements of the degree of Master of Science

Table of Contents

Abstract

Triple-negative breast cancer (TNBC) is an aggressive and difficult to treat breast cancer subtype as it lacks specific molecular targets that can be exploited therapeutically. Additionally, cancer metastasis is the cause of 90% cancer-related deaths, making the development of targeted therapies for the management of TNBC metastasis crucial to improved patient outcome.

Our lab has previously identified Glycoprotein NMB(GPNMB) as a cell surface protein over-expressed in a subset of TNBC patients, the expression of which is associated with poor prognosis and metastatic phenotypes. GPNMB has emerged as a stress-response gene, owing to its upregulation following nuclear translocation of members of the MiTF/TFE family of transcription factors. Two of these transcription factors, TFE3/TFEB, are known as master regulators of lysosomal biogenesis and autophagy that are activated as a cellular adaptation to stress, such as in response to oxidative stress due to elevated reactive oxygen species (ROS).

Interestingly, initial data from our lab suggests that cells deficient in the redox adaptor protein p66ShcA are unable to induce GPNMB expression. ShcA encodes 3 isoforms (p46, p52, and p66) of which p66ShcA is the longest. Importantly, in response to stress stimuli p66ShcA is trafficked to the mitochondria and promotes the formation of intracellular ROS. As such, we hypothesized that in response to pro-oxidant stimuli, p66ShcA modulates GPNMB expression in models of TNBC.

To investigate this theory, p66ShcA was knocked out in models of TNBC. These same cell lines were engineered to overexpress wild-type or mutant forms of p66ShcA that render the protein unable to generate ROS or localize to the mitochondria. Using these models, we analyzed GPNMB expression, ROS production, the involvement of TFE3/TFEB, and p66ShcA subcellular localization in response to a ROS-inducing compound, sodium arsenite ($NaAsO_2$).

Our data suggests that p66ShcA upregulates GPNMB independently of its ROS generating capabilities. p66ShcA promotes GPNMB expression by modulating the localization and activity of TFE3/TFEB, revealing a novel role for p66ShcA-dependent regulation of the TFE3/TFEB transcriptional network in TNBC.

Résumé

Notre laboratoire a identifié la glycoprotéine NMB (GPNMB) comme une protéine surexprimée à la surface des cellules de cancer du sein triples négatives (TNBC), dont l'expression est associée à un mauvais pronostic et au développement des métastases. GPNMB s'est révélé être un gène de réponse au stress, dont l'expression est contrôlée par la translocation nucléaire des facteurs de transcription de la famille MiTF/TFE. Deux de ces facteurs de transcription, TFE3/TFEB, sont des régulateurs majeurs de la biogenèse lysosomale et de l'autophagie et sont activés en réponse au stress cellulaire, dont le stress oxydatif qui est dû à une augmentation des espèces réactives de l'oxygène (ROS) dans la cellule.

De manière intéressante, les données initiales de notre laboratoire suggèrent que les cellules déficientes en la protéine adaptatrice p66ShcA sont incapables d'induire l'expression de GPNMB. Le gène ShcA code pour 3 isoformes (p46, p52 et p66) dont la plus longue est p66Shc. En réponse au stress, p66ShcA est acheminé vers les mitochondries et favorise la formation de ROS intracellulaires. Par conséquent, nous avons émis l'hypothèse que p66ShcA module l'expression de GPNMB dans des modèles de TNBC suite au stress oxydatif.

Pour valider cette hypothèse, p66ShcA a été déplété dans des modèles cellulaires de TNBC. La forme sauvage ou mutante de p66ShcA, qui rend la protéine incapable de générer des ROS ou de se localiser dans les mitochondries, a ensuite été surexprimé dans ces lignées. Dans ces modèles, nous avons analysé l'expression de GPNMB, la production de ROS, l'implication de TFE3/TFEB et la localisation subcellulaire de p66ShcA en réponse à l'arsénite de sodium (NaAsO2), un composé induisant la production de ROS.

Nos données suggèrent que p66ShcA induit l'augmentation d'expression de GPNMB en réponse à l'arsénite de sodium, indépendamment de ses capacités à générer des ROS. P66ShcA favorise l'expression de GPNMB en modulant la localisation et l'activité de TFE3/TFEB, révélant un nouveau rôle de p66ShcA dans la régulation du réseau transcriptionnel de TFE3/TFEB dans le cancer du sein triple négatif.

Acknowledgements

First and foremost, I would like to thank Dr. Peter Siegel for being an exceptional mentor throughout both my undergraduate and graduate studies. His intellect, input, and confidence in me to independently pursue this exciting project have guided this work into what it is today. We have had many productive conversations about science, my future, and shared many laughs since I first joined the lab. Dr. Siegel has inspired and encouraged me to continue my training as a scientist, and for that I am profoundly grateful.

I am also appreciative of the support and collaboration with Dr. Josie Ursini-Siegel and members of her lab: Eduardo Cepeda-Cañedo, Kyle Lewis, and Elias Maldonado. Eduardo, Kyle, and Elias generated many of the cell lines used throughout this thesis and validated their function. Elias was also integral to the BioID experiment. Dr. Ursini-Siegel's and her student's willingness to share reagents and knowledge in their areas of expertise has been central to the development of this project. I am also thankful for the collaboration with Dr. Jean-Francois Coté and Rebecca Cusseddu who processed and analyzed the BioID samples. Their assistance was crucial to the identification of some exciting avenues for future development of this project.

I would also like to thank my Research Advisory Committee members Dr. Ian Watson and Dr. Arnim Pause for their interest and constructive critiques of my project in our meetings. Their input directed the last several months of my efforts in the lab, and Dr. Pause was always supportive of collaboration with his students and sharing of resources.

I am grateful for financial support from the McGill Department of Biochemistry, as well as funding from the Research Institute of the McGill University Health Center and support from Dr. Siegel's CIHR grants.

I could not have learned several of the techniques required for conducting important experiments without training assistance from The Flow Cytometry Core Facility and The Advanced BioImaging Facility in the Goodman Cancer Institute and McGill Life Science Complex. A special thank you to Joel Ryan who helped with immunofluorescence quantification. Thank you to the IRCM mass spectrometry core who performed several steps of the BioID experiment.

Dr. Marco Biondini has been a close friend in the lab since my first days. I was fortunate enough to work under Marco's supervision as an undergraduate summer student, and he continued to provide support and advice as I worked on my own project in the lab. Marco's positive energy made coming to the lab a pleasure. I will miss working with him dearly.

A big thank you to the other Siegel Lab research associates Dr. Matthew Annis and Dr. Sébastien Tabariès who have helped with aspects of my training and undoubtedly keep the Siegel Lab running. Our lab would not run as smoothly as it does without Matt and Seb doing what they do for us every day.

Past and present members of the Siegel Lab have been incredible colleagues and friends. The Siegel Lab is very a close-knit group and saying goodbye to everyone was no easy task. Thank you to the current members I have spent a great deal of time with over the years: Dr. Afnan Abu-Thuraia, Dr. Charlotte Girondel, Dr. Leeanna El-Houjeiri, Matthew Dankner, Sarah Maritan, Jennie Huxham, Rima Ezzeddine, Anna Shen, Emilie Solymoss, Anna Lazaratos, Alex Nowakowski, Caitlyn Mourcos, Molly Shen, Georgia Kruck, and Celine Chen. Thank you to Leeanna for your thoughtful discussions with me on certain aspects of my project and providing reagents, and to Alex for your support with the technical elements of my microscopy studies. Also, I am grateful for protocols and input from former Siegel Lab member Dr. Alex Kiepas, whose previous work and assistance formed the basis for some of my immunofluorescence and flow cytometry experiments. It has been a privilege and pleasure to work with such talented and caring individuals.

And lastly, a huge thank you to my friends in Montreal and all my family in Alberta, Saskatchewan, and beyond. My sister Brette, father Glen, and mother Teira are a constant source of support, love, and guidance, and I credit much of my success to each of you. My mother remains the inspiration for my current and future research endeavours.

Author Contributions

Thank you to all the previously mentioned Siegel Lab members, core facilities and staff, and collaborators in Dr. Ursini-Siegel's lab.

Experimental design and conceptualization of the project and results were planned by Clark Thomson and Dr. Peter Siegel and collected by Clark Thomson. Dr. Peter Siegel edited the manuscript in its entirety, except for the French abstract which was translated by Marco Biondini and Charlotte Girondel.

Several cell lines were graciously shared by the Ursini-Siegel laboratory and were crucial for many of the experiments described in this thesis. Eduardo Cepeda-Cañedo generated the Hs578T p66ShcA KO, WT, QQ and SA cells, the HCC1954 p66ShcA VC and WT cells and the doxycycline-inducible MCF7 p66ShcA VC and WT cells. Kyle Lewis generated the 4T1-537 p66ShcA KO and WT cells. Elias Maldonado generated the Hs578T p52ShcA-BirA, p66ShcA-BirA and BirA-control cells and induced them with the appropriate treatments for BioID analysis and provided this information for the methods section.

Rebecca Cusseddu in the Coté laboratory processed the BioID samples and analyzed the mass spectrometry results generated by the IRCM mass spectrometry core. Rebecca also provided detailed methods for the BioID sample preparation.

Dr. Josie Ursini-Siegel analyzed TCGA data and constructed the figures presented in Figure 3.4A-B and Figure 3.9D-E. Figures were re-formatted slightly by Clark Thomson for consistency with other presented data.

All other experiments, data analysis, and figure preparation, as well as the writing of this thesis was performed by Clark Thomson.

List of Figures and Tables

Abbreviations

ADAM10	A Disintegrin and Metalloproteinase 10
ADC	Antibody-Drug Conjugate
AMPK	Adenosine 5’ Monophosphate-Activated Protein Kinase
ARF6	ADP-Ribosylation Factor 6
Arl8b	ADP-Ribosylation Factor-Like Protein 8b
As_2O_3	Arsenic Trioxide
BCA	Bicinchoninic Acid
BFDR	Bayesian False Discovery Rate
BioID	Proximity-Dependent Biotin Identification
BirA	Biotin Acetyl-Coenzyme A-Carboxylase Ligase
BRCA	Breast Cancer Gene
BSA	Bovine Serum Albumin
CAF	Core Amyloid Fragment
CH1/2	Collagen Homology 1/2
CLEAR	Coordinated Lysosomal Expression and Regulation
CNS	Central Nervous System
CTC	Circulating Tumour Cell
CTLA4	Cytotoxic T-Lymphocyte-Associated Protein
DC-HIL	Dendritic Cell-Heparin Integrin Ligand
DMEM	Dulbecco’s Modified Eagle Medium
E	Glutamic Acid
ECD	Extracellular Domain
ECM	Extracellular Matrix
EGFR	Epidermal Growth Factor Receptor
EMT	Epithelial to Mesenchymal Transition
ER	Estrogen Receptor
ERK	Extracellular Regulated Kinase
ETC	Electron Transport Chain
FACS	Fluorescence Activated Cell Sorting

FBS	Fetal Bovine Serum
FLCN	Folliculin
FNIP1/2	Folliculin Interacting Protein 1/2
GAP	GTPase Activating Protein
GEF	Guanine Nucleotide Exchange Factor
GPNMB	Glycoprotein NMB
GDP	Guanosine Diphosphate
GRB2	Growth Factor Receptor-Bound Protein 2
GSK3β	Glycogen Synthase Kinase 3 beta
GTP	Guanosine Triphosphate
H_2O_2	Hydrogen Peroxide
HEK293	Human Embryonic Kidney 293
hemiITAM	Half Immunoreceptor Tyrosine-Based Activation Motif
HER2	Human Epidermal Growth Factor Receptor 2
HGFIN	Hematopoietic Growth Factor Inducible, Neurokinin 1 Type
HIF1α	Hypoxia-Inducible Factor 1 Alpha
HO^-	Hydroxyl Radical
HOCl	Hypochlorous Acid
HPLC	High Pressure Liquid Chromatography
HR	Homologous Recombination
HSP70/90/90i	Heat Shock Protein 70/90/HSP90 inhibitors
IHC	Immunohistochemistry
JNK	c-Jun N-Terminal Kinase
KLD	Kringle-like Domain
KO	Knockout
LAMP1	Lysosomal Associated Membrane Protein 1
LINK-A	Long-Intergenic Noncoding RNA for Kinase Activation
MAFK	MAF BZIP Transcription Factor K
MAPK/i	Mitogen Activated Protein Kinase/MAPK Inhibitors
MCOLN1	Mucopilin TRP Cation Channel 1
MFI	Mean Fluorescence Intensity

MiTF	Microphthalmia-Associated Transcription Factor
MMP	Matrix Metalloproteinase
MMAE	Monomethylauristatin E
MTMR4	Myotubularin-Related Protein 4
mTOR/i	Mammalian Target of Rapamycin/mTOR Inhibitors
mTORC1	Mammalian Target of Rapamycin Complex 1
mtROS	Mitochondrial-Derived ROS
$NaAsO_2$	Sodium Arsenite
NAC	N-Acetyl-L-Cysteine
NADPH	Nicotinamide Adenine Dinucleotide Phosphate
NES	Nuclear Export Signal
NLS	Nuclear Localization Signal
NOX	NADPH Oxidase
noxROS	NOX-Derived ROS
NRF2	Nuclear Factor Erythroid 2-Related Factor
NRP1	Neuropilin 1
O_2	Singlet Oxygen
O_2^-	Superoxide Anion
ORR	Objective Response Rate
OS	Overall Survival
OXPHOS	Oxidative Phosphorylation
PARP/i	Poly-(ADP)-Ribose Polymerase/PARP Inhibitors
PD1	Programmed Cell Death 1
PDL1	Programmed Cell Death-Ligand 1
PERK	Protein Kinase R-Like Endoplasmic Reticulum Kinase
PFS	Progression-Free Survival
PI3K	Phosphoinositide-3-Kinase
PINK1	PTEN-Induced Kinase 1
PKC	Protein Kinase C
PKD	Polycystic Kidney Disease
PME1	Protein Phosphatase Methyl Esterase 1

Pmel17	Melanocyte Protein 17
PP2A	Protein Phosphatase 2A
PR	Progesterone Receptor
PRX1	Peroxiredoxin 1
PTB	Phosphotyrosine Binding
PTEN	Phosphatase and Tensin Homolog
PVDF	Polyvinylidene Difluoride
Q	Glutamine
RBD	Rag Binding Domain
RFS	Recurrence-Free Survival
RGD	Arginine-Glycine-Aspartic Acid
RhoA	Ras Homolog Family Member A
RIPA	Radioimmunoprecipitation Assay
RIPK1	Receptor-Interacting Serine/Threonine-Protein Kinase 1
ROI	Region of Interest
ROS	Reactive Oxygen Species
RPMI	Roswell Park Institute Media
RTK	Receptor Tyrosine Kinase
S	Serine
SAINT	Signficance Analysis of INTeractome
SD	Stable Disease
SH2	Src Homology 2
SH3BP4	SH3 Domain-Binding Protein 4
ShcA	Src Homology 2 Domain-Containing Protein A
siRNA	Small Interfering Ribonucleic Acid
SKIP	SifA and Kinesin Interacting Protein
SOS	Son of Sevenless
TIM20/23/44	Translocase of the Inner Mitochondrial Membrane 20/23/44
TMEM106B	Transmembrane Protein 106B
TNBC	Triple-Negative Breast Cancer
TFE3/B/C	Transcription Factor Binding to IGHM Enhancer 3/B/C

TGFβ	Transforming Growth Factor Beta
TROP2	Trophoblast 2
UV	Ultraviolet
v-ATPase	Vacuolar-Type Proton ATPase
VC	Vector Control/Empty Vector
VEGF	Vascular Endothelial Growth Factor
WT	Wild Type
Y	Tyrosine
ZEB1	Zinc-Finger E-Box-Binding Homeobox 1

Chapter 1: Literature Review

1.1 Breast Cancer

1.1.1 Breast Cancer Overview

Breast cancer is the broad term that encompasses tumour formation due to uncontrolled cellular growth within mammary tissues and can originate in various anatomical regions of the breast (ductal carcinoma, lobular carcinoma). Pre-malignant lesions can grow within their original site (*ductal carcinoma in situ*) or progress into adjacent tissues as invasive cancer. Additionally, breast cancer, like other forms of cancer, has the potential to develop into metastatic disease, spreading from its original site to distal organs and tissues in the body [1]. Among Canadian women, breast cancer remains the most commonly diagnosed cancer, with roughly 1 in 8 women projected to be diagnosed with the disease and 1 in 34 estimated to die from it over their lifetime [2]. The high incidence and sustained prevalence of breast cancer clearly illustrates the need for continued research into the underlying cellular and molecular causes, which may lead to better clinical management of this disease.

1.1.2 Breast Cancer Classification and Molecular Subtypes

Breast cancer is a highly heterogenous disease, with clear differences in the molecular characteristics of tumours arising between patients, and individual patients exhibiting both inter and intra-tumour heterogeneity. Because of these differences, several studies have employed gene expression analysis to classify tumours into specific molecular subtypes, each of which can be viewed as a distinct condition with varying clinical outcomes and treatment strategies. Tumours can thus be broadly categorized into one of five groups: luminal A, luminal B, human epidermal growth factor receptor 2^+ ($HER2^+$), triple-negative/basal-like breast cancer (TNBC/BLBC), and normal-like [3-6]. Luminal cancers are estrogen receptor (ER) and/or progesterone receptor (PR) positive and represent the highest proportion of breast cancer diagnoses. Prognosis for luminal cancers is generally positive, owing to their less aggressive characteristics and beneficial effects of hormone-targeting therapies [7]. In comparison, HER2 amplification is seen in 15-30% of patients, with these tumours typically characterized by low levels of hormone receptors and higher proliferation rates when compared to luminal cancers, resulting in a less favourable prognosis. However, those with $HER2^+$ tumours can benefit from treatment with monoclonal antibodies or other therapies targeting HER2, such as the widely administered therapeutic Trastuzumab [8].

Triple-Negative Breast Cancer

TNBC comprises between 10-20% of newly diagnosed patients, and is more common in African American women, pre-menopausal women, and carriers of breast cancer gene (BRCA) 1/2 mutations [9]. As the name suggests, TNBCs displays low or absent expression of hormone receptors and HER2 [3-6]. The majority of TNBCs exhibit characteristics reflective of basal epithelial cells such as high expression of epidermal growth factor receptor (EGFR), cytokeratins, and basal epithelial genes, however a smaller proportion of TNBC show genetic qualities reminiscent of luminal or $HER2^+$ cancers [10-12]. TNBC can be further stratified into an additional type known as claudin-low, owing to deficiencies in claudins 3,4 and 7, as well as enrichment in epithelial to mesenchymal transition (EMT) genes and stem-cell properties [12]. Phenotypically, TNBC is highly aggressive with significant metastatic potential, and has the worst prognosis among breast cancer patients, with a five-year overall survival (OS) of less than 80% [9,10,13-14]. This owes largely to a lack of druggable molecular targets (hormones/HER2) and the strong chance of recurrence after diagnosis and treatment, at which point resistance to conventional therapy as well as metastasis are commonly observed [13-14].

The lack of hormone receptors, HER2 and common genetic mutations seen in other subtypes highlights the need for molecular interrogation of TNBC, leading to the additional stratification of TNBC into six subtypes: basal-like 1, basal-like 2, immunomodulatory, mesenchymal-like, mesenchymal stem-like and luminal androgen receptor. Gene expression analysis of 21 data sets and hundreds of TNBC cases revealed distinct gene expression phenotypes, differing prognoses, and sensitivity to therapy across TNBC subtypes. These characteristics were also reproducible in cell models of TNBC. For example, cell lines within the mesenchymal subtypes are enriched in genes comprising cell motility/EMT pathways and displayed enhanced sensitivity to dasatinib, an inhibitor of the Src kinase that mediates cell migration [15]. These findings along with other studies emphasize the importance of analyzing the molecular and genetic basis of cancers to develop and determine appropriate treatment approaches and predict therapeutic response.

1.1.3 Breast Cancer Metastasis

Metastasis Overview

Despite widespread advancements in screening, diagnostics and treatment strategies, breast cancer is the second leading cause of cancer-related death, accounting for 14% of all cancer deaths [2]. Of these breast cancer deaths, the overwhelming majority are a result of metastasis [16-18]. The metastatic cascade is organ specific and comprises several steps before cancer colonization in a distant site. First, cancer cells proliferate in an initial site to form a primary tumour and invade into adjacent tissues. Cancer cell invasion can occur as single cells with highly invasive phenotypes and/or as cell clusters with intact adhesions [17]. Highly plastic cancer cells then escape the primary tumour and intravasate into the lymphatic system or blood stream. If circulating tumour cells (CTCs) survive in circulation, they then extravasate into a secondary site and establish a secondary tumour (metastasis) [16-18]. Because metastasis comprises several steps in various regions of the body, tumour cells must survive in vastly different environments. To do this, metastatic cells will leverage an array of biological processes and pathways to meet their specific needs. For example, invading tumour cells can undergo a partial or full EMT to dissociate cell adhesions, degrade the extracellular matrix (ECM) and thus increase motility at the onset of metastasis [17,19]. CTCs can also increase their capacity for survival in circulation by rewiring their metabolic programs, shifting from glycolysis to oxidative phosphorylation (OXPHOS), repressing immune pathways, and evading cell death pathways like anoikis, despite changes in the microenvironment and nutrient availability [20]. Due to the multi-step nature and constraints associated with studying certain stages of cancer progression, metastasis remains one of the most poorly understood aspects of the disease.

Additionally, two models of cancer cell dissemination have been proposed. The first model, which is arguably the conventional view of metastasis, involves the gradual accumulation of mutations in the primary tumour. These cells disseminate once their genetic and epigenetic alterations provide them with the fitness to survive the arduous metastatic process. Due to the development of malignancy within the initial site, these tumour cells reflect the characteristics of the primary tumour. Conversely, the parallel progression model posits that metastatic cells depart the lesion prior to malignancy. These disseminated tumour cells exhibited early metastatic potential and further evolve outside of the primary tumour, resulting in a primary tumour and

distant metastases with distinct molecular traits. Both proposed models have independent supporting lines of evidence, further adding to the complexity of metastatic cancer [21-22].

Though metastasis from a lesion to a distant site can be influenced simply by the anatomic design of the circulatory or lymphatic systems, it has long been hypothesised and supported by a large body of experimental and clinical evidence that colonization relies on the ability of tumour cells to initiate metastasis and survive the cascade, but also on interactions with the secondary site microenvironment [18,23]. First theorized by Stephen Paget at the turn of the 19th century and expanded on in following years, the "seed and soil" hypothesis and formation of the pre-metastatic niche describes a complex process in which primary tumours secrete various factors to prime distant tissues for secondary lesion formation, thus creating a microenvironment that supports survival of disseminated tumour cells [23-24]. Formation of the pre-metastatic niche also rationalizes how cancers preferentially colonize specific secondary sites, rather than metastatic distribution simply following dynamics of blood or lymphatic flow. It has become increasingly clear that interaction of the primary tumour, the surrounding microenvironment and the pre-metastatic niche has a profound influence on preferential metastasis to distant organs.

TNBC Metastasis

Unfortunately, though the five-year OS rate for breast cancer patients is high (approximately 90%), a significant proportion may develop metastases after diagnosis and/or treatment. The emergence of metastatic or treatment refractory disease drastically worsens prognosis, with a five-year OS rate of less than 30% [25]. The sites of breast cancer metastasis are diverse, commonly spreading to bone, lung, liver, and brain [26-27]. In TNBC, similar distributions of metastasis to bone and visceral organs have been reported, with slight variations. While bone is the most frequently colonized site for metastatic breast cancer overall with roughly 70% of patients experiencing bone metastasis [28], TNBC presents a preference for visceral organs, with increasing interest in TNBC metastasis to brain [29-31]. TNBC can also form secondary lesions in two or more of the aforementioned sites, with better prognosis in cases of single-organ metastasis [30].

Clinically, TNBC displays more aggressive phenotypes and a propensity for metastasis. In one study, 1,600 patients diagnosed with TNBC were more likely to experience distant recurrence compared to non-TNBC patients (33.9% vs 20.4%, respectively), and experience

lower recurrence-free survival (RFS) within five years of diagnosis. These same TNBC patients also exhibited a 1.5-fold higher chance of death and a shorter median time to death [32]. These trends in recurrence have been corroborated by another study with a cohort size of over 1,100 patients [31]. Both the underlying biology and clinical significance of TNBC recurrence reflect the need for further elucidation of metastatic pathways in this context, and development of treatment strategies for the prevention and management of TNBC metastasis.

1.1.4 TNBC Therapy

TNBC are characterized by a lack of hormone receptors and HER2; thus, TNBC is insensitive to conventional endocrine or HER2-targeting therapies and lacks viable targets to leverage for cancer treatment. As a result, surgical resection and systemic chemotherapy delivered in the adjuvant or neoadjuvant setting remain the front-line treatment approach for TNBC [33]. Several studies have analyzed survival of TNBC patients in the context of adjuvant versus neoadjuvant treatment, with a superior beneficial effect of either remaining unsettled. As such, neoadjuvant therapy will often be considered to minimize tumour volume prior to surgery [9]. A frustrating aspect of TNBC management with chemotherapy is the so-called “triple-negative paradox” in which TNBC patients initially respond favourably to adjuvant or neoadjuvant chemotherapy but experience rapid recurrence and eventual resistance to treatment [31,34]. As such, standard chemotherapies, particularly anthracyclines (doxorubicin)/cyclophosphamides and taxanes (paclitaxel), as well as alkylating agents (carboplatin), are typically recommended for initial treatment of TNBC, but such therapies can often be unsuccessful long term [9,35]. However, technological advancements, identification of pathways and specific cellular targets as well as a shift to personalized treatment approaches has resulted in several new areas of research into targeted TNBC therapies, a few of which are described below.

Immunotherapy

Immunotherapies have gained significant traction in recent years and represent a promising avenue for TNBC therapy. One immune checkpoint treatment that has received attention is targeting programmed cell death 1 (PD1) and programmed cell death-ligand 1 (PDL1). Binding of PD1 to PDL1 results produces several inhibitory effects on T-cells, thus

creating an immunosuppressive environment that facilitates tumour growth [33]. Conversely, inhibition of this immune checkpoint promotes the clearance of tumour cells by producing a microenvironment with a robust anti-tumor immune response. Several PD1/PDL1 checkpoint inhibitors are being used in ongoing clinical trials as first or second-line monotherapies or in conjunction with chemotherapy [35]. For example, a phase III trial testing the anti-PDL1 monoclonal antibody atezolizumab, in conjunction with paclitaxel resulted in improved progression-free survival (PFS) and OS in a cohort of PDL1-positive metastatic TNBC patients. Atezolizumab was subsequently granted accelerated approval by the food and drug administration (FDA) for PDL1-positive metastatic TNBC based on these results [36]. Other immune checkpoint inhibitors such as ipilimumab targeting the cytotoxic T-lymphocyte-associated protein 4 (CTLA4) are also being investigated in clinical trials for efficacy in TNBC [37].

PARP Inhibitors

A second area of research with promising possibilities for TNBC are poly-(ADP)-ribose polymerase (PARP) inhibitors (PARPi). PARP is a superfamily of enzymes implicated in the sensing of DNA-single strand breaks and base-excision repair responses that locates damaged DNA, binds to the site and in turn ribosylates and promotes the activation of downstream components of the DNA repair machinery [38-39]. PARPi are interesting therapeutically since TNBC patients harbour germline mutations in BRCA1/2 and possess deficiencies in homologous recombination (HR) repair. BRCA1/2 are well known tumour suppressors involved in DNA repair pathways that correct DNA-double strand breaks. When mutated, BRCA1/2 lead to deficiencies in HR repair [38-39]. Though it is likely not the sole mechanism explaining the anti-tumor effects of PARPi, this class of drugs leverage the concept of synthetic lethality, in which BRCA1/2 mutated cancers, in combination with PARPi, incapacitates two DNA-repair mechanisms. This ultimately results in the accumulation of DNA breaks and tumour cell death, whereas normal cells remain unaffected as their HR pathways are still intact [40]. Many PARPi have been approved by the FDA for use in numerous cancers, including Olaparib, which was the first PARPi to be approved as a monotherapy for metastatic, $HER2^-$ (TNBC), BRCA1/2 mutated cancers, demonstrating improved PFS survival of roughly 3 months and a 42% lower risk of disease progression or death in comparison to standard of care [41].

Antibody-Drug Conjugates

Another rapidly growing avenue of cancer research is antibody-drug conjugates (ADC). These therapies are an elegant approach to delivering chemotherapy specifically to cancerous cells, as ADCs are monoclonal antibodies that specifically target a tumour cell surface antigen linked to a potent cytotoxic drug [42]. By raising a monoclonal antibody against proteins that are present on cancerous cells and lowly expressed or absent in normal cells, ADCs can selectively deliver compounds to tumours, thus reducing the toxic effects that are seen with conventional systemic treatments. Regarding TNBC, an ADC that has garnered attention is Sacituzumab govitecan, which targets trophoblast 2 (TROP2) that is highly expressed in many cancers, including TNBC. Sacituzumab govitecan leverages a metabolite that triggers tumour cell death by interfering with DNA replication, inhibiting topoisomerase activity, and inducing DNA double-strand breaks [43]. This ADC demonstrated promise in metastatic TNBC patients that had previously undergone rigorous chemotherapy, as there was convincing data showing increased PFS compared to standard chemotherapy [44]. As such, Sacituzumab govitecan became the first ADC approved for use by the FDA in TNBC patients who experience metastasis and have previously undergone two previous chemotherapies [9]. ADCs represent an exciting and sophisticated form of cancer therapy, effectively combining immunotherapy and chemotherapy.

These 3 categories of emerging treatment strategies are by no means the only ongoing studies for targeted therapy in TNBC. Several other biological processes have therapeutic potential and are being or have been investigated, albeit with mixed results. For example, monoclonal antibodies targeting growth factors like EGFR [45] or vascular endothelial growth factor (VEGF) to inhibit angiogenesis [46] have been previously analyzed in clinical trials. Additionally, signaling pathways such as the phosphoinositide-3-kinase (PI3K)/AKT/mammalian target of rapamycin (mTOR) pathway [47], androgen receptor pathway [48], and ERβ signaling [49] have been interrogated for TNBC treatment. Due to the complexity of the disease, patients with TNBC still have largely unmet clinical needs. Further studies into the previously mentioned treatments both as monotherapies and in combination with other drugs, identification of new molecular targets for novel therapies, and a better understanding of the processes governing metastasis are needed for more effective and personalized medicine, and patient survival.

1.2 GPNMB

1.2.1 GPNMB Overview

An important molecular mediator of TNBC metastasis is Glycoprotein NMB (GPNMB). GPNMB was first characterized in melanoma cell lines that exhibited poor metastatic capabilities [50], however studies since its initial discovery have distinguished GPNMB as a pro-metastatic gene. GPNMB, also frequently referred to as osteoactivin [51], dendritic cell heparin integrin ligand (DC-HIL) [52], and hematopoietic growth factor inducible, neurokinin-1 type (HGFIN) [53], belongs to the melanocyte protein 17 (Pmel17)/NMB family and is found on the small arm of chromosome 7 (7p15) [50,53,54]. For simplicity, herein I will solely use the name GPNMB in the place of any other names or species-specific orthologues. GPNMB has two validated mRNA isoforms that result from alternative splicing: a short variant with 560 amino acids (aa) and a long variant with an additional 12 aa (572 aa) [55]. There are currently no studies reporting a functional difference between these isoforms. An additional transcript variant has also recently been reported in patients with amyloidosis cutis dyschromica [56].

GPNMB is a single-pass (type 1) transmembrane protein comprised of several domains that can be broadly separated into a large extracellular domain (ECD), a transmembrane anchor, and a short cytosolic tail. Within the ECD, GPNMB harbours an N-terminal secretory pathway targeting signal peptide, an integrin binding arginine-glycine-aspartic acid (RGD) motif, a polycystic kidney disease (PKD) domain, and a kringle-like domain (KLD). The cytosolic region of GPNMB harbours a half immunoreceptor tyrosine-based activation motif (hemiITAM) and a C-terminal dileucine-based endosomal/lysosomal sorting signal [52, 57-61]. Homology prediction modeling has also identified GAP1/2 and core amyloid fragment (CAF) domains conserved in Pmel17 and GPNMB; however, they have not been reported as functionally significant in GPNMB and thus are not discussed here [57, 60-61].

As the name suggests, GPNMB is heavily glycosylated on several sites in its N-terminus, [50, 58-59] and can also be subjected to further post-translational modifications such as tyrosine phosphorylation [62-63] and proteolytic release of the extracellular domain [57, 64]. Many of these modifications are intertwined with GPNMB's functions in normal as well as disease states. GPNMB may act as a cell surface receptor, be shed as a ligand, act as an adhesion molecule, melanosome or endosomal/lysosomal protein in different contexts and is involved in an array of biological processes, with its expression and action being characterized in various organs,

tissues, and systems such as bone, skin (especially melanocytes), eyes, the central nervous system (CNS), the immune system, and adipose tissue [59, 60, 65]. It is also possible for GPNMB to be expressed within multiple cell types in the same tissue and/or compartments within a cell, further adding to the widespread expression and implications of GPNMB under normal physiological conditions [59].

1.2.2 GPNMB as a Mediator of Metastasis in TNBC

In the context of cancer, nearly all studies of GPNMB indicate a pro-tumorigenic function *in vitro, in vivo*, and clinically [59, 65-67]. In comparison to normal tissues, GPNMB expression is elevated in numerous malignancies. GPNMB's overexpression and role in cancers of the lung, prostate, bladder, brain (gliomas and astrocytomas), liver, kidney, prostate, colon, pancreas, stomach, breast, and melanomas have been reviewed previously [59, 65-67], with additional studies suggesting GPNMB is involved in the progression and/or clinical outcome of cholangiocarcinoma [68], cervical [69], and ovarian cancers [70], as well as B-cell lymphomas [71]. However, the focus of this review revolves around the widespread implications of GPNMB in TNBC metastasis.

GPNMB Expression and Effect on Clinical Outcome in TNBC

Previous work done by our lab originally characterized the overexpression of GPNMB in murine TNBC 4T1 mammary carcinoma cell sub-populations *in vivo* selected for metastasis to bone. Highly metastatic populations exhibited elevated expression of GPNMB in comparison to parental 4T1, lowly-metastatic, or non-metastatic cell lines [72]. This observation was extended by our lab to show that GPNMB was also enriched in other 4T1 sub-populations aggressively metastasizing to lung [73] and liver [74]. The results in mice prompted further investigation of GPNMB expression in human breast tumours. Using several published data sets and tissue microarray data, it was shown that GPNMB is highly expressed in a proportion of all breast cancer subtypes, with TNBC exhibiting the most significant enrichment of GPNMB levels. Gene expression data revealed that 25.4% of tumours expressing high levels of GPNMB belonged to the TNBC/BLBC subtype, and similarly 29.1% of TNBC tumours were positive for immunohistochemistry (IHC) staining of GPNMB in the tumour epithelium [75]. In this same study, GPNMB expression was also shown to indicate recurrence and correlate with poorer OS

in breast cancer, and even within the TNBC subtype, GPNMB was associated with shorter RFS. These findings have been corroborated in independent investigations. One study utilizing patient specimens and publicly available breast tumour data showed elevated GPNMB gene and protein expression in comparison to non-TNBC patient samples, with high GPNMB levels correlating with significantly lower distant metastasis-free survival and RFS in comparison to low GPNMB-expressing patients. Visible trends were also observed for OS and local RFS, albeit not statistically significant [66]. The EMERGE clinical trial testing the effects of glembatumumab vedotin, an ADC that will be discussed later, also reported expression of GPNMB in the tumour epithelium of 40% of TNBC samples submitted, compared to 21% of all other samples [76]. Collectively, literature to date indicates a clear role for GPNMB expression in TNBC and as an indicator of poor prognosis within the subtype.

Mechanisms of GPNMB-Dependent Tumorigenesis

GPNMB has been implicated in several stages of TNBC tumor progression and the mechanisms through which GPNMB exerts its effects on metastasis have been extensively studied in both *in vitro* and *in vivo* models. Our lab has demonstrated in several papers that GPNMB is sufficient to drive migratory and invasive phenotypes in both breast cancer cells and mice, and enhance metastasis to organs such as bone, lung, and liver [72-75]. In one such study, it was shown that GPNMB expression decreased levels of apoptosis and increased angiogenesis *in vivo.* Further characterization of this mechanism in TNBC cell models revealed that the ECD of GPNMB is cleaved by the matrix metalloproteinase (MMP) a disintegrin and metalloproteinase 10 (ADAM10), and the shed form of GPNMB can subsequently stimulate endothelial cell migration and VEGF expression. This in turn enhances the angiogenic properties of cancer cells, thereby promoting tumour growth [73]. This is in line with a previous study in the lab positing that GPNMB is involved in the regulation of MMP3 expression, which may also contribute to the observed invasion in TNBC cell models [72]. Further evidence of the pro-invasive phenotype was also described with the MAF BZIP transcription factor K (MAFK) transcription factor shown to induce migration and invasion through upregulation of GPNMB (a MAFK transcriptional target). Interestingly, GPNMB expression was shown to promote metastatic phenotypes in this context by inducing an EMT [77]. TNBC metastasis has also been suggested to be promoted by GPNMB in a complex signaling cascade involving long-intergenic

noncoding RNA for kinase activation (LINK-A). LINK-A mediates heterodimer formation of GPNMB and EGFR, and their subsequent phosphorylation, which stabilizes downstream hypoxia-inducible factor 1 alpha (HIF1α). HIF1α signaling was then shown to promote tumour growth [63].

Other studies in our lab have also provided further insight into the role of GPNMB in tumour initiation and primary tumour growth through modulation of signaling pathways. For example, GPNMB was shown to exhibit tumour intrinsic functions by increasing the expression of neuropilin 1 (NRP1). GPNMB-dependent increases in NRP1 enhance proliferation and VEGF signaling and sustain AKT activation, contributing to primary tumour growth. However, this mechanism was dispensable for metastasis [78]. Additionally, tumour initiation and growth in Wnt-dependent cancer was previously demonstrated to be enhanced by GPNMB, as GPNMB increases the transcriptional activity of β-catenin through modulation of the PI3K/AKT/mTOR pathway [79]. Regulation of AKT, as well as altered proliferation and apoptosis by GPNMB observed in this study, are in agreement with previous work conducted in the lab [73, 78].

Some of the pro-metastatic functions associated with GPNMB have been mapped to specific domains within the protein, in addition to the previously described ECD shedding. In the same paper describing NRP1-dependent primary tumour growth, the RGD motif of GPNMB was also shown to interact with the tumour-specific integrin α5β1. The GPNMB RGD motif was shown to not only increase expression of the integrin receptor but also activate downstream signaling and promote tumour growth and lung metastasis [78]. Deletion of the KLD in GPNMB's extracellular region in breast cancer cells has also been shown to impair the molecular functions of GPNMB, with reduced potential to induce EMT and a reduction of tumour volume and frequency when injected into mice in comparison to wild-type GPNMB-expressing cells [80]. This was proposed to be a result of dysfunctional Wnt/β-catenin signaling, and although this theory has not been robustly tested, it is line with previous reports that GPNMB regulates the Wnt/β-catenin pathway [69, 71, 79-80]. Tyrosine phosphorylation of key residues within the cytosolic hemiITAM domain have also been demonstrated to be critical for GPNMB's functions in inducing EMT and stabilizing HIF1α. The mutation of tyrosine to phenylalanine in either of these contexts ablates the pro-tumorigenic capabilities of GPNMB [63, 77]. Finally, though not validated in the context of cancer, the PKD domain of GPNMB has been shown to bind to syndecan 4, a transmembrane protein upregulated on T-cells. GPNMB engagement of syndecan

4 in turn leads to T-cell inhibition, which in tumour cells may create an immunosuppressive environment conducive to the progression of metastasis [81].

Clearly, GPNMB can leverage diverse signaling pathways and biological processes to exert its pro-tumorigenic effects. GPNMB is multi-faceted in that in can produce both tumour intrinsic functions and impact the tumour microenvironment to promote metastasis. As such, further investigation into GPNMB's underlying mechanisms and potential in TNBC therapeutics is warranted.

1.2.3 GPNMB Targeted Therapy: CDX-011

Due to GPNMB's expression in a considerable proportion of TNBC cancer patients, and its reported implications on clinical outcome and various aspects of metastasis, GPNMB has been identified as a potential target for TNBC therapy. It represents a particularly attractive treatment option as in normal tissues GPNMB is predominantly intracellular, but in breast cancer cells GPNMB expression is increased at the cell surface, making it readily available for therapeutics specifically targeting tumours cells [75]. GPNMB-targeting therapy arose from transcript profiling of metastatic melanomas, in which GPNMB was identified as a potential target and thus a human monoclonal antibody dubbed CR011 was generated for characterization of efficacy in melanoma. CR011 alone exhibited no inhibitory effect on melanoma cell growth, so it was developed into an ADC by fusing CR011 to monomethylauristatin E (MMAE), a cytotoxic tubulin destabilizer. This ADC, termed CR011-vcMMAE, CDX-011 or glembatumumab vedotin, herein referred to as CDX-011, is internalized into GPNMB-expressing cells and subsequently cleaved, with the free cytotoxin inducing cell death. The study showed an inhibition of melanoma tumour growth with CDX-011 administration, setting the stage for future trials in GPNMB-expressing melanoma and breast cancer [82].

After initial observations in our lab that CDX-011 impaired breast cancer growth *in vitro* and *in vivo* [75], the first instance of CDX-011 use in breast cancer clinical trials was conducted in advanced/metastatic breast cancer patients subjected to previous cycles of chemotherapy. Of particular interest were the results in the TNBC patients within the phase II cohort. Of the 10 TNBC cases, 60% experienced 12-week PFS, 80% displayed stable disease (SD) and overall patients had a 20% objective response rate (ORR) and longer median PFS in comparison to non-TNBC. TNBC patients stratified for GPNMB-positive tumours exhibited further responsiveness

to CDX-011, with this cohort having the longest median PFS, 100% 12-week PFS and 100% with SD [83]. Further evidence of CDX-011 activity was seen in the phase II EMERGE clinical trial, with an ORR of 18% and 40% in TNBC patients and TNBC patients overexpressing GPNMB, respectively, treated with CDX-011, in comparison to those same patients treated with other chemotherapy who exhibited a 0% ORR [76]. However, clinical trials were ultimately discontinued in 2018 after the larger METRIC clinical trial failed to demonstrate any significant differences in response or any secondary survival outcome between patients in the CDX-011 arm and the capecitabine arm of the study [84].

Despite halting clinical trials for CDX-011 in breast cancer, there are still opportunities for its application in TNBC therapeutics. The previously mentioned studies all employed CDX-011 as a single agent. It is possible given the diverse functions of GPNMB in promoting tumour progression that CDX-001 combination therapies could improve its efficacy. For example, a previous study in the lab showed that melanoma tumour growth was significantly inhibited by treatment with CDX-011 in combination with mitogen activated protein kinase inhibitors (MAPKi). Treatment with MAPKi induces the transcriptional activity of microphthalmia-associated transcription factor (MiTF), of which GPNMB is a target gene. Subsequent treatment with CDX-011 then targets GPNMB-expressing cells, impairing tumour growth and acquired resistance to MAPKi [85]. It is important to note that the clinical efficacy of CDX-011, particularly in TNBC, appears to directly hinge on the level of GPNMB expression. This is consistent with the initial observation in melanoma that the inhibitory effect of CDX-011 can be enhanced with ectopic GPNMB expression or mitigated with transient knockdown of GPNMB [82]. A recent publication from our lab has provided further evidence that other therapies enhance CDX-011 sensitivity in models of breast cancer. Inhibition of the MAPK pathway or treatment with mTOR inhibitors (mTORi) upregulates GPNMB expression by promoting the nuclear shuttling of transcription factor binding to IGHM enhance 3 (TFE3), another transcription factor that that will be discussed extensively in future sections. In response to MAPKi/mTORi, enhanced localization of TFE3 to the nucleus upregulates GPNMB expression, resulting in reduced TNBC tumour growth when combined with CDX-011. In this same study, it was determined that though MAPKi/mTORi increase GPNMB levels, they only marginally enhance GPNMB cell surface expression. Interestingly, treatment with heat shock protein 90 (HSP90) inhibitors (HSP90i) was shown to not only upregulate GPNMB expression through

repression of PI3K/Akt/mTOR signaling, but also deliver GPNMB to the cell surface through lysosomal scattering and subsequent fusion with the plasma membrane. As such, exposure to HSP90i substantially enhanced sensitivity to CDX-011 *in vivo* [86]. This recent finding strengthens the notion that high GPNMB expression, as well as cell surface localization, dictate response to CDX-011. Further investigation into drug combinations that interfere with specific aspects of GPNMB's pro-tumorigenic roles, while increasing GPNMB expression and cell surface availability for CDX-011 targeted therapy, could reveal novel treatment strategies for metastatic TNBC and other GPNMB-expressing cancers.

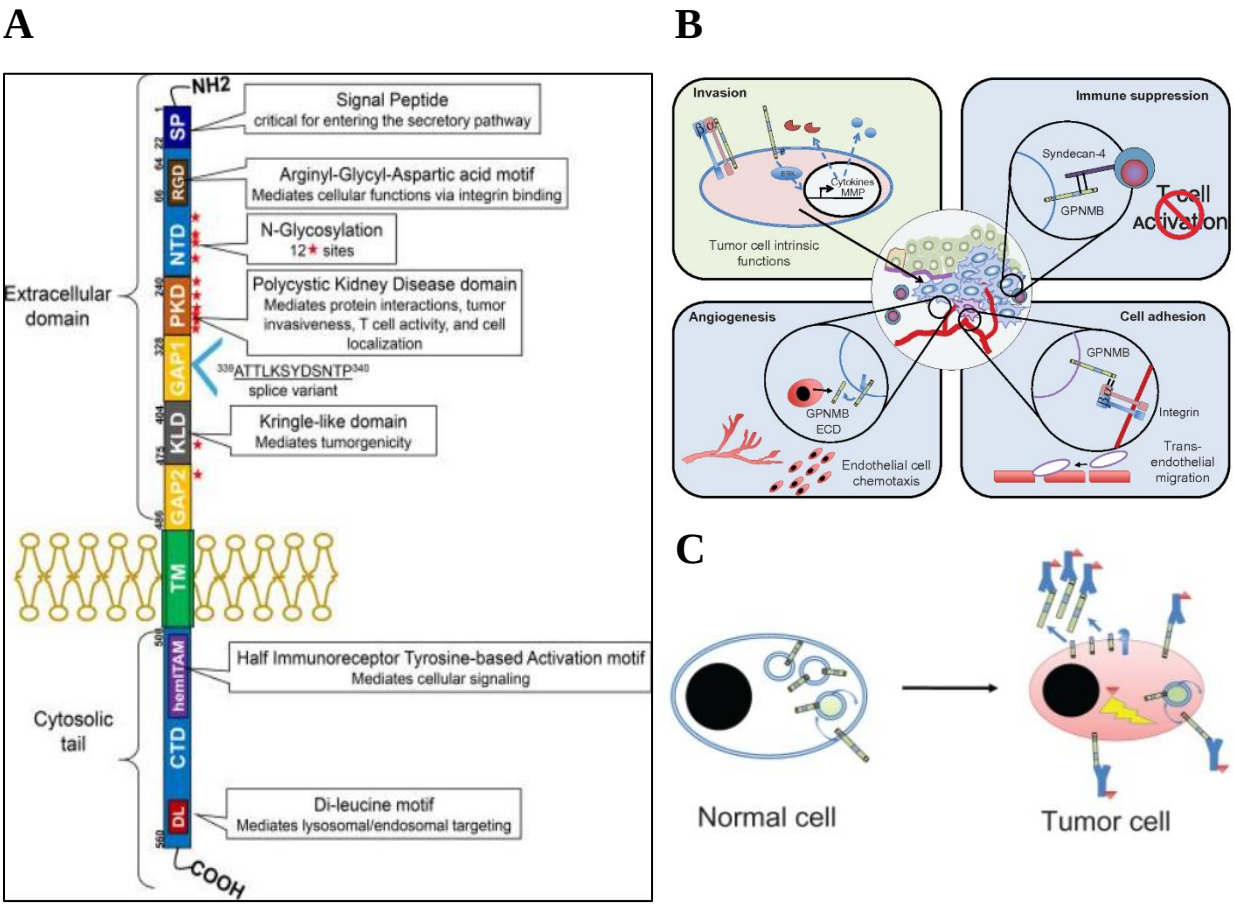

1.1 Structure and Function of GPNMB in Cancer. (**A**) Schematic depiction and functional role of GPNMB domains. Figure adapted from Tsou and Sawalha, 2020 [60]. (**B**) Possible pro-tumorigenic mechanisms and (**C**) differential localization of GPNMB in malignant cells. The enhanced cell surface expression of GPNMB in tumour cells underlies its potential for targeted therapy. Figures adapted from Maric et al., 2013 [59].

1.2.4 GPNMB as a Stress Response Gene

Given the harsh conditions of the tumour microenvironment, as well as the numerous obstacles encountered by CTCs throughout the metastatic cascade, it is plausible that GPNMB is expressed or functions in contexts of elevated cellular or physiological stress. An increasing body of work has focused on GPNMB in the context of inflammation, particularly in neurological conditions. The presence of GPNMB in Alzheimer's and Parkinson's Disease, as well as Amyotrophic Lateral Sclerosis has been recently reviewed, with GPNMB induction following exposure to cytokines or pro-inflammatory stimuli reported to be neuro-protective [87]. Consistent with its previously described role in immune inhibition, GPNMB upregulation has also been reported in phagocytic macrophages and patient samples in autoimmune disorders, including lupus and psoriatic arthritis [60].

At the cellular level, GPNMB has also been studied in the context of stress response pathways. GPNMB expression is elevated in response to lysosomal stress or damage, with lysosomal dysfunction in a variety of tissues and cell types causing Parkinson's and lysosomal storage disorders such as Niemann Pick type C and Gaucher Disease [88-90]. The endoplasmic reticulum stress response has also been reported to upregulate GPNMB, which in turn protects cells by promoting the expression of molecular chaperone proteins [91]. Using a genetic approach to identify downstream phenotypes in glaucoma, GPNMB has also been proposed to function as a part of a gene network with pathways associated with oxidative stress and apoptosis, thus contributing to pathogenesis [92].

Clearly, cellular stress can contribute to the expression and activity of GPNMB in tumorigenesis and other disease states. This can likely be explained in part by the stress-induced activation of GPNMB's upstream transcription factors, which will be discussed in detail in the following section. The diversity of stress response systems that are influenced by or promote GPNMB expression emphasizes the therapeutic potential for targeting GPNMB and its associated pathways, as well as GPNMB's function as a stress-response gene.

1.3 TFE3/TFEB

1.3.1 TFE3/TFEB Overview

The MiTF/TFE family of transcription factors is comprised of the evolutionarily conserved MiTF, and transcription factor binding to IGHM enhancer 3/B/C (TFE3/TFEB/TFEC). These transcription factors are basic helix-loop-helix leucine zipper structural proteins and bind DNA regions of target genes as homo or heterodimers [93]. For the purposes of this review, I will primarily focus specifically on TFE3/TFEB. TFE3/TFEB play many biological roles and control the expression of a myriad of downstream genes, particularly as an adaptation to stress. Though they are in some ways functionally redundant, it has been proposed that both TFE3 and TFEB are required for optimal response to cellular stress [94]. TFE3/TFEB activation has been extensively reviewed in response to endoplasmic reticulum, metabolic and oxidative stress, mitochondrial and DNA damage, pathogen infection, starvation, and as part of the immune response [95]. Chromosomal translocations of TFE3/TFEB or their aberrant activation has also been widely reported in neurological conditions, lysosomal storage disorders, and numerous cancers [95-97].

TFE3/TFEB can be considered as cellular adaptation transcription factors, and they are most widely known as master regulators of lysosomal biogenesis and autophagy. TFEB was first characterized as a regulator of lysosomal and autophagy genes by Sardiello *et al.* in which a specific 10 base-pair DNA motif was determined to be bound by TFEB. This motif, dubbed the Coordinated Lysosomal Expression and Regulation (CLEAR) element, was found in the promoter of many lysosomal genes, the majority of which were upregulated in response to TFEB overexpression [98]. TFE3 was subsequently shown to bind to the CLEAR element and TFE3 overexpression induces the expression of the same subset of lysosomal and autophagy related genes as TFEB [94]. The regulation of lysosomal biogenesis and autophagy is important not only for the maintenance of cellular homeostasis, but also has widespread implications in disease, such as cancer. Though autophagy can play a dual role as a tumour suppressor or promoter in malignant cells, it has been posited that autophagy can promote tumour progression by helping malignant cells meet their high energetic needs, often in nutrient or energy sparse microenvironments [99]. This exact mechanism has been reported in models of lung cancer, with TFE3/TFEB activation promoting cancer progression in glucose-starved conditions [100]. The importance of lysosomes in cancer metastasis has also been described, with the TFEB-target

transmembrane protein 106B (TMEM106B) having been reported to promote lung cancer metastasis by inducing lysosomal gene expression and release of lysosomal enzymes through exocytosis. This has been suggested to provide a route for metastatic progression through degradation of the ECM [101]. Additionally, TFE3/TFEB pro-tumorigenic mechanisms independent of autophagy or lysosomes have also been described previously, including regulation of the cell cycle, angiogenesis, and cell differentiation [95]. As such, TFE3/TFEB proteins have drawn attention as potential oncogenic therapeutic targets.

Importantly, TFE3/TFEB have further implications in cancer as regulators of GPNMB expression. Though GPNMB regulation by MiTF had been reported in melanosomes, GPNMB was initially proposed as a direct MiTF/TFE family transcriptional target when a bioinformatics approach revealed that GPNMB harboured a M box sequence in its promoter; a sequence that is highly conserved and directly recognized by the MiTF/TFE transcription factors. In this study, GPNMB was shown to be directly regulated by TFEB through activity on the M box promoter [102]. GPNMB was additionally confirmed as a direct target of TFE3 in an independent study of TFE3 chromosomal translocations in renal cell carcinoma [103]. Regarding breast cancer, TFE3/TFEB may have particular importance in TNBC. A recent study reported that TNBC/BLBC cell lines exhibited a higher percentage of cells with nuclear TFE3, where TFE3 upregulates target genes such as GPNMB, in comparison to luminal models [104]. This is in line with the previously discussed importance of GPNMB in TNBC progression. As mentioned, GPNMB is an emerging stress response gene, which is likely owed to its regulation by TFE3/TFEB, known regulators of cellular adaptation to therapy and stress [86]. Further investigation into TFE3/TFEB-dependent stress response mechanisms that induce GPNMB could unveil innovative approaches for TNBC management.

1.3.2 Regulation of TFE3/TFEB Activity

mTORC1-Dependent Regulation of TFE3/TFEB

TFE3/TFEB transcriptional activity is directly associated with its subcellular localization, both of which are tightly regulated. To initiate transcription of their target genes, TFE3/TFEB must be shuttled from the cytosol to the nucleus where they can bind M box or CLEAR elements. Early evidence of TFEB nuclear translocation was observed in response to sucrose treatment [98]. This has been corroborated with a variety of pharmacological agents and stress

stimuli, with observable nuclear accumulation of TFE3/TFEB in comparison to untreated cells [105]. Mechanistically, TFE3/TFEB regulation has been best characterized in the context of nutrient deprivation in a mTOR complex 1 (mTORC1)-dependent manner. Under nutrient replete conditions, TFE3/TFEB are diffused in the cytosol, or localized at the lysosomal surface through recruitment by the Rag guanosine triphosphatases (Rag GTPases). Specifically, TFE3/TFEB are bound to active Rag complexes, consisting of a heterodimer of Rag A/B bound to GTP and Rag C/D bound to guanosine diphosphate (GDP) through an N-terminal Rag binding domain (RBD) [96, 106]. At the lysosome, TFE3/TFEB are then phosphorylated by mTORC1 on serine (S) 321 [94] and S142/211 [107-109], respectively, resulting in transcription factor binding to the 14-3-3 chaperone protein. This phosphorylation and subsequent binding event renders TFE3/TFEB cytosolic, potentially masking a nuclear localization signal (NLS), thus preventing their activation [107-109]. In contrast, when there are insufficient amino acids, the Rag GTPases and mTORC1 are inactive, thus preventing TFE3/TFEB phosphorylation and 14-3-3 binding, allowing TFE3/TFEB translocation to the nucleus and subsequent transcription. Phosphorylation of mTORC1-phosphorylated residues has also been shown to be removed by the phosphatase calcineurin in starved cells, resulting in further nuclear accumulation of TFE3/TFEB [110]. This mechanism was delineated roughly a decade ago, and since its initial characterization additional layers of regulation have been described. For example, TFEB shuttling back to the cytosol following restoration of nutrient supplies has been demonstrated to occur through Exportin-1 mediated trafficking. This has also been shown to be mTORC1-dependent, with phosphorylation of S138/142, which are encompassed by a nuclear export signal (NES), by mTORC1 required for efficient shuttling [111]. S122 of TFEB has also been shown to be phosphorylated by mTORC1, and although mutation of this residue does not render TFEB constitutively nuclear, it has been demonstrated to enhance nuclear shuttling when co-mutated with S211 [112]. Due to the direct regulation of TFE3/TFEB by mTORC1, it is important to consider that changes to the activity, lysosomal localization, and/or expression of mTORC1 regulatory elements may also have an impact on TFE3/TFEB transcriptional activity. Because TFE3/TFEB subcellular localization is rigorously controlled, changes in any component of this cascade can have profound impacts on TFE3/TFEB activity and downstream effects on target gene transcription.

A

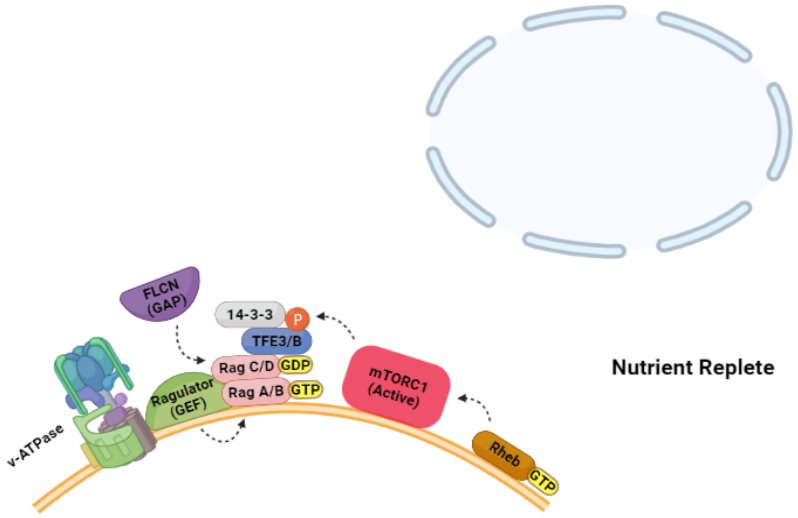

B

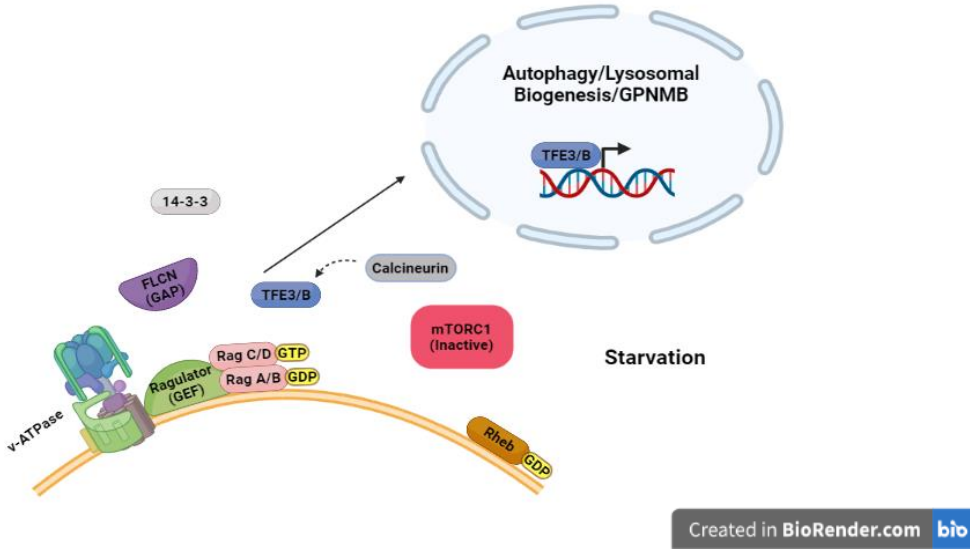

Figure 1.2 Regulation of TFE3/TFEB by mTORC1. (**A**) With sufficient levels of amino acids, mTORC1 is recruited to the lysosome by active Rag GTPases. An active Rag GTPase complex consists of a heterodimer of Rag A/B bound to GTP and Rag C/D bound to GDP. Loading of GTP/GDP is facilitated by the GEF/GAP activity of Ragulator and FLCN, respectively. Ragulator provides a physical link between Rag GTPases and the v-ATPase, which stimulates the GEF activity of Ragulator. mTORC1 is activated by the small GTPase Rheb, resulting in mTORC1-dependent phosphorylation of TFE3/TFEB on specific serine residues at the lysosomal surface. TFE3/TFEB phosphorylation creates a binding site for 14-3-3, retaining TFE3/TFEB in the cytosol where they are inactive. (**B**) In response to starvation/cellular stress, mTORC1 is not recruited to the lysosome and its activity is inhibited. TFE3/TFEB are dephosphorylated by calcineurin, and the lack of mTORC1 phosphorylation events promotes TFE3/TFEB nuclear accumulation and target gene transcription. Figures created using BioRender.

Regulation of TFE3/TFEB by Other Kinases

Though regulation by mTORC1 has been thoroughly studied, many other mTORC1-independent or concomitant mechanisms involving other factors have been reported. Notably, a recent study identified the adenosine 5' monophosphate-activated protein kinase (AMPK) as a critical mediator of TFE3/TFEB activity during starvation. Phosphorylation of a cluster of serine residues in the C-terminus of TFE3/TFEB, S567/568/570 and S466/467/469, respectively, by AMPK was shown to be essential for TFE3/TFEB gene transcription even when the transcription factors are constitutively nuclear [113]. When combined with the extensively studied mTORC1 starvation mechanism, these investigations collectively suggest that mTORC1 controls the subcellular localization of TFE3/TFEB and AMPK controls transcriptional activity upon accumulation in the nucleus. Phosphorylation of previously described residues can also occur through kinases other than mTORC1. Extracellular regulated kinase 2 (ERK2), has been reported to phosphorylate TFEB on S142 and result in TFEB retention in the cytosol, the mechanism of which remains unclear [114]. Cytosolic retention of TFEB has additionally been reported following phosphorylation of S134/138 by glycogen synthase kinase 3 beta (GSK3β). TFEB activation in this context was shown to occur through a protein kinase C (PKC)-dependent mechanism in which PKC-mediated inhibition of GSK3β alleviates phosphorylation of TFEB, allowing its subsequent nuclear translocation. However, GSK3β phosphorylation was shown to recruit TFEB to lysosomes, so it cannot be definitively stated that this is an entirely mTORC1-independent mechanism [115]. Additionally, GSK3β activity on S138 has also been shown to mediate nuclear export of TFEB in response to glucose by activating a NES [116]. PKC, specifically PKCβ, has also been shown to regulate the stability of TFEB and downstream effects on lysosomal biogenesis in osteoclasts by phosphorylating several C-terminal serine residues [117]. Furthermore, the mitochondrial components phosphatase and tensin homolog (PTEN)-induced kinase 1 (PINK1), Parkin, and the autophagy proteins Atg5/9 all contribute to a mechanism during mitophagy that promotes the accumulation of TFEB in the nucleus, independently of mTORC1 inactivation [118]. Finally, phosphorylation of TFE3/TFEB on S565/467, respectively, by AKT has also been shown to promote the cytosolic retention and inactivation of TFE3/TFEB, which also suggests that many of the phosphorylation events reported in TFEB may be conserved in TFE3 and the other MiTF/TFE family members [119-120].

TFE3/TFEB Regulation by Phosphatases

As previously described, calcineurin dephosphorylates TFE3/TFEB on critical serine residues under starvation conditions when mTORC1 activity is inhibited [110]. However, an additional mechanism for calcineurin-mediated TFE3/TFEB activation in response to endoplasmic reticulum stress has also been described, which does not require the inhibition of mTORC1. This study described a mechanism for TFE3/TFEB activation that requires protein kinase R-like endoplasmic reticulum kinase (PERK) and calcineurin as part of the unfolded protein stress response. PERK was shown to increase the activity of calcineurin, leading to dephosphorylation of TFE3 and its subsequent nuclear translocation, even in the context of active mTORC1 [121]. This suggests that calcineurin not only acts independently of mTORC1 in specific cellular contexts, but the enzymatic activity of calcineurin is sufficient to drive TFE3/TFEB nuclear accumulation. TFE3/TFEB activity is also stimulated by the activity of protein phosphatase 2A (PP2A) in response to oxidative stress induced by sodium arsenite ($NaAsO_2$). Following the production of reactive oxygen species (ROS), PP2A dephosphorylates TFE3 at S321, and TFEB at 4 serine residues (including S211). This mechanism was also shown to be independent of mTORC1 inactivation, as expression of downstream phosphorylation targets of mTORC1 were not reduced [122]. Though the precise mechanism has not been fully elucidated, in lung A549 cells myotubularin-related protein 4 (MTMR4), a PI3 specific phosphatase was also shown to influence the phosphorylation status and localization of TFEB, with MTMR4 knockdown cells exhibiting higher levels of phosphorylated, and thus cytosolic, TFEB [124].

In summary, an extensive body of work has been directed to identify the regulatory mechanisms of TFE3/TFEB, particularly in the context of nutrient starvation, in which mTORC1 plays a key role in the suppression of TFE3/TFEB activation. However, there are a considerable number of studies that have identified mTORC1-indpendent mechanisms of TFE3/TFEB activation. Evidently, TFE3/TFEB regulation is complex and the engagement of various signaling pathways, kinases and phosphatases appears to be cell line, tissue and context dependent based on stress stimuli.

1.3.3 TFE3/TFEB and Oxidative Stress

The role of TFE3/TFEB activation in responding to various cellular stressors is an ongoing area of research in many diseases, including cancer. Of particular interest to this project is the implication of TFE3/TFEB in the context of oxidative stress due to elevated ROS. ROS is an umbrella term referring to highly reactive and unstable intermediates formed by the reduction of oxygen, including H_2O_2, superoxide anion (O_2^-), hydroxyl radical (HO^-), singlet oxygen (O_2), and hypochlorous acid (HOCl) [123]. Numerous studies report a link between ROS-dependent TFE3/TFEB activation and the regulation of downstream lysosomal and autophagy processes. These results encompass various cell types, tissues, treatment conditions and diseases, all of which contribute to the diverse regulation of TFE3/TFEB transcription factors. A few selected studies regarding TFEB highlight this complexity. For example, one of the earliest characterized mechanisms of ROS-dependent, TFEB-mediated induction of autophagy and lysosomal biogenesis was shown to be dependent on mucopilin TRP cation channel 1 (mCOLN1). In response to treatment with various oxidants, ROS production was enhanced and caused mCOLN1-dependent release of calcium. This in turn activates calcineurin, resulting in transcriptional activity of TFEB after dephosphorylation and nuclear accumulation. This mechanism of TFEB activation was shown to be independent of mTORC1 inactivation [125]. In contrast, treatment with pterostilbene, a plant-derived phenol, causes increased levels of ROS and stimulates TFEB nuclear translocation, downstream of mTORC1 inhibition. Interestingly, this paper also investigated the simultaneous convergence of other TFEB regulatory aspects, such as AMPK signaling and release of cytosolic calcium, both of which also contribute to TFEB activation [124]. This concept is likely true for many ROS-inducing compounds. It is logical to suggest that ROS may modulate TFE3/TFEB by engaging various signaling cascades depending on stimuli, cell type and disease state, and this is further supported by various studies reporting ROS-mediated regulation of TFE3/TFEB by AMPK [126], PI3K/AKT/mTOR [127], caspase 3 [128], mTORC1 inhibition [126] or lack thereof [125], and other additional mechanisms.

The complex nature of oxidative stress induced TFE3/TFEB activation can also be seen in the downstream effects exerted by TFE3/TFEB. This can be illustrated by comparing two independent studies, both of which investigate ROS-induced TFEB activation in osteosarcoma models. The first study demonstrates that oxidative stress induced by treatment with arsenic trioxide (As_2O_3) engages TFEB through dephosphorylation of S142, upregulating the expression

of an autophagy gene signature, thereby resulting in osteosarcoma cell death [129]. On the other hand, inhibition of ERK was shown to elevate ROS levels by suppressing glutathione production, which in turn abolishes TFEB-14-3-3 binding and shuttles TFEB to the nucleus. The authors showed that co-treatment with an ERK plus an autophagy inhibitor had a synergistic effect on tumour cell death in osteosarcoma, suggesting that osteosarcoma cells in this scenario rely on TFEB-dependent autophagy for survival [130]. The conflicting results generated by these studies, though not experimentally validated in either paper, could be due in part to the mechanism of TFEB activation. Neither study extensively investigated the upstream factors (phosphatases, kinases) involved in promoting the nuclear accumulation of TFEB. The difference in effect could also be due to the stimulus used in each study, and the source of ROS the various treatments utilized. Sources of ROS and their potential impact on biological processes will be discussed later in this review. Regardless, these studies reflect the duality of autophagy and the complexity of ROS signaling in biological pathways.

The effect of ROS on TFE3 has also been characterized in several reports, such as ROS-TFE3-dependent induction of autophagy in melanoma [131] and breast cancer [132] models. It has become increasingly clear that in many cellular environments or in response to certain stressors, individual members of the MiTF/TFE family are specifically activated. However, due to the partial redundancy of TFE3/TFEB, and the high degree of conservation in terms of structural domains and critical regulatory residues, it is plausible that the effect of ROS on TFEB is similar to the effects on TFE3. This is exemplified by the observation that $NaAsO_2$ treatment causes dephosphorylation of both TFE3 and TFEB on their conserved serine residues by PP2A [122]. Furthermore, in human embryonic kidney 293 (HEK293) cells stimulated with hydrogen peroxide (H_2O_2), TFEB/TFE3 and MiTF were shown to rapidly translocate to the nucleus following oxidative stress due to cysteine residue oxidation. The specific residue was identified as cysteine 212 in TFEB, corresponding to cysteine 322 in TFE3, the mutation of which rendered both transcription factors cytosolic. Oxidation of these residues by H_2O_2 was demonstrated to inhibit interaction with the active Rag GTPases, thus promoting nuclear accumulation [133]. This finding was especially intriguing as it provided further evidence of shared regulation of TFE3/TFEB by ROS, but also demonstrated that ROS can have a direct effect on these transcription factors through modification of critical residues, rather than indirectly activating an upstream regulator element. In summary, the engagement of TFE3/TFEB in response to

oxidative stress involves a plethora of mechanisms that mediate TFE3/TFEB-dependent effects on autophagy and lysosomal biogenesis.

1.4 Implications for Oxidative Stress and the Redox Protein p66ShcA in TNBC

1.4.1 Reactive Oxygen Species Overview

As mentioned, ROS are unstable molecular intermediates of reduced oxygen. The proper management of cellular ROS is critical for the prevention of ROS-induced damage, and when the levels of ROS and antioxidants are out of balance, oxidative stress occurs. During oxidative stress elevated levels of ROS can result in mutation and damage to DNA, RNA, proteins and lipids, which can contribute to the progression of various diseases, including cancer [134]. Within cells, the majority of ROS are produced in the mitochondrial electron transport chain (ETC) as a biproduct of cellular respiration. The ETC is located in the inner mitochondrial membrane and primarily generates O_2^- at complexes I and III through electron leakage; however, ROS can also be produced at other sites of the ETC [135]. The generation of ROS through the Fenton reaction [136], in which iron reacts with H_2O_2, has also been reported [123, 137]. ROS formation can also occur through enzymatic sources such as xanthine oxidases, lipoxygenases, nitric oxide synthase, cyclooxygenases, thymidine phosphorylase, and most notably, nicotinamide adenine dinucleotide phosphate (NADPH) oxidases (NOX enzymes) [138-139]. NOX is a family of seven structurally homologous isoforms known to produce O_2^- and in some instances H_2O_2, that are widely recognized as a major component of cellular ROS production, along with mitochondrial-derived ROS (mtROS) [140]. While expression levels can vary across different cell types and tissues, all NOX enzymes are transmembrane proteins that share a common catalytic core. NOX are largely localized to the plasma membrane, with some expression also observed in intracellular organelles [141]. Mechanistically, ROS are produced in the catalytic core of NOX enzymes upon binding of NADPH, which triggers the sequential transfer of an electron to the inner and outer heme groups within the transmembrane portion of these proteins. This electron is then transferred to oxygen to produce NOX-derived ROS (noxROS) [141]. ROS production can also be stimulated by exogenous stimuli, such as exposure to ultraviolet (UV) light, alcohol, drugs, smoke, pollutants and certain foods [142]. Studying ROS and their effects can be complex, as ROS are incredibly dynamic and can be derived from multiple sources, with many types of ROS simultaneously contributing to the same downstream

cellular responses. Some stimuli can also promote ROS production from more than one intracellular source [123, 134-143]. ROS derived from one intracellular source may also drive the production of ROS from another. Such crosstalk has been described previously in the case of mtROS stimulating noxROS and vice versa [143]. However, ROS from one source can also drive signaling and biological processes independently of others. In pericytes, increased glucose was shown to stimulate noxROS and promote apoptosis, whereas mtROS generated under the same cellular context had no effect [144]. Conversely, in pancreatic β-cells, palmitate treatment has been shown to induce cell death, with the bulk of this effect being attributed to increases in mtROS [145]. Therefore, it is important to consider not only the effects of oxidative stress, but also the intracellular source of ROS that is driving the observed phenotypes.

The traditional view of ROS has been that these highly reactive molecules are simply waste products of naturally occurring cellular processes. However in recent years, an emerging concept argues that ROS function as secondary messengers in numerous signaling pathways under normal conditions and in disease states. At low concentrations, ROS are undoubtedly important for the induction of signaling and various cellular processes like proliferation, differentiation, regulation of metabolism, homeostasis and adaptation to stress; however, at toxic levels they can lead to the induction of cell death pathways [123,134, 138-139, 146]. This dichotomy is also present within the tumour microenvironment, and thus ROS, as well as their specific intracellular sources, are an active area of research to leverage for therapeutics.

1.4.2 Oxidative Stress and Cancer

The role of ROS in cancer is multi-faceted. The accumulation of DNA damage by ROS can contribute to genomic instability, which inherently drives tumour initiation [147]. However, tolerable levels of ROS in tumour cells can activate signaling cascades that promote tumour cell survival and the progression of cancer. One mechanism that is well characterized is the ROS-dependent stabilization of HIF1α. ROS levels increase during hypoxia, which stabilizes HIF1α and promotes HIF1α-dependent gene transcription [148]. HIF1α, which is expressed in numerous cancers, subsequently promotes tumour progression by stimulating angiogenesis and metabolic adaptation to hypoxia [149]. ROS can also promote tumour cell growth and proliferation by regulating PI3K/AKT/mTOR and ERK signaling pathways [146]. ROS can inactivate phosphatases implicated in the control of ERK signaling, the dysregulation of which

results in sustained activation and unchecked proliferation of tumour cells [150]. ROS can also inactivate phosphatases such as PTEN [151] and PP2A [152], both of which are responsible for modulating PI3K/AKT activity, resulting in AKT activation and subsequent cancer cell proliferation and growth. ROS may further promote survival of tumour cells by enhancing processes discussed previously in this review, such as autophagy [130] and suppression of the immune system [139]. ROS can also regulate the progression of metastasis. For example, ROS have been shown to regulate the activity of several genes known to be important for induction of EMT, including MMPs [153], Snail [154] and the Smad pathway [155]. Additionally, transforming growth factor beta (TGFβ) is widely known as a highly potent inducer of EMT, and exhibits a reciprocal regulatory relationship with ROS, in turn promoting metastatic phenotypes [156]. It has also been suggested that ROS may indirectly contribute to chemoresistance, as the modulation of growth and survival pathways, metabolism, and modification of cancer stem cells may produce a sub-population of highly adaptive tumour cells that are unresponsive to therapy [157].

Conversely, supra-physiological levels of ROS can initiate cell death pathways such as apoptosis, necroptosis and ferroptosis, and as such a harsh pro-oxidative environment may promote tumour cell death [158]. There is also evidence that ROS may have the capacity to be tumour suppressive by inducing cellular senescence, thereby preventing malignant transformation and proliferation [159].

It has been established in several studies that tumour cells exhibit higher levels of ROS than non-cancerous cells. Some of the earliest evidence of this came over three decades ago in a study reporting elevated levels of H_2O_2 in several different cell models of cancer [160]. Interestingly, to combat excessive accumulation of ROS, cancer cells can leverage existing antioxidant systems to detoxify ROS and maintain concentrations at a level conducive to survival [123]. For instance, the antioxidant response is largely regulated by the transcription factor nuclear factor erythroid 2-related factor 2 (NRF2; also known as NFE2L2/NFE2), which when activated attenuates intracellular ROS production [161]. One important study characterized the upregulation of NRF2 due to common oncogenic mutations, such as KRas, BRaf and Myc mutations in murine models and human pancreatic cancer. Genetic mutations in NRF2 were demonstrated to impair KRas-dependent tumour growth, suggesting that the activation of NRF2 and detoxification of ROS in cancer cells is a critical aspect of tumorigenesis [162].

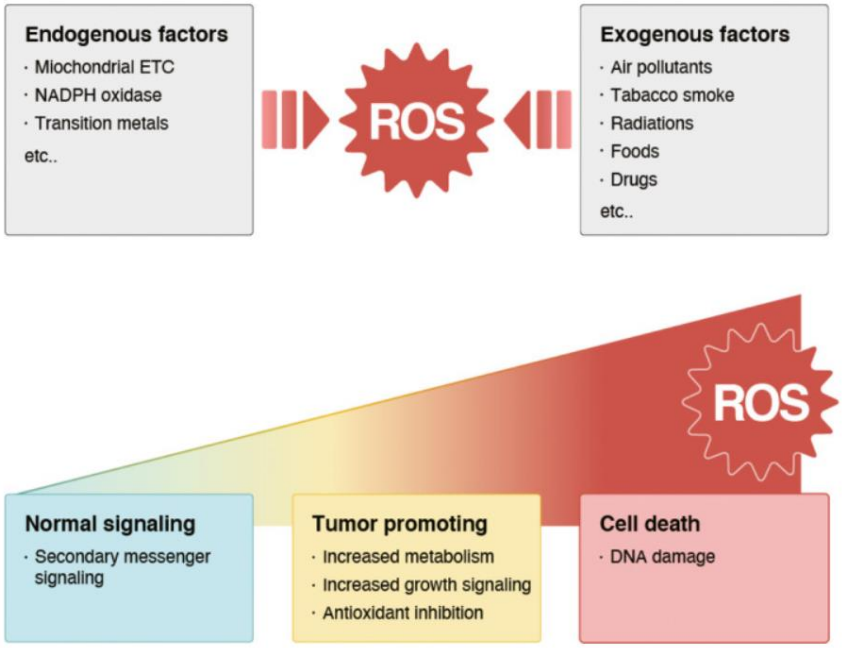

Figure 1.3 Sources of ROS and Dual Role in Cancer Progression. ROS can be produced from various sources endogenously, primarily from the mitochondrial ETC and NADPH oxidases, and in response to exogenous stimuli. ROS function in normal cellular signaling and based on cellular concentrations can promote cancer progression through oncogenic signaling or tumour cell death during excessive oxidative stress. Figure adapted from Nakamura and Takada, 2021 [123].

ROS as a Therapeutic Target in Cancer

Since the levels of ROS govern cell fate and signaling in cancer cells, modulating the concentration of ROS in tumours represents in intriguing therapeutic target. As such, antioxidants may help alleviate ROS-induced tumorigenesis and many antioxidant chemicals or naturally occurring vitamins have been used in studies reporting anti-tumour effects [158, 162-164]. However, the efficacy of antioxidants in cancer remains controversial, as anti-tumour effects may be seen in scenarios in which cancer cells utilize ROS to promote survival and growth, but treatment with antioxidants may also reduce the levels of ROS in established malignant cells, aiding in the survival of tumour cells during oxidative stress. Therefore, pro-oxidative therapies are also a potential therapeutic option for cancer management. Pro-oxidant chemicals that directly induce ROS and/or inhibit antioxidant systems like glutathione are being evaluated in clinical trials both as single agents and in combination with other therapies [158]. For example, the ROS-inducing compound metformin is being investigated in clinical trials with

immunotherapies, anthracyclines, and other standard of care chemotherapies in several cancers, including breast cancer [139].

TNBC may represent a cancer type that is particularly susceptible to ROS-inducing therapies. TNBC displays a high level of intrinsic genome instability, especially in BRCA1/2 mutant cases [14]. This inherit instability could be exploited in TNBC if treated with pro-oxidant agents, as the added accumulation of mutations could push tumour cells towards cell death pathways, particularly if DNA-repair pathways are ineffective. TNBC cell models have also been demonstrated to exhibit much higher levels of baseline ROS production in comparison to luminal breast cancers and non-cancerous tissues [165]. Though this may present an opportunity for antioxidant therapy-mediated inhibition of cellular processes needed for cancer cells to survive in TNBC, enhancing ROS production in the already stressful baseline oxidative environment may more effectively promote tumour cell death in TNBC/BLBC.

1.4.3 p66ShcA Overview

One protein that is critical in the formation of intracellular ROS is the redox adaptor protein p66ShcA. The Src homology 2 domain-containing protein A (ShcA) gene encodes three different isoforms: p46ShcA, p52ShcA and p66ShcA [166-168]. Of these, p46/p52ShcA are expressed ubiquitously and arise from alternative translational start sites, whereas p66ShcA displays variable expression and is regulated by a different promoter [169-170]. All ShcA isoforms share a common structure with an N-terminal phosphotyrosine binding (PTB) domain, a central proline-rich collagen homology (CH) 1 domain, and an N-terminal Src homology 2 (SH2) domain, with p66ShcA containing an additional N-terminal CH2 domain [169-171]. The significance of the CH2 domain in executing the biological redox functions of p66ShcA will be discussed in a future section. Within the CH1 domain, ShcA proteins contain phosphorylation sites on three specific tyrosine (Y) residues, Y239/240/317, that transmit intracellular signals downstream of receptor tyrosine kinases (RTKs) through activation of Ras/MAPK, EGFR, and PI3K/AKT/mTOR [167-175]. However, these cellular signaling nodes are not transmitted by p66ShcA, as the CH2 domain exerts inhibitory effects on transduction of Ras/MAPK mitogenic signaling sequestering by growth factor receptor-bound protein 2 (GRB2)/son of sevenless (SOS) from the other ShcA isoforms [169, 176]. Knockout of the ShcA gene in mice is embryonic lethal [177]; however, specific deletion of p66ShcA results in extended lifespan, as

well as resistance to oxidative stress and apoptosis [178]. This is due to the pro-apoptotic functions of p66ShcA [176], as well as its contribution to the formation of endogenous and stress-induced ROS, which are known to be important contributors to the ageing process [178]. The concept of p66ShcA inhibition offering protection from oxidative stress has been reported in various models of disease beyond cancer, including cardiac diseases [179-180], metabolic conditions like diabetes and obesity [181-182], neuroprotective effects in neurons [183] and multiple sclerosis [184], as well as renal injury [181,185] and alcohol-induce liver damage [186], among others. As such, the p66ShcA-dependent production of ROS has a profound impact on the progression of overall lifespan and a myriad of diseases.

1.4.4 Mechanism of mtROS Production by p66ShcA

The role of p66ShcA as a redox protein and the mechanism through which p66ShcA produces mtROS have been extensively characterized. Under basal conditions, significant pools of p66ShcA exist in the cytosol and mitochondria. The mitochondrial pool is bound by a complex containing heat shock protein (HSP) 70 [187] and the translocase of the inner mitochondrial membrane (TIM) proteins (TIM20/23/44) [188], which inhibits the pro-apoptotic functions of p66ShcA. The N-terminal CH2 domain unique to p66ShcA is essential for its ROS producing capabilities as it contains key residues that facilitate its mitochondrial localization and mechanism of action once in the mitochondria [178, 188-195]. Specifically, phosphorylation of the S36 residue is critical for trafficking of p66ShcA to the mitochondria and its redox function [178, 188-195]. S36 phosphorylation can be triggered by diverse stimuli, particularly those that induce apoptosis, such as cell detachment, hypoxia, exposure to UV irradiation and chemotherapy [189-190]. Arguably the best characterized trigger for p66ShcA mitochondrial localization is the induction of oxidative stress by H_2O_2. In response to oxidative stress, p66ShcA dissociates from peroxiredoxin 1 (PRX1) [191] and is phosphorylated on S36 by stress kinases such as c-Jun N-terminal kinase (JNK) [192], PKCβ [193], ERK [194] and MAPK-activated protein kinase 2 [195]. Phosphorylation of S36 within p66ShcA results in isomerization of the protein by the prolyl isomerase PIN1 [193]. Following subsequent dephosphorylation of S36 by PP2A, p66ShcA is then imported into the mitochondria [189, 195] increasing the existing mitochondrial p66ShcA fraction. The endogenous mitochondrial p66ShcA pool may also become activated in response to ROS-inducing or pro-apoptotic stressors, as treatment with such

stressors results in destabilization of the p66ShcA-HSP70-TIM20/23/44 complex [188]. Thus, oxidative stimuli create a biologically active pool of mitochondrial p66ShcA that can exert its redox function.

Within the ETC, cytochrome c serves as an intermediate in the shuttling of electrons between complex III and IV [196]. By binding to and oxidizing reduced cytochrome c, p66ShcA diverts electrons away from the ETC, transferring electrons onto free O_2, resulting in the production of ROS (H_2O_2). ROS generation is necessary for p66ShcA-mediated induction of mitochondrial apoptosis, strengthening the notion that the pro-apoptotic role of p66ShcA is attributed to its redox function. Also in the CH2 domain, a specific cytochrome c binding region within p66ShcA was identified proximal to the PTB domain. Glutamic acids 132/133 (EE132/133) were demonstrated to be critical for mediating downstream redox functions, as mutating these residues to glutamine (Q) in p66ShcA abrogated binding to cytochrome c, impaired ROS production, and inhibited apoptosis [188].

Collectively, the numerous studies into p66ShcA functions have revealed that this adaptor is a critical redox protein, which enables cellular adaptation to a wide variety of stressors, including oxidative stress. Key residues within the CH2 domain have also been determined to be essential for p66ShcA-mediated ROS production: S36, the phosphorylation of which is required for translocation of p66ShcA to the mitochondria, and EE132/133 which constitute the redox center and cytochrome c binding site. These residues are thus indispensable to generate mtROS.

A

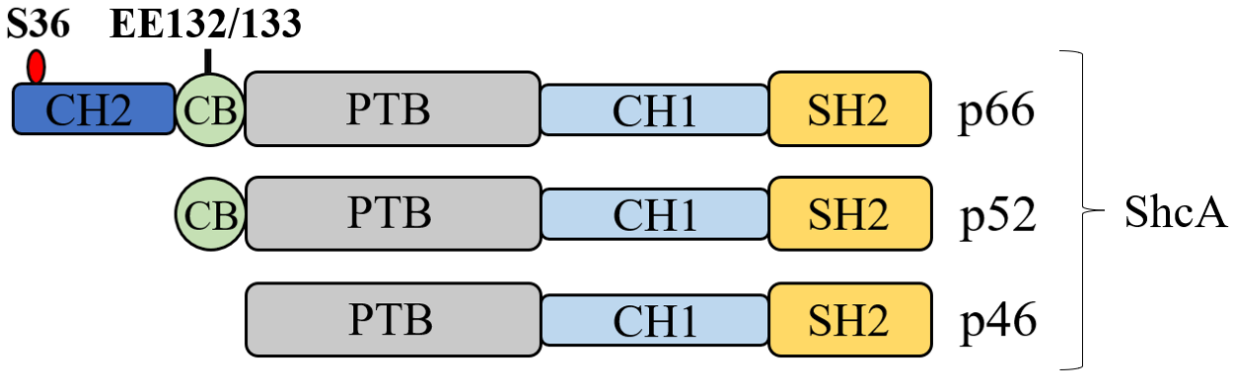

B

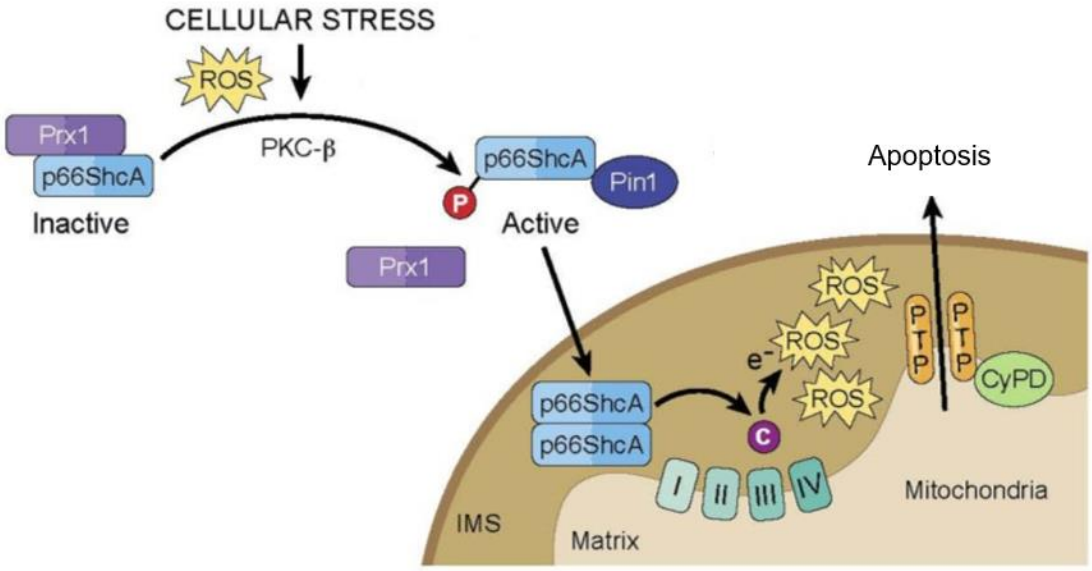

Figure 1.4 p66ShcA Structural Organization and Mechanism of mtROS Production. (**A**) Schematic depiction of ShcA isoform architecture. All isoforms share a N-terminal PTB domain and a C-terminal SH2 domain with a central CH1 domain. p66ShcA contains an additional N-terminal CH2 domain and residues crucial for its ROS-generating function **(in bold).** (**B**) In response to stress stimuli p66ShcA is phosphorylated on **S36** by stress kinases and is localized to the mitochondria after Pin1-mediated isomerization. Mitochondrial p66ShcA binds to cytochrome c through its cytochrome c binding domain, **EE132/133**, and facilitates electron transfer onto oxygen, producing ROS. ROS generated by p66ShcA mediates p66ShcA's pro-apoptotic role. Figure adapted from Su, Bourdette, and Forte, 2013 [206].

1.4.5 p66ShcA in TNBC and Metastasis

Anti-Tumorigenic Functions of p66ShcA

p66ShcA has been widely studied in several models of cancer, revealing contrasting effects on tumour progression that can be attributed to cancer type and context. This is entirely consistent with the role of p66ShcA as a redox protein, since ROS can exert both pro- and anti-tumorigenic functions depending on ROS levels. For example, high p66ShcA expression in lung cancer reduces metastasis and correlates with improved clinical outcome [197-198]. p66ShcA can also inhibit oncogenic EMT by acting in a negative feedback loop with the mesenchymal transcription factor zinc-finger E-box-binding homeobox 1 (ZEB1) [199], as well as by suppressing Ras signaling typically activated by the other ShcA isoforms [198]. Additionally, p66ShcA can promote anoikis (a form of cell death stemming from cell detachment from the ECM) [200] through Ras homolog family member A (RhoA) and focal adhesion targeting, resulting in further suppression of EMT [198, 201]. p66ShcA has also been proposed to promote autophagy and apoptosis under nutrient deprivation, with p66ShcA expression resulting in apoptotic cell death of lung cancer cells [202]. Another study also reported a pro-apoptotic role for p66ShcA in melanoma cell death [203] and a model of TNBC in response to sulforaphane [204]. Phosphorylation of a CH1 domain tyrosine residue in the ShcA proteins, combined with low expression of p66ShcA was also shown to predict stage, nodal status, and relapse of breast cancer patients [205].

Pro-Tumorigenic Functions of p66ShcA

Despite evidence for anti-tumorigenic functions of p66ShcA, a prominent body of work exists supporting pro-tumorigenic properties of p66ShcA in numerous cancers. The acquisition of phenotypes that promote tumour growth and metastasis, particularly proliferation and cell migration and invasion (EMT) have been previously characterized, with high expression of p66ShcA reported in esophageal cancer [207], gastric/colorectal cancers [208], ovarian cancer [209], thyroid cancer [210] and hormone sensitive cancers such as prostate, testicular and luminal breast [211]. Of particular interest to this project are reports that p66ShcA is enriched in TNBC/BLBC relative to other subtypes [212] and within breast cancer cell lines or primary tumours that display elevated propensity to metastasize [213]. Interestingly, both studies implicate p66ShcA in basal-like/metastatic breast cancer progression independently of

p46/p52ShcA expression, providing some of the earliest evidence that the p66ShcA isoform may be especially important in TNBC metastasis.

Several p66ShcA-dependent pro-tumorigenic and metastatic mechanisms have been described in the context of breast cancer. The contribution of p66ShcA in the development of migratory phenotypes has been particularly well studied. In the same study reporting high p66ShcA expression in TNBC/BLBC, p66ShcA was demonstrated to cooperate with Met signaling to induce an EMT in luminal models. An EMT signature was consistent across all breast cancer subtypes, suggesting that in luminal tumours, p66ShcA can increase tumour plasticity through induction of EMT, and in TNBC/BLBC tumours can drive the already plastic cancer cells into a full mesenchymal state [212]. Similarly, p66ShcA has been shown to modulate the activity ADP-ribosylation factor 6 (ARF6) by recruiting ARF6 to the EGFR, resulting in potentiation of ARF6/Ras/MAPK signaling and breast cancer cell growth and migration [214]. p66ShcA-dependent activation of the Rho family small GTPase Rac1, known to control cytoskeletal organization, has also been demonstrated to facilitate ROS production, wound healing, and migration of breast cancer cells [215]. Pro-proliferative effects of p66ShcA also contribute to breast cancer progression, as independent studies have reported enhanced proliferation in p66ShcA-expressing cells, spanning luminal [211], HER2+ [213] and TNBC [190] subtypes. A unique p66ShcA-dependent mechanism involving self-renewal and survival under hypoxia has also been described regarding breast cancer progression. In response to hypoxia, p66ShcA expression is induced and modulates the expression of Notch 3. p66ShcA and Notch 3 then cooperate to promote the expression of Jagged 1 and carbonic anhydrase, a hypoxia-survival gene, downstream of activated ERK. The p66ShcA/Notch 3/Jagged 1/carbonic anhydrase signaling cascade then promotes the survival of *in vitro* mammospheres under hypoxic stress and enhances self-renewal of both normal and cancerous tissues [216].

As mentioned, p66ShcA exists in distinct subcellular pools, with a significant fraction present in the mitochondria [187]. Interestingly, a recent study conducted by members of our lab and the Ursini-Siegel lab reported a complex collaboration between mitochondrial and cytosolic p66ShcA in the context of TNBC lung metastasis. By utilizing a non-phosphorylatable p66ShcA mutant in which S36 is mutated to alanine (SA), thus inhibiting translocation of p66ShcA to the mitochondria, the contribution of mitochondrial and cytosolic p66ShcA to metastasis was examined. Interestingly, wild type (WT) p66ShcA and p66ShcA SA were both shown to

promote primary tumour growth, suggesting that mitochondrial p66ShcA pools are not required for tumour proliferation in the primary site (breast) [190]. Cytosolic p66ShcA was also shown to contribute to various stages of the metastatic cascade. Both p66ShcA WT and p66ShcA SA modulated adhesion dynamics such as adhesion size and disassembly rate, and increased activation of Src family kinase signaling to promote cell migration and invasion [190]. Additionally, both forms of p66ShcA demonstrated comparable effects on the potentiation of metastasis through increased Akt/mTOR signaling, extravasation, and survival and proliferation of cancer cells in the metastatic site (lung). However, in mice injected with cells harbouring p66ShcA SA mutation, the ability to form spontaneous metastases in the lung was drastically reduced. This implies that mitochondrial p66ShcA is required at a specific stage of the metastatic cascade. It was ultimately determined that mitochondrial p66ShcA is necessary for survival in the blood stream after invasion, as mice injected with p66ShcA SA cells exhibited lower levels of CTCs in the blood, and in culture p66ShcA SA cells could not promote cell survival following detachment from the ECM [190]. Collectively, the results of this study indicate that many of the pro-tumorigenic functions of p66ShcA in the context of TNBC lung metastasis are independent of mitochondrial p66ShcA. This study illustrates that the function of p66ShcA in cancer, as in normal physiology or other disease states, is very complex and often dependent on stress stimuli and context. The obvious contribution of p66ShcA to TNBC metastasis reported in this study and others constitutes an interesting avenue to pursue for prognostic and therapeutic value. Thus, detailed interrogation of cytosolic and mitochondrial p66ShcA-dependent mechanisms may reveal unique approaches for TNBC management.

1.5 Project Rationale and Objectives

TNBC/BLBC represents the most aggressive breast cancer subtype, with an increased propensity for metastasis and poor overall prognosis [31, 32]. TNBC lacks viable molecular features that can be exploited therapeutically; thus, surgery in conjunction with chemotherapy remains the standard of care for TNBC [33]. As such, investigation into specific targets for TNBC management is essential. Our lab has previously described identified GPNMB as a mediator of metastatic phenotypes such as invasion, migration, and proliferation, with specific enrichment in a subset of TNBC patients [72-75]. Due to GPNMB's intracellular localization in normal cells and increased expression at the cell surface in tumour cells, GPNMB represents an

attractive therapeutic target. As such, the ADC CDX-011 targeting GPNMB was generated and assessed in clinical trials. Although initial experimental and clinical results were promising, clinical trials were halted in 2018 due to lack of improved survival in TNBC patients [84]. Currently, interest has been drawn to investigation of pathways and combinatorial treatment strategies to enhance the efficacy of CDX-011 [85-86].

GPNMB expression is upregulated in response to a variety of cellular stressors, including oxidative stress [86]. Like GPNMB, p66ShcA is highly expressed in models of TNBC [212], as well as primary tumours with high metastatic potential [213]. This is intriguing when one considers that TNBC exhibits particular high levels of baseline ROS production [165], and p66ShcA has been extensively described as a redox protein with the capability to produce mtROS [178, 188]. Furthermore, GPNMB and p66ShcA can both be considered stress response genes, with biological functions that contribute to cellular stress adaptation. In the case of GPNMB, this may be due in large part to its regulation by the transcription factors TFE3/TFEB. Interestingly, TFE3/TFEB activation in response to oxidative stress has been reported in several publications [122, 125-133], implying that GPNMB may be induced in response to ROS.

Based on these observations, I have explored the hypothesis that p66ShcA regulates GPNMB expression in TFE3/TFEB-dependent manner in response to oxidative stress in TNBC/BLBC. To address this hypothesis, I pursued two main objectives. The first was to determine if p66ShcA is required for GPNMB upregulation in response to oxidative stress. The second was to investigate the regulation of TFE3/TFEB by p66ShcA. Insights into the mechanism of p66ShcA-dependent GPNMB upregulation following oxidative damage may reveal novel approaches/combinatorial strategies to improve the efficacy of CDX-011 in TNBC.

Chapter 2: Materials and Methods

Cell Culture

Hs578T, 4T1, HCC1937, HCC1954, MDA-MB-231, MDA-MB-436, BT20, and MCF7 breast cancer cell lines were obtained from the American Type Culture Collection (Manassas, VA, USA). Hs578T, MDA-MB-231, MDA-MB-436, BT20 and MCF7 cells were cultured in Dulbecco's Modified Eagle Medium (DMEM; cat. no. 319-005-CL, Wisent Bioproducts) supplemented with 10% fetal bovine serum (FBS; cat. no. 10082-147, ThermoFisher Scientific) and 1% penicillin-streptomycin (cat. no. 450-201-EL, Wisent Bioproducts). HCC1937 and HCC1954 cells were cultured in Roswell Park Institute Media (RPMI; cat. no. 350-000-CL, Wisent Bioproducts) supplemented with 10% FBS and 1% penicillin-streptomycin.

The isolation of 4T1-derived explants from primary tumour (152), lung-aggressive (537), bone-aggressive (592), and liver-aggressive (2776) populations have been described previously [72-74]. Parental 4T1 and all 4T1-derived cells were cultured in DMEM supplemented with 10% FBS, 1.5g/L sodium bicarbonate (cat. no. 609-105-EL, Wisent Bioproducts), 10mM HEPES (cat. no. 330-050-EL, Wisent Bioproducts), 1mM sodium pyruvate (cat. no. 600-110-EL, Wisent Bioproducts), and 1% penicillin-streptomycin.

The breast cancer cell lines (Hs578T, 4T1-537) harboring a p66ShcA KO and those engineered to express the various p66ShcA isogenic forms generated as described previously [190, 217]. Briefly, p66ShcA was deleted from the genome of parental Hs578T and 4T1-537 cells and engineered to re-express empty vector (KO), C-terminally tagged p66ShcA WT, p66ShcA QQ and p66ShcA SA-harbouring pMSCV/puromycin vectors (cat. no. 68469, Clontech).

p66ShcA VC and p66ShcA WT expression in parental HCC1954 and MCF7 cells was conducted in the same fashion without prior deletion of p66ShcA, due to low endogenous p66ShcA expression. HCC1954 cells were infected with empty vector (VC) and C-terminally tagged p66ShcA WT pMSCV/puromycin vectors, while MCF7 cells were infected with doxycycline-inducible empty vector (VC) and C-terminally tagged p66ShcA WT pCW57-MCS1-P2A-MCS2/hygromycin vectors (cat. no. 80922, Addgene).

Hs578T-BirA expressing cells were also generated according to the same protocol. Hs578T cells were infected with BirA control, p52ShcA-BirA orp66ShcA-BirA pQCXIB/blasticidin vectors (cat. no. 22800). Fusion proteins are C-terminally tagged on BirA and N-terminally tagged on p52/p66ShcA.

All cells were selected and maintained in 2µg/mL puromycin (cat. no. ant-pr-1, Invivogen), except the MCF7 and Hs578T-BirA expressing cells which were selected and maintained in 100µg/mL hygromycin (cat. no. 450-141-XL, Wisent Bioproducts) and 10µg/mL blasticidin (cat. no. ant-bl-1, Invivogen), respectively.

Treatment Conditions

The indicated breast cancer cell models were treated with actinomycin D (cat. no. A1410, Sigma-Aldrich), doxorubicin (cat. no. S1208, Selleckchem), oligomycin A (cat. no. S1478, Selleckchem), phenformin (cat. no. P7045, Sigma-Aldrich), H_2O_2 (cat. no. H1009, Sigma-Aldrich) or sodium arsenite ($NaAsO_2$; cat. no. S7400, Sigma-Aldrich) for the indicated time points. Where specified, cells were pre-treated for 24h with indicated doses of N-Acetyl-L-cysteine (cat. no. A9165, Sigma-Aldrich) or apocynin (cat. no. 178385, Sigma-Aldrich).

Immunoblot Analysis

At experimental end points, breast cancer cells were lysed in cold TNE lysis buffer, collected in tubes, and rotated for 10 min at 4°C. Lysates were centrifuged at max speed for 10 min at 4°C, supernatants collected, and protein concentrations measured using the Pierce bicinchoninic acid (BCA) protein assay (cat. no. 23227, Thermo Fisher). Total protein (40-50ug) was loaded onto 7.5% acrylamide gels and transferred onto polyvinylidene difluoride (PVDF) membranes (cat. no. IPVH00010, Millipore). Membranes were blocked in 5% bovine-serum albumin (BSA) or 5% fat-free milk for 1h and incubated overnight at 4°C with primary antibodies. Human breast cancer cell lines were incubated with the following antibodies: GPNMB XP (1:1000; cat. no. 38313, Cell Signaling), ShcA (1:2000; cat. no. 610082, BD Transduction Laboratories), TFE3 (1:1000; cat. no. 14779, Cell Signaling), TFEB (1:1000; cat. no. 37785, Cell Signaling) and α-tubulin (1:25,000; cat. no. T9026, Sigma-Aldrich). 4T1 murine beast cancer cell lines were incubated with the same antibodies, except for mouse GPNMB (1:1000; cat. no. ab188222, Abcam) and mouse TFEB (cat. no. A303-673A, Bethyl Laboratories). Corresponding horseradish peroxidase–conjugated secondary antibodies (1:10,000; Jackson Immuno Research Laboratories) were added to membranes for 1h at room temperature. Membranes were then visualized using the SuperSignal™ West Pico PLUS Chemiluminescent Substrate (cat. no. 34578, Thermo Fisher Scientific).

qRT-PCR Analysis

At experimental end points, breast cancer cells were processed and RNA extracted using the RNeasy Mini Kit (cat. no. 74106, Qiagen) according to manufacturer's protocol. RNA was eluted in RNAse-free water and quantified using the nanodrop instrument (ThermoFisher Scientific). Total RNA (1ug) was subsequently reverse transcribed into cDNA using the high-capacity cDNA reverse transcription kit (cat. no. 4368814, Applied Biosystems) according to manufacturer's instructions. Resulting cDNA was then used as template in a qPCR reaction with the LightCycler® FastStart Universal SYBR Master (Rox) (cat. no. 4913914001, Roche), primers amplifying gene of interest, and the CFX connection real-time PCR detection system (BioRad). Cycling conditions have been described previously [72]. All qRT-PCR targets were normalized to the housekeeping genes *β2M* or *GAPDH* in human and murine cells, respectively. Normalized gene expression levels were generated from Cq values obtained using the CFX Maestro^{TM} Software (BioRad) according to manufacturer's instructions. qRT-PCR primer sequences can be found in table 2.1.

ROS Production Quantification

At experimental end points, breast cancer cells were washed with pre-warmed fluorescence-activated cell sorting (FACS) buffer (1x PBS supplemented with 2% FBS). Cells were then incubated with 2.5µM CM-H_2DCFDA probe (cat. no. C6827, Invitrogen) diluted in FACS buffer for 30 min at 37°C to detect total cellular ROS. Cells were washed once more with FACS buffer, trypsinized, and collected in microcentrifuge tubes. For mtROS detection, cells were first collected by trypsinization and resuspended with 5µM MitoSOX^{TM} (cat. no. M36008, Invitrogen) in complete media. Cells were then incubated for 20 min at 37°C. For both total and mtROS, 500,000 cells were collected and centrifuged at 900 x g for 2 min. Pellets were resuspended in 300uL FACS buffer and analyzed by flow cytometry on a BD Bioscience FACSCantoII cell analyzer. Analysis was conducted using FlowJo 10 software (TreeStar), with cell debris and doublets being excluded in all conditions.

siRNA Transfections

For siRNA experiments, Hs578T and 4T1-537 breast cancer cells were reverse-transfected at the time of seeding with siRNAs targeting TFE3, TFEB, or non-targeting control

using the Lipofectamine™ RNAiMAX Transfection Reagent (cat. no. 13778150, ThermoFisher Scientific) according to manufacturer's instructions. Cells were transfected overnight, and media was changed the following morning. Post-transfection (24h), breast cancer cells were then treated with the indicated dose $NaAsO_2$ for 48h and subsequently processed for immunoblot or qRT-PCR analysis.

siRNAs used in this study were ON-TARGETplus SMARTpool siRNAs purchased from Dharmacon. Non-targeting siRNA (cat. no. D-001810-10-05) was used as a control. Specific targeting siRNAs are as follows: human TFE3 (7030: cat. no. L-00933-00-005) and TFEB (7942: cat. no. L-009798-00-0005). Mouse TFE3 (209446: cat. no. L-054750-00-0005) and TFEB (21425: cat. no. L-050607-02-0005).

Immunofluorescence

For all immunofluorescence studies, breast cancer cells were seeded onto coverslips coated with fibronectin (cat. no. F0895, Sigma-Aldrich) and treated with $NaAsO_2$ for the indicated time (2, 4, 6, 24 or 48h). Cells were subsequently fixed in 3% paraformaldehyde containing 0.1% Triton X-100 for 10 minutes at room temperature. Fixed cells were then rinsed with 100mM glycine in 1X PBS, permeabilized with 0.2% Triton X-100 for 10 minutes at room temperature, rinsed again with PBS, and stained with primary antibodies.

For visualization of TFE3 nuclear localization, primary antibody against TFE3 (1:200) was applied for 1h at room temperature. Rabbit Alexa Fluor™ 555 dye-conjugated secondary antibody (1:500; cat no. A31572, Invitrogen) and 4′,6-diamidino-2-phenylindole (DAPI; 1:10,000; cat. no. D1306, Invitrogen) were then added for 1h at room temperature to visualize TFE3 and nuclei, respectively.

For co-localization analysis of p66ShcA (FLAG) and lysosomes (LAMP1), primary antibodies against FLAG (1:200; cat. no. F1804, Sigma–Aldrich) or LAMP1 XP (1:200; cat. no. 9091, Cell Signaling) were applied overnight at 4°C. Mouse Alexa Fluor™ 488 (1:500; cat. no. A11001, Invitrogen), rabbit Alexa Fluor 555™ (1:500) and DAPI (1:10,000) were then added for 1h at room temperature to visualize p66ShcA, lysosomes, and nuclei, respectively.

For co-localization analysis of biotinylated proteins (streptavidin) and LAMP1, cells were prepared as described for FLAG and LAMP1 co-immunofluorescence experiments with the following adjustments. Approximately 6h prior to fixation, 50µM biotin (cat. no. B4501, Sigma-

Aldrich) was added to all coverslips to facilitate biotinylation. Cells were then processed and stained with LAMP1 as previously described. Streptavidin Alexa Fluor™ 488 (1:500; cat. no. S11223, Invitrogen), rabbit Alexa Fluor 555™ (1:500), and DAPI (1:10,000) were then added for 1h at room temperature to visualize biotinylated proteins, lysosomes, and nuclei, respectively.

In all experiments cells were mounted onto glass coverslips and stored at 4°C until imaging. Images were acquired on a Zeiss Axiovert 1 inverted microscope (TFE3) or a Zeiss LSM710 laser scanning confocal microscope (co-localization) and adjusted for contrast in Fiji.

Quantification of TFE3 nuclear positivity was separated into TFE3 negative, weak, and strong proportions based on mean fluorescence intensity (MFI) values obtained using a home-made macro in Fiji. At least 100 cells were quantified per condition.

BioID Sample Preparation

24h after seeding, Hs578T cells stably expressing BirA or BirA-p52/p66ShcA fusion proteins were treated with either 50μM biotin alone or in combination with 10μM $NaAsO_2$. After 24h treatment cells were harvested, washed with 1X PBS, and collected in microcentrifuge tubes. Cells were then centrifuged for 2 min at 5000 RPM, supernatant was removed, and cell pellets were stored at -80°C.

Cell pellets were then processed for streptavidin pulldown and mass spectrometry. All buffers were made in high pressure liquid chromatography (HPLC) grade water, all pipette tips were non-autoclaved, and all glassware was rinsed two times with HPLC water (no plastic except for Falcon and Eppendorf tubes). All Eppendorf tubes were rinsed three times with 50% acetonitrile in HPLC water and dried using SpeedVac for 30 min. 1.5 mL of fresh radioimmunoprecipitation assay (RIPA) buffer was used to resuspend cells pellets by pipetting up and down and lysates were transferred into 2mL Eppendorf tubes. 250U/μL of benzonase was added to each sample to digest nucleic acids. Samples were sonicated on ice for three cycles, 10 sec ON, 2 sec OFF at 30 % amplitude. Samples were centrifuged for 30 minutes at 12,000 g at 4°C to pellet the cell debris. After optimization, 15μL of Streptavidin Sepharose High Performance (cat. no. GE-17-5113-01, Cytiva) beads were used per sample. Streptavidin beads were washed three times in 1mL of RIPA buffer supplemented with inhibitors with centrifugation at 375g for 1 min at 4°C. After centrifugation, clarified supernatant was transferred into new Eppendorf tubes and 40μL was saved to monitor expression, lysis efficiency

and solubility as an input control. Pre-washed beads were added to the cell lysate and incubate at 4°C with rotation for three hours. Beads were spin down by centrifugation at 375g for 1 min at 4°C, and 40uL was saved as an unbound control. 1mL of RIPA buffer supplemented with inhibitors was added to the beads and transferred into new Eppendorf tubes to remove unwanted material. Beads were washed two times with RIPA buffer at 4°C and three times with fresh 50 mM ammonium bicarbonate. Beads were finally resuspended in 75µL of 50mM ammonium bicarbonate.

Beads tryptic digestion, reduction and alkylation, collection of peptide and mass spectrometry injection were performed by the mass spectrometry platform at the IRCM. Mass spectrometry results were generated in Dr. Jean-Francois Cote's laboratory and normalized to a BirA-control. Results were further analyzed by normalizing the $NaAsO_2$ gene set to untreated samples. The resulting gene list is thus representative of interactions specifically gained in treated conditions. Only genes satisfying a Significance Analysis of INTeractome (SAINT) score ≥ 0.9 and Bayesian False Discovery Rate (BFDR) ≤ 0.02 were included in the dot plot (created using the ProHitz viz website: Lunenfeld-Tanenbaum Research Institute) and exported as Figure 3.10B. The SAINT score, BFDR, and average spectral count (AvgSpec: number of times the gene is detected by mass spectrometry) values were used in ProHitz viz as a semi-quantitative representation of proximal biotinylated proteins.

RIPA Lysis Buffer:

5mL NP40
5mL 10% SDS
25mL 1M Tris-HCl pH 7.4
15mL 5M NaCl
2.5g Sodium Deoxycholate
1mL 0.5M EDTA
Up to 500mL with HPLC Water

Supplement 50mL Aliquot for Daily Use with:

500µL 100mM PMSF
50µL 1M DTT
100µL Protease Inhibitors

Co-Localization Quantification

Quantification of co-localization was conducted in Fiji, with images manually cropped to display individual cells. Lysosomal image noise was reduced by applying a gaussian blur filter in the LAMP1 channel. Automatic thresholding was then performed using Otsu's method to produce a region of interest (ROI) corresponding to LAMP1-positive organelles (lysosomes). To analyze p66ShcA (ant-FLAG) or protein biotinylation (streptavidin) within lysosomes, fluorescent signals were measured using the LAMP1 ROI and the MFI was recorded. A second ROI was manually outlined surrounding the entire cytoplasmic area containing LAMP1-positive structures and used for an additional measurement to serve as background fluorescence signal of p66ShcA or biotinylation in the cytoplasm. Finally, the FLAG or streptavidin MFI measured in lysosomes was subsequently divided by their MFI in the cytoplasm to produce a normalized p66ShcA or biotinylation signal within lysosomes. Each data point represents the normalized MFI of an individual cell in the FLAG or streptavidin channel. At least 30 cells were quantified per condition.

Statistical Analysis

Graphpad Prism 9 Software was used to graph and perform all statistical analysis. Statistical significance (*p* values) was obtained using an unpaired, 2-tailed Student's *t te*st, 1-way ANOVA with Tukey's multiple comparisons test, or Mann-Whitney *U* test as indicated in figure legends. RT-qPCR and flow cytometry data are presented with column height representing the means, whereas mean values are depicted as horizontal bars in the immunofluorescence data. All figures excluding TCGA data are representative of at least three independent experiments and error bars indicate ± SEM. TCGA data are displayed as box and whisker graphs with horizontal bars depicting median values, and box and whiskers representing 25^{th} to 75^{th} percentiles and 5^{th} to 95^{th} percentiles, respectively. Data points plotted on the graphs lie outside the 5^{th} to 95^{th} percentiles.

Table 2.1: List of qRT-PCR Primers

Gene	Species	Forward (5' – 3')	Reverse (5'– 3')
GPNMB	Human	CTTCTGCTTACATGAGGGAGC	CTGGTCACTGAGTGGTCGG
TFE3	Human	CCGTGTTCGTGCTGTTGGA	TAGGACTGTCGAAGATGCTC
TFEB	Human	ACCTGTCCGAGACCTATGGG	CTGTTTGTAATACGCAGACCTGC
LAMP1	Human	ACGTTACAGCGTCCAGCTCAT	TCTTTGGAGCTCGCATTGG
HEXA	Human	CAACCAACACATTCTTCTCCA	CGCTATCGTGACCTGCTTTT
ATP6V1H	Human	GGAAGTGTCAGATGATCCCCA	CCGTTTGCCTCGTGGATAAT
TPP1	Human	CCTCCACACGGTGCAAAAATG	CTCTGCTTGTCGGATGCTCAG
CTSD	Human	AACTGCTGGACATCGCTTGCT	CATTCTTCACGTAGGTGCTGG
β2M	Human	TATCCAGCGTACTCCAAAGA	CACCTCGTAAGTCTGAACA
GPNMB	Mouse	AGCACAACCAATTACGTGGC	CTTCCCAGGAGTCCTTCCA
TFE3	Mouse	TGCGTCAGCAGCTTATGAGG	AGACACGCCAATCACAGAGAT
TFEB	Mouse	CCACCCCAGCCATCAACAC	CAGACAGATACTCCCGAACCT
GAPDH	Mouse	CAAGTATGATGACATCAAGAAGGTGG	GGAAGAGTGGGAGTTGCTGTTG

Chapter 3: Results

3.1 ROS-Inducing Compounds Upregulate GPNMB

Given the existing relationship between GPNMB and cellular adaptation to stress [86], we first investigated whether ROS-inducing compounds increase GPNMB expression. The Hs578T breast cancer (TNBC) cell line was exposed (48h) to a variety of ROS-inducing compounds that can be broadly categorized into chemotherapies (red), mitochondrial inhibitors (red) and general oxidative stressors (green) and GPNMB protein and mRNA levels were assessed. GPNMB expression was upregulated in response to several compounds, with the most robust increases in GPNMB protein and mRNA levels observed following $NaAsO_2$ treatment (Figure 3.1A-B). We next examined the time course of GPNMB induction following oxidative stress. GPNMB proteins levels were clearly evident at 48h post-treatment with 7.5µM $NaAsO_2$, with the appearance of *GPNMB* mRNA beginning as early as 6 hours (Figure 3.1C-D). We thus selected 7.5µM $NaAsO_2$ as our ROS-inducer for subsequent experiments at a fixed treatment time of 48h.

To confirm that $NaAsO_2$ was indeed inducing ROS, we next analyzed total intracellular and mtROS production using the fluorescent probes CM-H_2DCFDA and MitoSOX, respectively. The CM-H_2DCFDA probe diffuses into cells where it undergoes acetate group cleavage and reacts with intracellular thiols through its chloromethyl group. It is then oxidized by various ROS into a fluorescent derivative that can be measured with appropriate excitation as a readout of total cellular ROS [218]. In contrast, the MitoSOX probe is targeted to the mitochondria where it is oxidized by O_2^-, the predominant oxygen radical produced in this organelle [135, 219]. The selective accumulation of MitoSOX is due to its cationic triphenylphosphonium-based modification that promotes uptake into respiring mitochondria, with the final oxidized form acting as a measure of mtROS due to its high fluorescence [219]. As anticipated, analysis of ROS levels by flow cytometry revealed a 2-fold increase in total ROS and a 1.5-fold increase in mtROS in Hs578T cells treated with $NaAsO_2$ when normalized to baseline (untreated) ROS levels (Figure 3.1E-H).

To determine whether the changes observed in GPNMB expression were a result of elevated ROS, we employed the ROS-scavenger N-acetyl cysteine (NAC) to quench cellular ROS prior to and during $NaAsO_2$ treatment. Hs578T breast cancer cells treated with NAC showed attenuated ROS production following $NaAsO_2$ addition (Figure 3.1E-H), concomitant with a reduction of GPNMB protein and mRNA expression to baseline levels (Figure 3.1E-J).

Together, these data suggest that ROS production is required for increased GPNMB expression following oxidative stress and establish treatment conditions for further experimentation.

3.2 TNBC Cell Models with Higher Endogenous p66ShcA Expression Show an Increase in GPNMB Levels in Response to ROS.

GPNMB is most frequently overexpressed and exerts its pro-metastatic functions within the TNBC subtype [72-75]. To extend our results to other TNBC models, we analyzed GPNMB protein and mRNA expression in several human and murine cell lines. Importantly, several of the breast cancer cell lines tested cell revealed elevated GPNMB expression in response to oxidative stress. Human breast cancer cell lines that express higher endogenous levels of p66ShcA exhibited higher baseline levels of GPNMB (BT20, MDA-MB-436) or a greater fold induction of GPNMB (Hs578T) following $NaAsO_2$ treatment when compared to cell lines lacking endogenous p66ShcA (HCC1937, HCC1954) (Figure 3.2A-B). One outlier to this trend is the MDA-MB-231 breast cancer cell line; however, this is consistent with our previous observations that this model exhibits extremely low baseline and stress-induced GPNMB protein expression in response to several cellular stressors and chemotherapies (data not shown).

Similar results were seen in the murine 4T1 cells. Both 4T1 parental and primary explant (152) tumour cells exhibited low basal levels of p66ShcA and GPNMB and were unable to induce the latter's expression in response to elevated ROS. Conversely, 4T1 cells with enhanced metastatic potential to distal organs, namely lung (537), bone (592), and liver (2776) had higher expression of both p66ShcA and GPNMB, and upregulated GPNMB further following exposure to $NaAsO_2$ (Figure 3.2C-D). These findings in both human and murine cells suggest that endogenous p66ShcA promotes GPNMB expression and upregulation in response to oxidative stress.

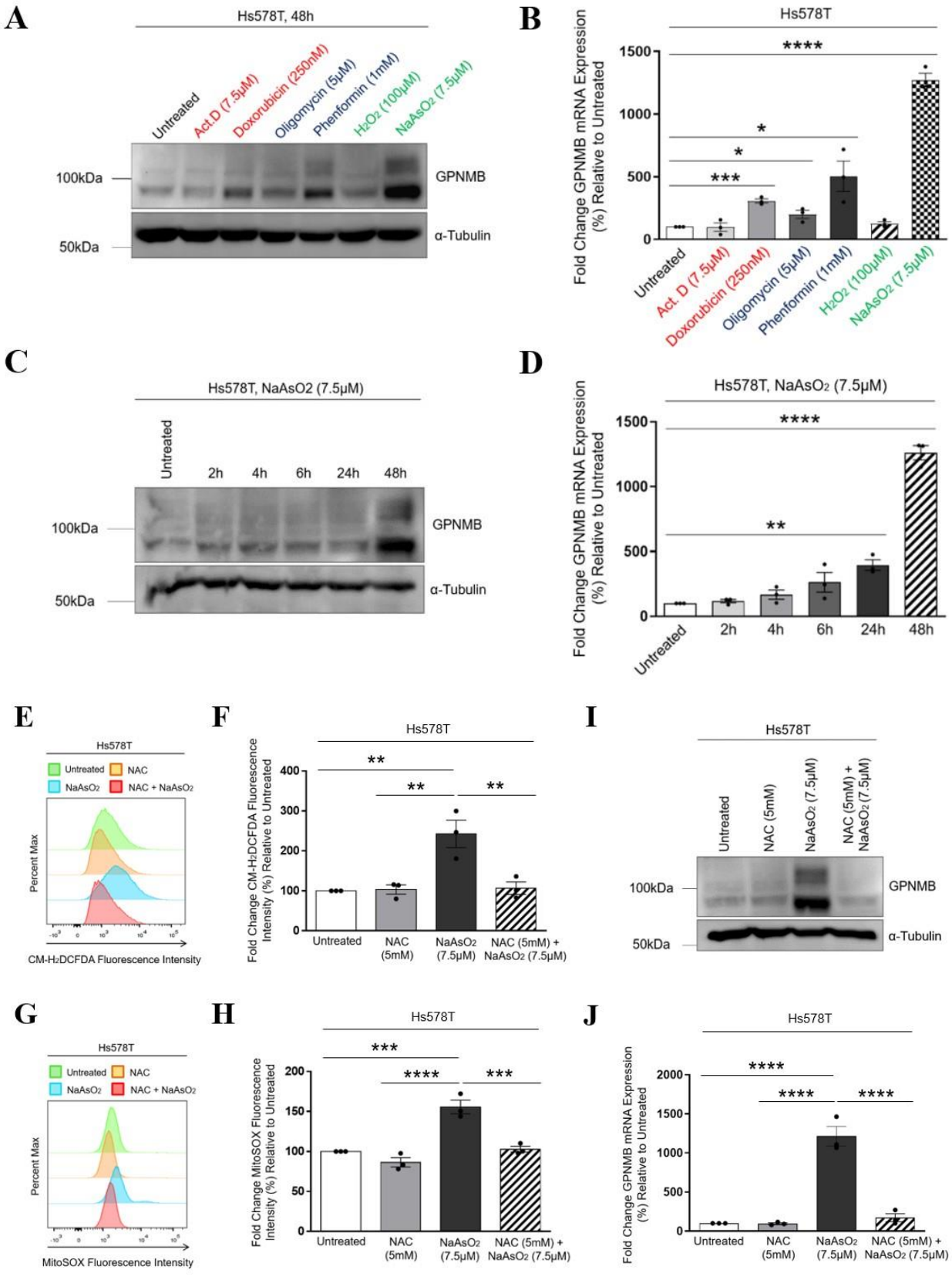
A
Hs578T, 48h
Untreated
Act.D (7.5μM)
Doxorubicin (250nM)
Oligomycin (5μM)
Phenformin (1mM)
H2O2 (100μM)
NaAsO2 (7.5μM)
100kDa
GPNMB
50kDa
α-Tubulin
B
Hs578T
Fold Change GPNMB mRNA Expression (%) Relative to Untreated
1500
1000
500
0
****
*
*
***
Untreated
Act. D (7.5μM)
Doxorubicin (250nM)
Oligomycin (5μM)
Phenformin (1mM)
H2O2 (100μM)
NaAsO2 (7.5μM)
C
Hs578T, NaAsO2 (7.5μM)
Untreated
2h
4h
6h
24h
48h
100kDa
GPNMB
50kDa
α-Tubulin
D
Hs578T, NaAsO2 (7.5μM)
Fold Change GPNMB mRNA Expression (%) Relative to Untreated
1500
1000
500
0
****
**
Untreated
2h
4h
6h
24h
48h
E
Hs578T
Untreated
NAC
NaAsO2
NAC + NaAsO2
Percent Max
CM-H2DCFDA Fluorescence Intensity
F
Hs578T
Fold Change CM-H2DCFDA Fluorescence Intensity (%) Relative to Untreated
400
300
200
100
0
**
**
**
Untreated
NAC (5mM)
NaAsO2 (7.5μM)
NAC (5mM) + NaAsO2 (7.5μM)
I
Hs578T
Untreated
NAC (5mM)
NaAsO2 (7.5μM)
NAC (5mM) + NaAsO2 (7.5μM)
100kDa
GPNMB
50kDa
α-Tubulin
G
Hs578T
Untreated
NAC
NaAsO2
NAC + NaAsO2
Percent Max
MitoSOX Fluorescence Intensity
H
Hs578T
Fold Change MitoSOX Fluorescence Intensity (%) Relative to Untreated
200
150
100
50
0
***
****
***
Untreated
NAC (5mM)
NaAsO2 (7.5μM)
NAC (5mM) + NaAsO2 (7.5μM)
J
Hs578T
Fold Change GPNMB mRNA Expression (%) Relative to Untreated
2000
1500
1000
500
0
****
****
****
Untreated
NAC (5mM)
NaAsO2 (7.5μM)
NAC (5mM) + NaAsO2 (7.5μM)

Figure 3.1. ROS-Inducing Compounds Upregulate GPNMB (**A**) Immunoblot analysis of GPNMB protein expression in Hs578T breast cancer cells cultured in the absence (untreated) or presence of the specified compound/drug for 48h at the indicated dose. α-Tubulin served as a loading control. (**B**) Corresponding RT-qPCR analysis of *GPNMB* mRNA expression. Cells were treated as in (A). Data are presented as fold change mean values ± SEM (n = 3 biological replicates): *, $P < 0.05$; ***, $P < 0.001$; ****, $P < 0.0001$ by unpaired Student's *t* test. (**C**) Immunoblot analysis of GPNMB protein expression in Hs578T cells cultured in the presence of $NaAsO_2$ (7.5μM) for the indicated times. α-Tubulin served as a loading control. (**D**) Corresponding RT-qPCR analysis of *GPNMB* mRNA expression. Cells were treated as in (C). Data are presented as fold change mean values ± SEM (n = 3 biological replicates): **$P < 0.01$; ****, $P < 0.0001$ by unpaired Student's *t* test. Representative histograms (**E**) and quantification (**F**) of total cellular ROS by flow cytometry in Hs578T breast cancer cells. ROS levels were analyzed by CM-H_2DCFDA staining. Data are presented as fold change CM-H_2DCFDA fluorescence (geometric mean) ± SEM (n = 3 biological replicates): **, $P < 0.05$ by 1-way ANOVA with Tukey's multiple comparisons test. Representative histograms (**G**) and quantification (**H**) of mtROS by flow cytometry in Hs578T breast cancer cells. ROS levels were analyzed by MitoSOX staining. Data are presented as fold change MitoSOX fluorescence (geometric mean) ± SEM (n = 3 biological replicates): **, $P < 0.01$ by 1-way ANOVA with Tukey's multiple comparisons test. (**I**) Immunoblot analysis of GPNMB protein expression in Hs578T breast cancer cells. α-Tubulin served as a loading control. (**J**) Corresponding RT-qPCR analysis of *GPNMB* mRNA expression. Data are presented as fold change mean values ± SEM (n = 3 biological replicates): **, $P < 0.01$; ***, $P < 0.001$ by 1-way ANOVA with Tukey's multiple comparisons test. Breast cancer cells in (E-J) were cultured with NAC or $NaAsO_2$, alone or in combination, at the indicated doses. Breast cancer cells were treated with NAC at the time of seeding, followed by the addition of $NaAsO_2$ 24h later and then further cultured for 48h.

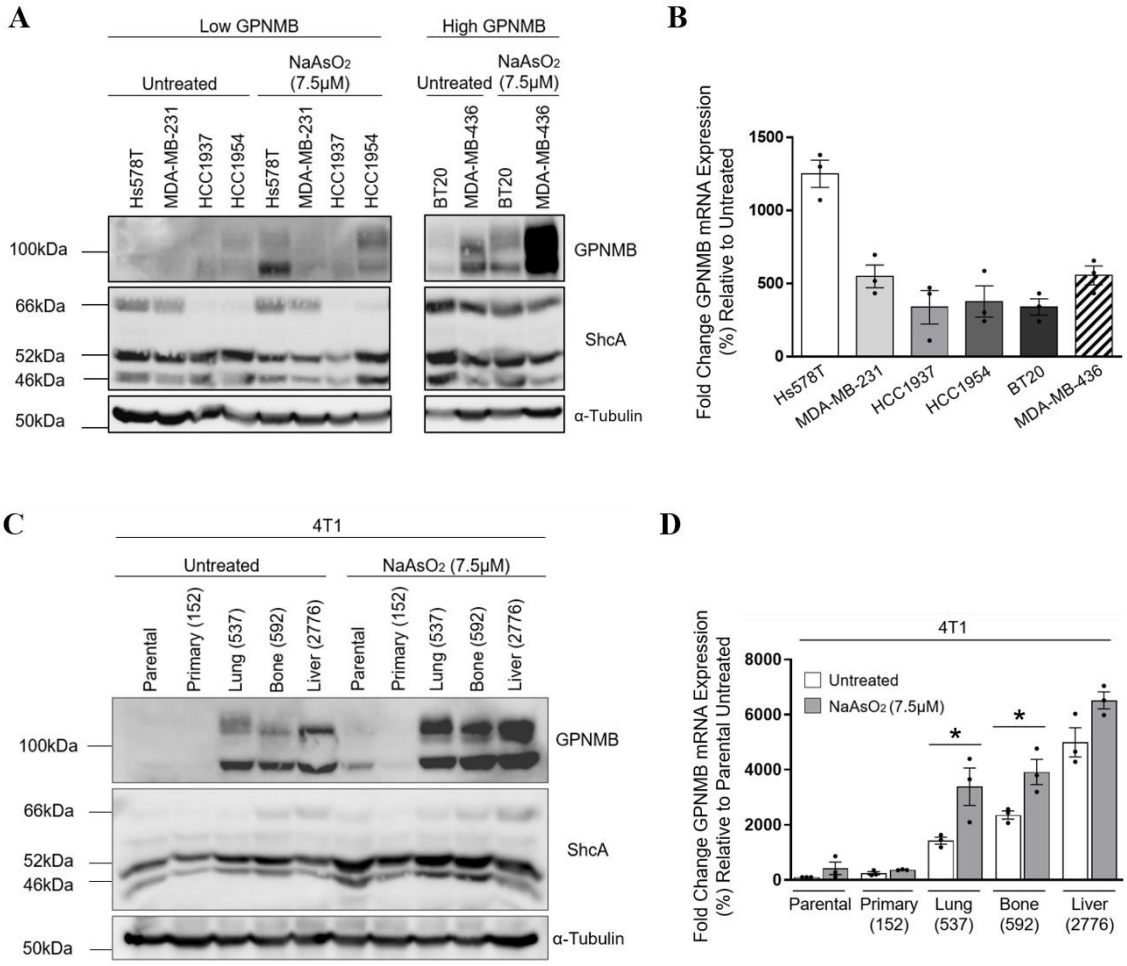

Figure 3.2. TNBC Cell Models with Higher Endogenous p66ShcA Expression Show an Increase in GPNMB Levels in Response to ROS. (**A**) Immunoblot analysis of GPNMB and ShcA protein expression in the indicated TNBC/BLBC cell lines cultured in the absence (untreated) or presence of $NaAsO_2$ (7.5μM) for 48h. Blots are from the same membrane, cropped, and adjusted for contrast based on endogenous GPNMB expression for clarity. α-Tubulin served as a loading control. (**B**) Corresponding RT-qPCR analysis of *GPNMB* mRNA expression in indicated cell lines. Breast cancer cells were treated as in (A). Data are presented as fold change mean values ± SEM (n = 3 biological replicates). (**C**) Immunoblot analysis of GPNMB and ShcA protein expression in the indicated 4T1 and 4T1 organ-specific metastatic cell lines cultured in the absence (untreated) or presence of $NaAsO_2$ (7.5μM) for 48h. α-Tubulin served as a loading control. (**D**) Corresponding RT-qPCR analysis of *GPNMB* mRNA expression in indicated cell lines. Breast cancer cells were treated as in (C). Data are presented as fold change mean values ± SEM (n = 3 biological replicates): *, $P < 0.05$ by unpaired Student's *t* test.

3.3 TCGA Data Reveals a Correlation Between *p66ShcA* and *GPNMB* mRNA Expression in Human Breast Tumors

With the discovery that TNBC cells expressing endogenous p66ShcA exhibit high baseline GPNMB and/or elevated fold increases in GPNMB expression in response to oxidative stress, we interrogated TCGA data to strengthen the notion that p66ShcA plays a role in the regulation of GPNMB. First, we segregated gene expression data into quartiles (1-4) based on *p66ShcA* expression, with quartile 1 containing tumours with the lowest *p66ShcA* levels and quartile 4 containing tumours with the highest *p66ShcA* levels. Interestingly, analysis of *GPNMB* expression within these quartiles revealed that tumours exhibiting high *p66ShcA* expression likewise express elevated *GPNMB* (Figure 3.3A) and show approximately 2-fold higher *GPNMB* expression versus tumours with the lowest *GPNMB* expression (Figure 3.3B). These data corroborate results seen in our *in vitro* experiments, and further build a rationale for p66ShcA as a modulator of GPNMB upregulation.

3.4 Knockout of p66ShcA Ablates GPNMB Upregulation in Response to Oxidative Stress

To directly assess the role that p66ShcA plays in GPNMB upregulation following oxidative stress, we employed TNBC/BLBC cell lines (Hs578T, 4T1-537) to generate models with a deletion of endogenous p66ShcA. Furthermore, p66ShcA mutants that lack the ability to translocate to the mitochondria (p66ShcA SA) or generate ROS (p66ShcA QQ) were expressed in these breast cancer cells lacking endogenous p66ShcA. Thus, both of these mutations render p66ShcA functionally unable to generate mtROS, albeit through different mechanisms (Figure 3.4A). The p66ShcA SA mutant cannot be phosphorylated on S36, preventing mitochondrial localization and mtROS production [190]. The p66ShcA QQ mutant is capable of localizing to the mitochondria; however, mutation of the cytochrome c binding site prevents binding and oxidation of reduced cytochrome c, disrupting electron transfer to oxygen and inhibiting the formation of mtROS [188].

GPNMB upregulation at the protein and mRNA levels, in response to $NaAsO_2$ treatment, was severely impaired in both Hs578T and 4T1 breast cancer cells lacking endogenous p66ShcA (Figure 4B-E). Importantly, induction of GPNMB expression was fully rescued by expression of p66ShcA WT (Figure 3.4B-C). Consistent with our previous experiments conducted in parental cells, p66ShcA WT expressing Hs578T and 4T1-537 breast cancer cells increased GPNMB

mRNA and protein levels in response to oxidative stress, which was blocked by NAC-dependent ROS scavenging (Figure 4B-E). Unexpectedly, we also observed upregulation of GPNMB protein and mRNA levels in Hs578T cells expressing p66ShcA QQ or p66ShcA SA, which are defective in ROS production (Figure 3.4B-C). This observation suggests a more complex mechanism in which p66ShcA regulates GPNMB following ROS exposure but exerts its regulatory effects independently of its role as a redox protein.

We next asked whether p66ShcA overexpression in basal breast cancer cells, which possess low endogenous p66ShcA levels, could enhance GPNMB upregulation following oxidative stress. HCC1954 breast cancer cells lack observable endogenous p66ShcA by immunoblot blot (Figure 3.2A) and were engineered to harbour an empty vector (VC) or express p66ShcA WT. Parental HCC1954 breast cancer cells did not display appreciable baseline GPNMB levels and exhibited only modest increases in GPNMB mRNA and protein expression following $NaAsO_2$ treatment (Figure 3.4F-G). Interestingly, HCC1954 cells that overexpress exogenous p66ShcA WT display the same magnitude of $NaAsO_2$-induced GPNMB upregulation observed in Hs578T and 4T1-537 breast cancer cells (high endogenous p66ShcA) (Figure 3.4F-G). Taken together, these data support p66ShcA-dependent regulation of GPNMB following oxidative stress in both human and murine breast cancer cells. Interestingly, this process does not rely on p66ShcA's ability to generate ROS and may rather be a result of an adaptor function of p66ShcA.

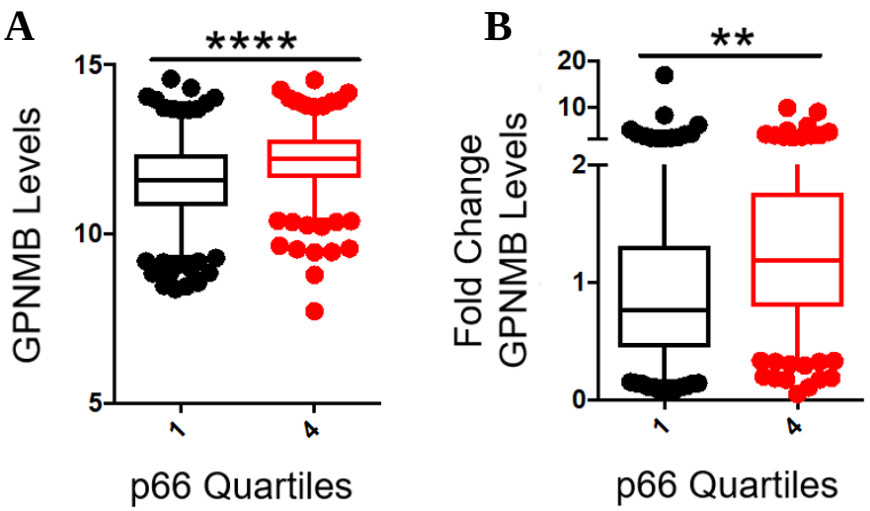

Figure 3.3: TCGA Data Reveals a Correlation Between *p66ShcA* and *GPNMB* mRNA Expression. Interrogation of TCGA data was performed by stratifying gene expression into quartiles. Quartiles 1 and 4 represent tumours with the lowest and highest levels of *p66ShcA* gene expression, respectively. Each quartile was then used to compare levels of *p66ShcA* with *GPNMB* expression. Data in (**A**) are presented as overall *GPNMB* expression and data in (**B**) are presented as fold change in *GPNMB* expression based on *p66ShcA* levels. n = 275 in each quartile. Horizontal bars depict median values, with the box and whiskers representing 25th to 75th percentiles and 5th to 95th percentiles, respectively. Data points plotted on the graphs lie outside the 5th to 95th percentiles. **, $P < 0.01$; ****, $P < 0.0001$ by unpaired Student's *t* test.

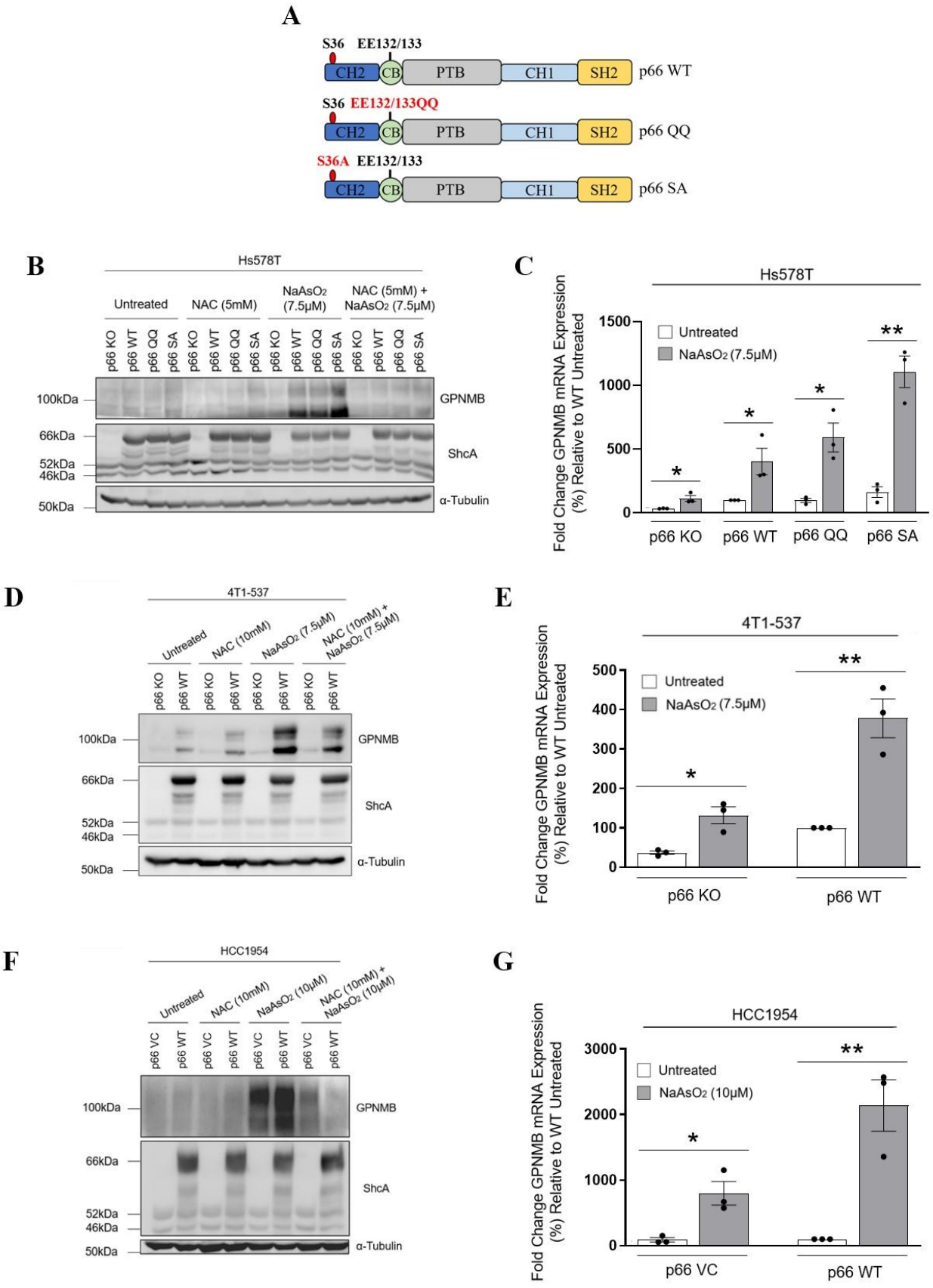
A
S36 EE132/133
CH2 CB PTB CH1 SH2
p66 WT
S36 EE132/133QQ
p66 QQ
S36A EE132/133
p66 SA
B
Hs578T
Untreated
NAC (5mM)
NaAsO2 (7.5μM)
NAC (5mM) + NaAsO2 (7.5μM)
p66 KO
p66 WT
p66 QQ
p66 SA
100kDa
66kDa
52kDa
46kDa
50kDa
GPNMB
ShcA
α-Tubulin
C
Hs578T
Fold Change GPNMB mRNA Expression (%) Relative to WT Untreated
Untreated
NaAsO2 (7.5μM)
p66 KO
p66 WT
p66 QQ
p66 SA
D
4T1-537
NAC (10mM)
NaAsO2 (7.5μM)
NAC (10mM) + NaAsO2 (7.5μM)
E
4T1-537
F
HCC1954
NaAsO2 (10μM)
p66 VC
G
HCC1954

Figure 3.4: Knockout of p66ShcA Ablates GPNMB Upregulation in Response to Oxidative Stress. (**A**) Schematic of p66ShcA WT and p66ShcA SA and QQ mutants. (**B**) Immunoblot analysis of GPNMB and ShcA protein expression (all isoforms) in p66ShcA KO, WT, QQ and SA expressing Hs578T cells. α-Tubulin served as a loading control. (**C**) RT-qPCR analysis of *GPNMB* mRNA expression in the same panel of cell lines. Data are presented as fold change mean values ± SEM (n = 3 biological replicates): *, $P < 0.05$; **, $P < 0.01$ by unpaired Student's *t* test. (**D**) Immunoblot analysis of GPNMB and ShcA protein expression in p66ShcA KO and p66ShcA WT expressing 4T1-537 cells. α-Tubulin served as a loading control. € RT-qPCR analysis of *GPNMB* mRNA expression in the same cell lines. Data are presented as fold change mean values ± SEM (n = 3 biological replicates): *, $P < 0.05$; **, $P < 0.01$ by unpaired Student's *t* test. (**F**) Immunoblot analysis of GPNMB and ShcA protein expression in VC and p66ShcA WT expressing HCC1954 cells. α-Tubulin served as a loading control. (**G**) RT-qPCR analysis of *GPNMB* mRNA expression in the same cell lines. Data are presented as fold change mean values ± SEM (n = 3 biological replicates): *, $P < 0.05$; **, $P < 0.01$ by unpaired Student's *t* test. Cells in (B), (D) and (F) were cultured with NAC or $NaAsO_2$ alone or in combination at the indicated dose. Cells were treated with NAC at the time of seeding, with the addition of $NaAsO_2$ 24h later. Cells were then cultured for 48h. Cells in (C), (E), and (G) were only cultured in the absence (untreated) or presence of $NaAsO_2$ (7.5μM) for 48h.

3.5 Breast Cancer Cells Expressing p66ShcA SA and QQ Mutants Exhibit Lower Intracellular ROS Following $NaAsO_2$ Treatment

The ability of p66ShcA mutants defective in ROS production to induce GPNMB expression following oxidative stress was surprising. To confirm that Hs578T cells expressing p66ShcA SA and p66ShcA QQ were indeed impaired in ROS production, total ROS levels were analyzed in these cells following $NaAsO_2$ treatment using the CM-H_2DCFDA fluorescence indicator of ROS production. As anticipated, p66ShcA KO expressing cells showed little change in cellular ROS across all conditions; whereas p66ShcA WT expressing cells exhibited a marked increase in ROS when treated with $NaAsO_2$. The observed elevation in ROS levels could also be dramatically reduced by pre-treatment with NAC. Importantly, we observed that Hs578T breast cancer cells expressing the p66ShcA SA or p66ShcA QQ mutants produced less $NaAsO_2$-induced ROS production when compared to p66ShcA WT expressing cells (Figure 3.5A-B). Coupled with the significant upregulation of *GPNMB* seen by RT-qPCR and immunoblot analysis in each of the p66ShcA-expressing Hs578T cell lines, these data support the mechanism in which p66ShcA exerts its regulatory effects on GPNMB following oxidative stress independently of it being able to generate mtROS.

3.6 Expression of p66ShcA in Luminal Breast Cancer Cells does not Enhance GPNMB Levels Following ROS Exposure

Given that our studies to this point were limited to TNBC/BLBC cell models (Hs578T, 4T1-537, HCC1954), we sought to investigate the effect of oxidative stress on GPNMB expression in a luminal model, and the role of p66ShcA in this context. MCF7 breast cancer cells treated with $NaAsO_2$ exhibited no increases in GPNMB mRNA or protein expression (Figure 3.6A-B). This result was anticipated due to the fact that MCF7 breast cancer cells express very little endogenous p66ShcA (Figure 3.6A). Given that p66ShcA overexpression was sufficient to induce GPNMB expression in response to oxidative stress in HCC1954 basal like breast cancer cells (Figure 3.4F-G), we assessed whether the same result could be achieved in the less aggressive MCF7 luminal subtype. MCF7 breast cancer cells were engineered to express a doxycycline-inducible p66ShcA WT (p66ShcA) construct or an empty vector control (VC). Inducing p66ShcA expression by escalating concentrations of doxycycline failed to increase GPNMB levels under both basal and $NaAsO_2$ stimulated conditions, regardless of p66ShcA

protein levels (Figure 3.6C). Therefore, our findings suggest that p66ShcA does not promote GPNMB expression in luminal models following oxidative stress and appear restricted to TNBC/BLBC breast cancer.

3.7 GPNMB Induction in Response to $NaAsO_2$ is Dependent on NADPH Oxidases

The ability of p66ShcA to produce ROS is dispensable for the increase of GPNMB expression following oxidative stress, yet ROS are nonetheless critical for GPNMB upregulation. One possible explanation for this finding is the source of intracellular ROS that is generated in response to $NaAsO_2$. $NaAsO_2$ has been previously reported to promote the formation of ROS through stimulation of NOX activity as well as upregulation and phosphorylation of key NOX subunits [220-222]. Since p66ShcA produces mainly mtROS, we hypothesized that GPNMB upregulation following $NaAsO_2$ treatment was specifically dependent on extra-mitochondrial noxROS. To test this theory, parental Hs578T cells were pre-treated with apocynin, a routinely employed inhibitor that prevents assembly and activity of the NOX complex [223]. In a manner consistent with previous experiments conducted with NAC, apocynin was added at the time of seeding to block noxROS production prior to and during treatment with $NaAsO_2$. Intriguingly, inhibition of NOX prior to stimulation with $NaAsO_2$ completely abrogated GPNMB protein upregulation (Figure 3.7A). To verify that apocynin reduced overall ROS production, we conducted flow cytometry analyses using CM-H_2DCFDA under the same treatment conditions in the Hs578T cells. The addition of apocynin prior to $NaAsO_2$ exposure significantly reduced the amount of cellular ROS that was generated (Figure 3.7B-C), in agreement with our findings that GPNMB expression is drastically reduced in the presence of apocynin (Figure 3.7A). These results are reminiscent of our previous results, where Hs578T cells exhibited attenuated GPNMB expression and total ROS production when pre-treated with NAC (Figure 3.1G-J). Taken together, our results suggest that NOX is the primary source of ROS production in response to $NaAsO_2$ treatment, and GPNMB upregulation in this context is dependent on non-mitochondrial noxROS.

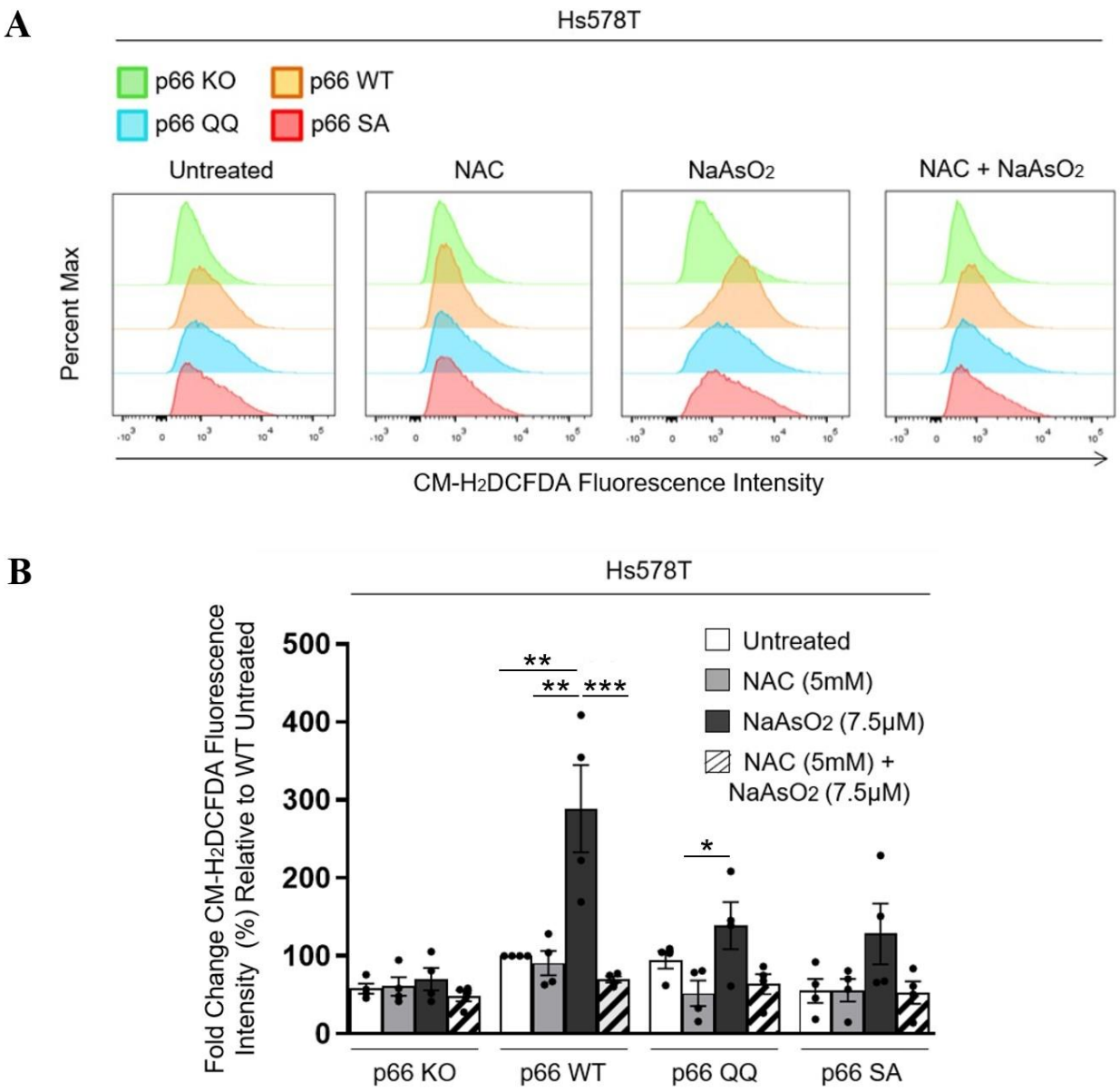

Figure 3.5: Breast Cancer Cells Expressing p66ShcA SA and QQ Mutants Exhibit Lower Intracellular ROS Following $NaAsO_2$ Treatment (**A**) Representative histograms and (**B**) quantification of total cellular ROS by flow cytometry in p66ShcA KO, WT, QQ and SA expressing Hs578T cells. ROS levels were analyzed by CM-H_2DCFDA staining. Breast cancer cells were cultured with NAC or $NaAsO_2$ alone, or in combination, at the indicated doses (B). Brest cancer cells were treated with NAC at the time of seeding, with the addition of $NaAsO_2$ 24h later. Cells were then cultured for 48h. Data are presented as fold change CM-H_2DCFDA fluorescence (geometric mean) ± SEM (n = 4 biological replicates): **, $P < 0.01$. ***, $P < 0.001$ by 1-way ANOVA with Tukey's multiple comparisons test.

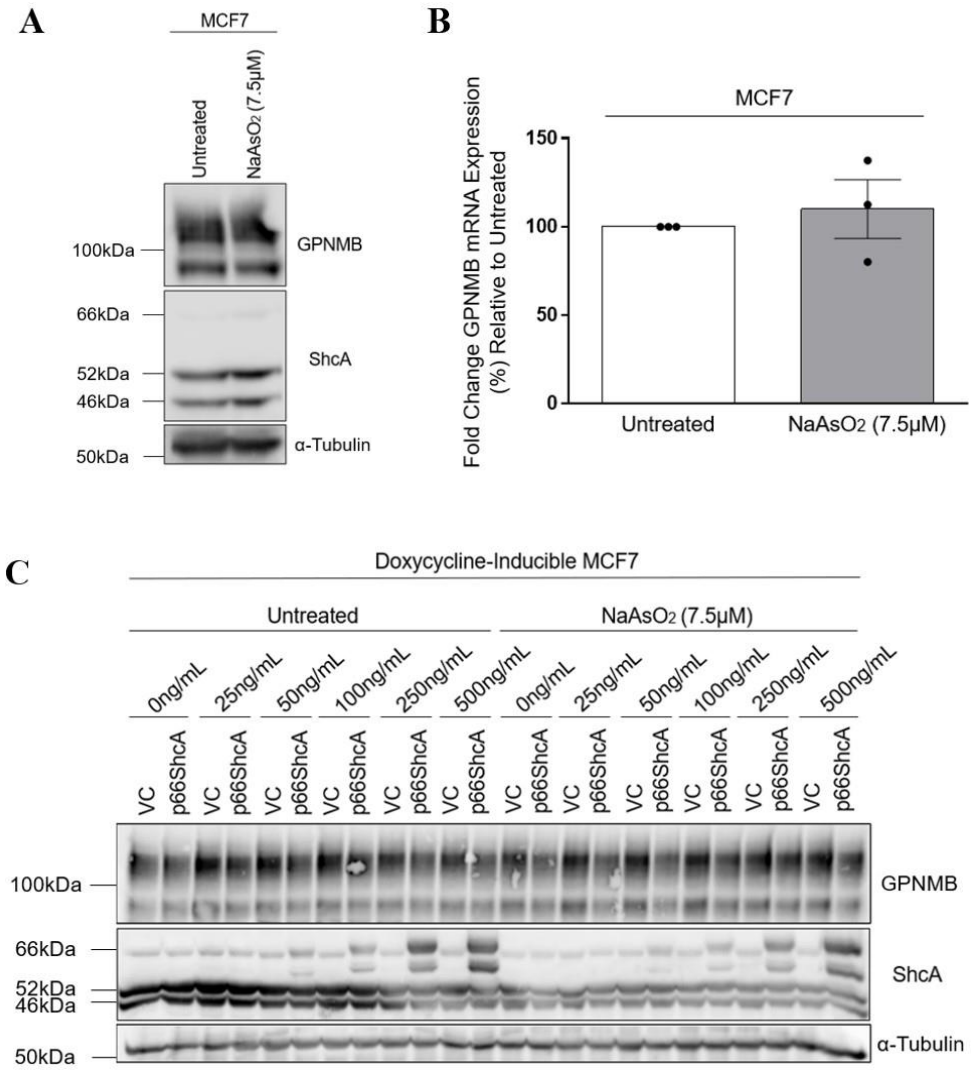

Figure 3.6: Expression of p66ShcA in Luminal Breast Cancer Cells does not Enhance GPNMB Levels Following ROS Exposure. (**A**) Immunoblot analysis of GPNMB and ShcA protein expression in MCF7 cells cultured in the absence (untreated) or presence of $NaAsO_2$ (7.5μM) for 48h. α-Tubulin served as a loading control. (**B**) RT-qPCR analysis of *GPNMB* mRNA expression in the same cells. Breast cancer cells were treated as in (A). Data are presented as fold change mean values ± SEM (n = 3 biological replicates): data not significant by unpaired Student's *t* test (**C**) Immunoblot analysis of GPNMB and ShcA protein expression in doxycycline-inducible p66ShcA expressing MCF7 cells cultured in the absence (untreated) or presence of $NaAsO_2$ (7.5μM) for 48h. Prior to treatment with $NaAsO_2$, cells were cultured in the absence or presence of doxycycline for 48h and maintained at the indicated dose to induce p66ShcA. α-Tubulin served as a loading control.

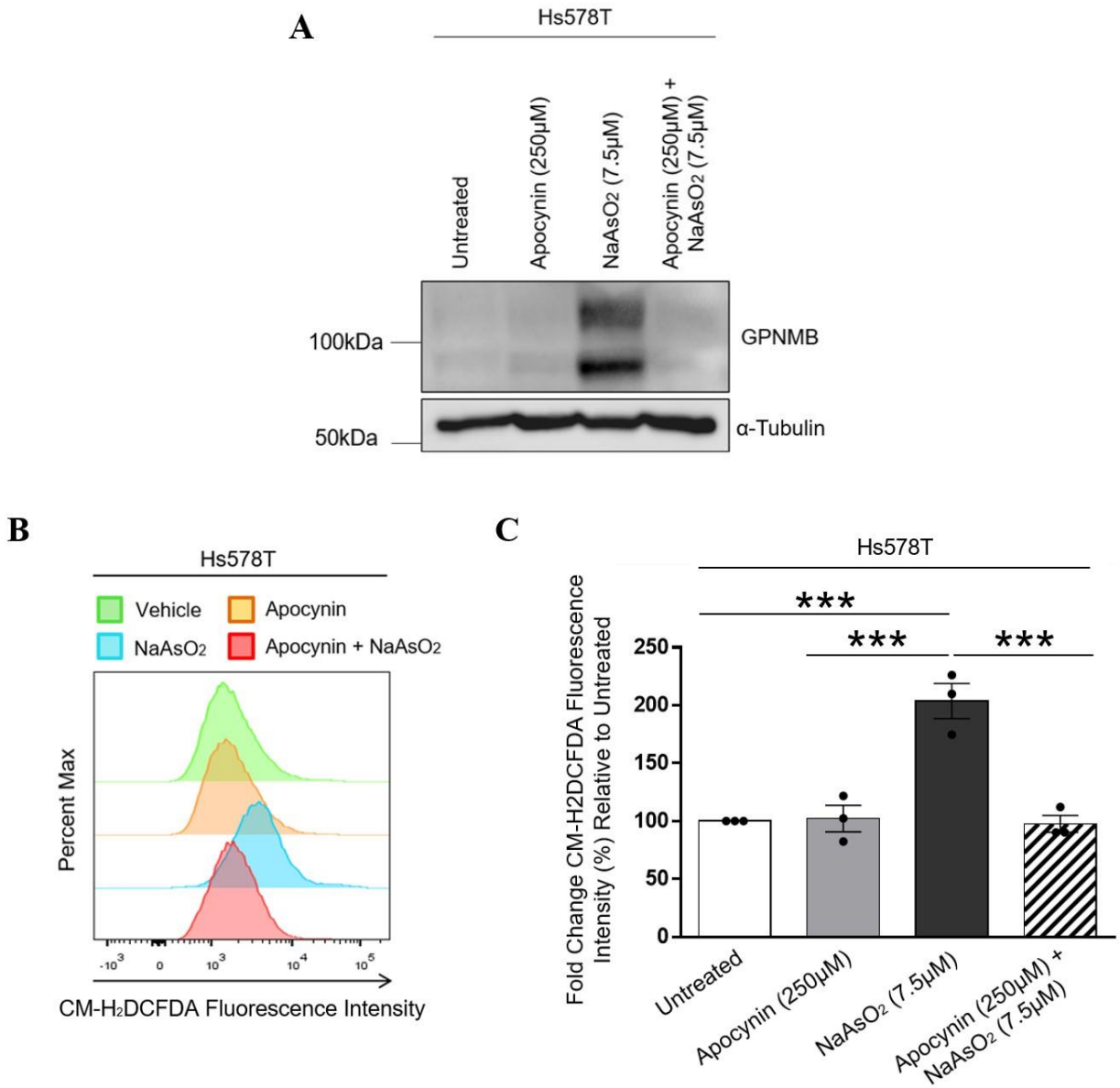

Figure 3.7: GPNMB Induction in Response to $NaAsO_2$ is Dependent on NADPH Oxidases. (**A**) Immunoblot analysis of GPNMB protein expression in Hs578T cells. α-Tubulin served as a loading control. Representative histograms (B) and quantification of total cellular ROS by flow cytometry (**C**) in Hs578T cells. ROS levels were analyzed by CM-H_2DCFDA staining. Data are presented as fold change CM-H_2DCFDA fluorescence (geometric mean) ± SEM (n = 3 biological replicates): ***, $P < 0.001$ by 1-way ANOVA with Tukey's multiple comparisons test. Cells in (A-C) were cultured with apocynin or $NaAsO_2$ alone, or in combination, at the indicated doses. Cells were treated with apocynin at the time of seeding, with the addition of $NaAsO_2$ 24h later. Cells were then cultured for 48 hours.

3.8 TFE3 and TFEB are Required for GPNMB Upregulation Following Oxidative Stress

GPNMB expression is regulated by the transcription factors TFE3 and TFEB in TNBC cells, and TFE3/TFEB are activated in response to diverse cellular stressors, such as ROS (including $NaAsO_2$) [86, 122, 125-133]. Thus, we investigated whether TFE3 and TFEB were necessary for GPNMB induction in response to oxidative stress. p66ShcA KO and p66ShcA WT expressing Hs578T breast cancer cells were depleted of TFE3 or TFEB by transient siRNA-mediated knockdown prior to exposure to $NaAsO_2$. Reduction of TFE3 and TFEB levels impaired GPNMB protein and mRNA expression in both untreated conditions and following oxidative stress (Figure 3.8A-B). Reduced TFEB levels did not attenuate GPNMB expression to the same level as diminished TFE3expression; however, there was a clear contribution of both transcription factors to GPNMB upregulation following $NaAsO_2$ treatment. Interestingly, there was also a noticeable mobility shift in the molecular weight of TFE3 in the treated condition in comparison to untreated cells (Figure 3.8A). This decrease in molecular weight suggests that TFE3 is being dephosphorylated following ROS exposure, and presumably translocating to the nucleus where it is subsequently transcribing its target genes, including GPNMB.

We extended our studies to the murine p66ShcA KO and p66ShcA WT expressing 4T1-537 breast cancer cells to determine if this TFE3/TFEB-dependent mechanism was conserved in multiple TNBC models. Knockdown of TFE3 and TFEB under basal conditions again attenuated GPNMB protein and mRNA expression (Figure 3.8C-D). Furthermore, targeting of TFE3 and TFEB largely ablated the increase in GPNMB levels observed following $NaAsO_2$ treatment. As seen in human TNBC cells, TFE3 appears to be play a more significant role in inducing GPNMB expression following oxidative stress when compared to TFEB in 4T1-537 cells. Collectively, these data suggest that TFE3 and TFEB are both required for the robust induction of GPNMB expression following oxidative stress in both human and murine cell models.

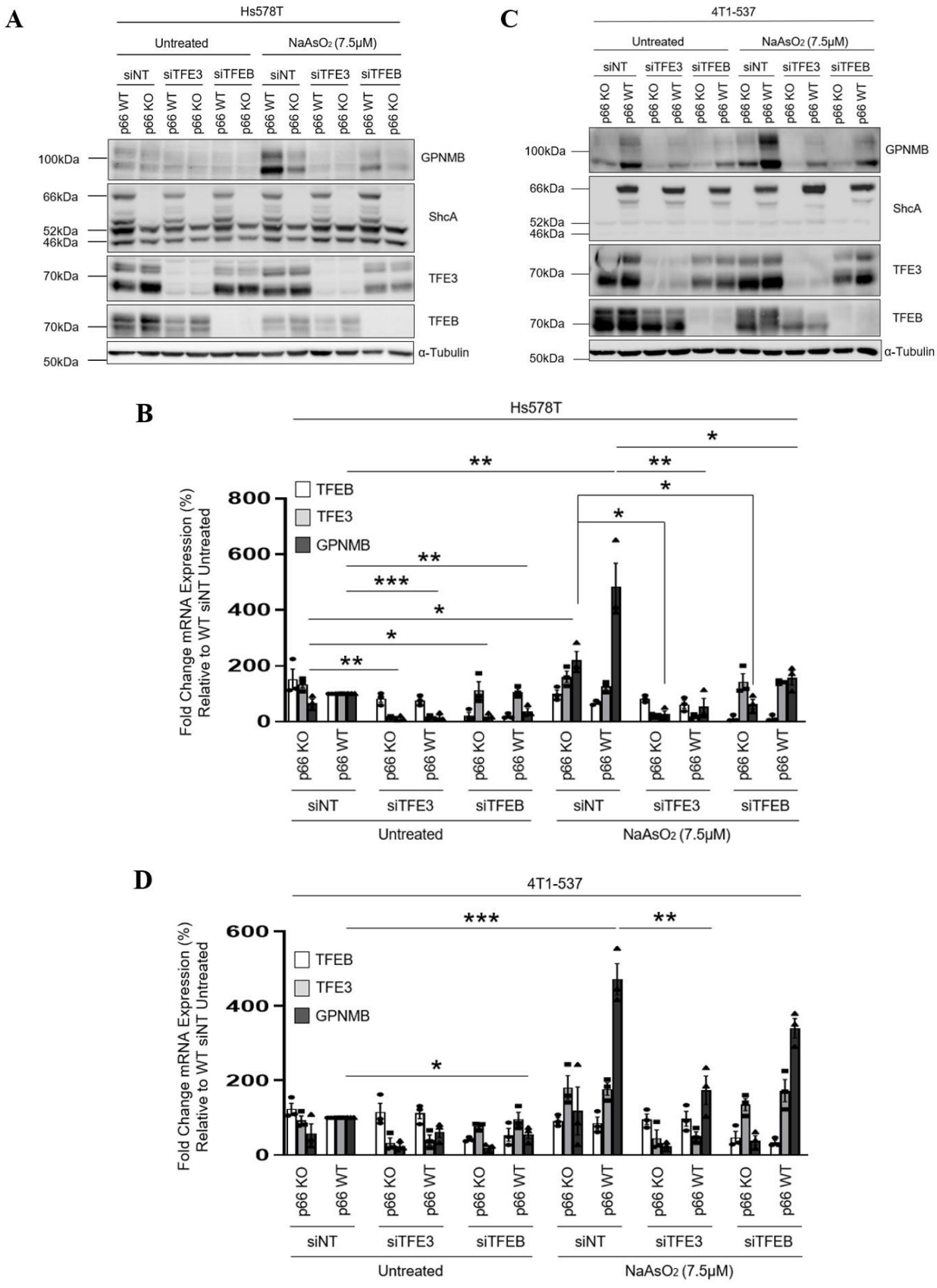
A
Hs578T
Untreated
NaAsO2 (7.5μM)
siNT
siTFE3
siTFEB
p66 WT
p66 KO
100kDa
66kDa
52kDa
46kDa
70kDa
50kDa
GPNMB
ShcA
TFE3
TFEB
α-Tubulin
C
4T1-537
B
Hs578T
Fold Change mRNA Expression (%) Relative to WT siNT Untreated
TFEB
TFE3
GPNMB
D
4T1-537

Figure 8: TFE3 and TFEB are Required for GPNMB Upregulation Following Oxidative Stress. (**A**) Immunoblot analysis of GPNMB, ShcA, TFE3 and TFEB protein expression in p66ShcA KO and p66ShcA WT expressing Hs578T cells. α-Tubulin served as a loading control. (**B**) RT-qPCR analysis of *GPNMB, TFE3* and *TFEB* mRNA expression in the same panel of breast cancer cells. Data are presented as fold change mean values ± SEM (n = 3 biological replicates): *, $P < 0.05$; **, $P < 0.01$; ***, $P < 0.001$ by unpaired Student's *t* test. (**C**) Immunoblot analysis of GPNMB, ShcA, TFE3 and TFEB protein expression in p66ShcA KO and WT 4T1-537 cells. α-Tubulin served as a loading control. (**D**) RT-qPCR analysis of *GPNMB, TFE3* and *TFEB* mRNA expression in the same panel of breast cancer cells. Data are presented as fold change mean values ± SEM (n = 3 biological replicates): *, $P < 0.05$; **, $P < 0.01$; ***, $P < 0.001$ by unpaired Student's *t* test. Cells in (A-D) were reverse-transfected with non-targeting control (siNT), TFE3 (siTFE3) or TFEB (siTFEB) targeting siRNAs at the time of seeding. Cells were transfected overnight, washed, and supplied with fresh media the following morning. 24h after transfection cells were then cultured in the absence (untreated) or presence of $NaAsO_2$ (7.5μM) for 48h.

3.9 p66ShcA Regulates the Localization, Transcriptional Activity, and Expression of TFE3

The transcriptional activity of TFE3 and TFEB is controlled, in part, by regulation of their cytoplasmic/nuclear translocation. Thus, we next investigated the subcellular localization of TFE3 following oxidative stress, in the presence or absence of p66ShcA. TFE3 was selected for further investigation as our data suggests that TFE3 has a larger contribution to GPNMB upregulation in response to ROS (Figure 3.8A-D). This is supported by published work from our lab demonstrating that TFE3 is the MiTF/TFE member responsible for GPNMB expression in TNBC following treatment with chemotherapy or other stressors [86]. Experiments were performed on p66ShcA KO and p66ShcA WT expressing Hs578T cells treated with $NaAsO_2$ for time points ranging from 2h to 48h. TFE3 began to accumulate in the nucleus as early as 2 hours following $NaAsO_2$ treatment, with most nuclei in p66ShcA WT cells showing nuclear TFE3 signal by 24 hours, as well as an increased proportion of nuclei with strong TFE3 staining (Figure 3.9A-B). In contrast, the dynamics and signal strength of TFE3 accumulation in Hs578T cells lacking p66ShcA was significantly delayed at 24 and 48h time points (Figure 3.9A-B). The lag in TFE3 nuclear accumulation in p66ShcA KO cells may point to a role for p66ShcA in influencing the subcellular localization of TFE3 and could also offer an explanation as to why GPNMB is not induced in response to $NaAsO_2$ at a 48h time point in p66ShcA KO cells.

Given the profound delay in $NaAsO_2$ –induced TFE3 nuclear localization observed in the absence of p66ShcA, we reasoned that multiple TFE3 transcriptional target genes could be adversely affected in a manner similar to GPNMB. TFE3 target genes related to lysosomes and autophagy were selected as readouts of a broader TFE3-dependent transcriptional program. $NaAsO_2$ treatment of Hs578T breast cancer cells expressing p66ShcA WT resulted in a significant upregulation of several TFE3 target genes, which was blunted in cells deficient in p66ShcA (Figure 3.9C). These results provide evidence for p66ShcA-dependent regulation of TFE3 transcriptional activity; thus, we revisited TCGA data to determine if p66ShcA levels also correlate with TFE3 expression. It was revealed that tumour expressing the highest levels of p66ShcA also expressed significantly higher overall levels of TFE3 (Figure 3.9D) and fold change in TFE3 expression (Figure 3.9E). The combination of *in vitro* data and TCGA data from human tumours indicates that p66ShcA modulates TFE3 nuclear accumulation, transcriptional activity, and expression, and places p66ShcA at the interface of an oxidant-induced autophagy and lysosomal gene network.

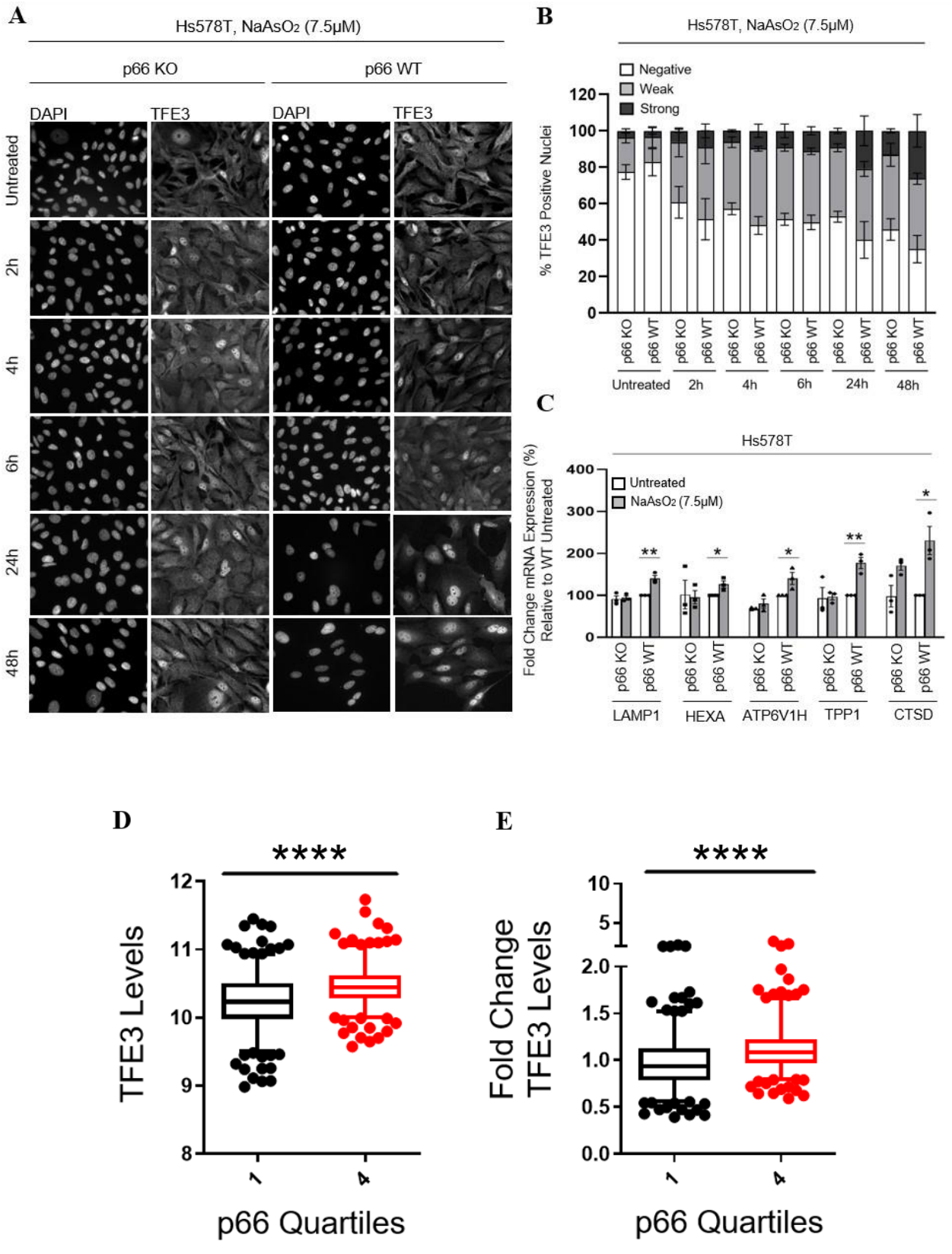
A
Hs578T, NaAsO2 (7.5μM)
p66 KO
p66 WT
DAPI
TFE3
DAPI
TFE3
Untreated
2h
4h
6h
24h
48h
B
Hs578T, NaAsO2 (7.5μM)
Negative
Weak
Strong
% TFE3 Positive Nuclei
120
100
80
60
40
20
0
p66 KO
p66 WT
Untreated
2h
4h
6h
24h
48h
C
Hs578T
Untreated
NaAsO2 (7.5μM)
Fold Change mRNA Expression (%) Relative to WT Untreated
400
300
200
100
0
**
*
*
**
*
LAMP1
HEXA
ATP6V1H
TPP1
CTSD
D
****
TFE3 Levels
12
11
10
9
8
1
4
p66 Quartiles
E
****
Fold Change TFE3 Levels
10
5
2.0
1.5
1.0
0.5
0.0
1
4
p66 Quartiles

Figure 3.9: p66ShcA Regulates the Localization, Transcriptional Activity, and Expression of TFE3. Representative immunofluorescence images (**A**) and quantification (**B**) of TFE3 nuclear localization in p66ShcA KO and p66ShcA WT expressing Hs578T breast cancer cells. Hs578T were cultured in the absence (untreated) or presence of $NaAsO_2$ (7.5µM) for the indicated times. Scale bar is 20µM and applies to all images. (**C**) RT-qPCR analysis of *LAMP1*, *HEXA*, *ATP6V1H*, *TPP1* and *CTSD* mRNA expression in p66ShcA KO and WT Hs578T cells. Cells were cultured in the absence (untreated) or presence of $NaAsO_2$ (7.5µM) for 48h. Data are presented as fold change mean values ± SEM (n = 3 biological replicates): *, $P < 0.05$; **, $P < 0.01$ by unpaired Student's *t* test. TCGA data were divided into quartiles as in Figure 3.3. Data in (**D**) are presented as overall TFE3 expression and data in (**E**) are presented as fold change TFE3 expression based on p66ShcA levels. n = 275 in each quartile. Horizontal bars depict median values, with the box and whiskers representing 25^{th} to 75^{th} percentiles and 5^{th} to 95^{th} percentiles, respectively. Data points plotted on the graphs lie outside the 5^{th} to 95^{th} percentiles. ****, $P < 0.0001$ by unpaired Student's *t* test.

3.10 BioID Mass Spectrometry Reveals an Endosomal-Lysosomal Gene Signature in $NaAsO_2$ Treated Cells

Collectively, our data suggests that p66ShcA does not need to generate ROS in order to promote GPNMB upregulation. Coupled with the finding that p66ShcA also modulates the localization and transcriptional activity of TFE3, we hypothesized that p66ShcA functions as an adaptor protein and may interact with as yet unidentified proteins to exert its regulatory effects under conditions of oxidative stress. As such, a BioID approach was employed to elucidate proteins in proximity to p66ShcA in response to oxidative stress. Both p52ShcA-BirA and p66ShcA-BirA fusion proteins were generated and expressed in parental Hs578T cells to examine potential interactions (Figure 3.10A). p52ShcA-BirA and p66ShcA-BirA cells were treated for 24h with biotin alone or in combination with $NaAsO_2$ to induce BirA-meditated biotin labeling under unstimulated and pro-oxidant conditions. Intriguingly, unbiased gene ontology analysis [224-225] of hits identified in p66ShcA-BirA cells treated with $NaAsO_2$ revealed that 2/7 genes, Folliculin (FLCN) and Receptor-Interacting Serine/Threonine-Protein Kinase 1 (RIPK1), are localized to the endosomal-lysosomal system (Figure 3.10B). FLCN has been well characterized as a GTPase activating protein (GAP) for the Rag C/D GTPases at the lysosomal surface, promoting the activation of Rag C/D by binding to and facilitating GDP loading onto the GTPases [104, 226-228]. Additionally, gene ontology analysis indicates endosomal localization of RIPK1; however, existing literature also suggests that RIPK1 is recruited to the lysosomal membrane where it interacts with mTORC1 regulatory elements, such as the Rag-Ragulator complex [229] and AMPK [230]. This was a compelling discovery, as to our knowledge p66ShcA localization to lysosomes has not been described. Thus, close proximity of p66ShcA to FLCN and RIPK1 may represent novel shuttling mechanism of p66ShcA to a previously unreported subcellular compartment following oxidative stress. Importantly, the dot plot shown in Figure 3.10B includes only candidate proteins whose proximity to p66ShcA is specifically gained in $NaAsO_2$ treated conditions (normalized to untreated samples) suggesting that p66ShcA may traffic to lysosomes in response to ROS creating an oxidative stress-induced lysosomal pool.

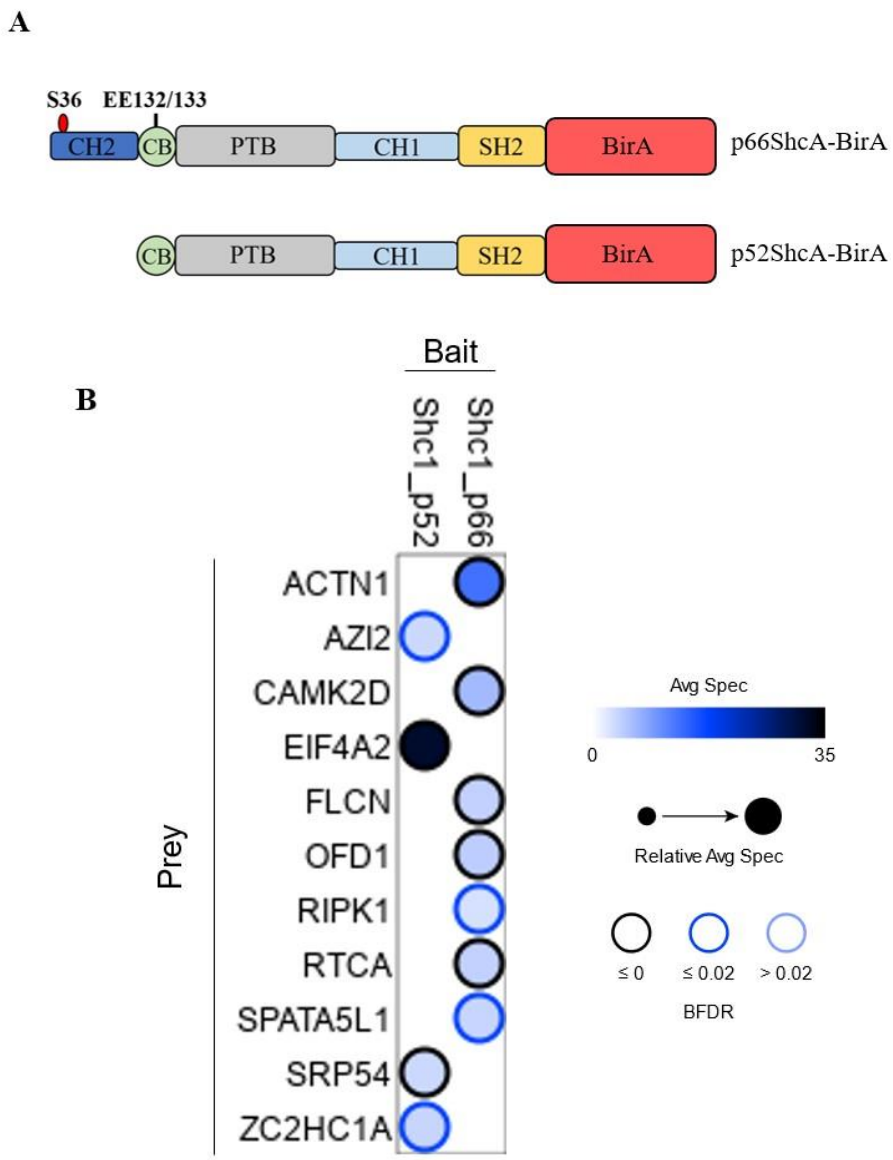

Figure 3.10 BioID Mass Spectrometry Reveals an Endosomal-Lysosomal Gene Signature in $NaAsO_2$ Treated Cells (**A**) Schematic of p52ShcA-BirA and p66ShcA-BirA fusion proteins used for BioID experiments. (**B**) Dot plot of genes identified in mass spectrometry results. Hs578T-BirA fusion proteins were treated in the absence or presence of 10μM $NaAsO_2$ combined with 50μM biotin for 24 hours. Post-treatment, cell pellets were sent for streptavidin pull-down and mass spectrometry sample preparation. Mass spectrometry results were normalized to a Hs578T-BirA control in each replicate, as well as untreated samples. Dot colour represents average spectral count, dot size represents relative abundance, and dot circumference colour represents BFDR of each prey (biotinylated) protein. Dot plot was generated using ProHitz-viz and is representative of 3 biological replicates.

3.11 $NaAsO_2$ Treatment Promotes p66ShcA Localization to Lysosomes

The observation that a significant proportion (roughly 30%) of proteins biotinylated by p66ShcA-BirA following $NaAsO_2$ treatment are associated with the lysosomal system, coupled with the fact that p66ShcA loss impairs TFE3 nuclear localization, was compelling given the well characterized mechanism of TFE3 regulation at the lysosomal surface. These findings led us to hypothesize that a fraction of the p66ShcA cytoplasmic pool may translocate to lysosomes in response to oxidative stress. Since the Hs578T breast cancer cells lacking endogenous p66ShcA were engineered to express a FLAG-tagged version of p66ShcA WT, we performed co-immunofluorescence experiments with anti-FLAG and anti-LAMP1 antibodies. Interestingly, with increasing exposure to $NaAsO_2$, Hs578T p66ShcA WT expressing cells exhibited an increase in FLAG fluorescence signal within LAMP1-positive structures, suggesting an increase in the co-localization of p66ShcA with lysosomes at 24h, and to an even higher degree at 48h post-treatment (Figure 3.11A-B).

To further corroborate these co-localization results, we assessed the degree of protein biotinylation (mediated by p66ShcA-BirA) that colocalized with LAMP1 following treatment with $NaAsO_2$. Hs578T breast cancer cells expressing p66ShcA-BirA were treated with $NaAsO_2$ for 18 hours, at which time biotin was added for an additional 6 hours prior to fixation (24 hours of $NaAsO_2$ exposure) (Figure 3.11C). Fluorescent-tagged streptavidin coupled with indirect LAMP1 immunofluorescence revealed that exposure to $NaAsO_2$ for 24h produced an increase in the streptavidin signal within LAMP1-positive organelles (Figure 3.11D-E). Interestingly, the ability of ShcA to translocate to the lysosome is not unique to the p66ShcA isoform, as p52ShcA-BirA expressing Hs578T cells also exhibited elevated co-localization of biotin with LAMP1 following $NaAsO_2$ exposure (Figure 3.11D-E). However, once at the lysosome, it appears that unique interactions between p66ShcA and lysosomal protein(s) or distinct functions of p66ShcA are implicated in the nuclear translocation of TFE3 and subsequent upregulation of GPNMB.

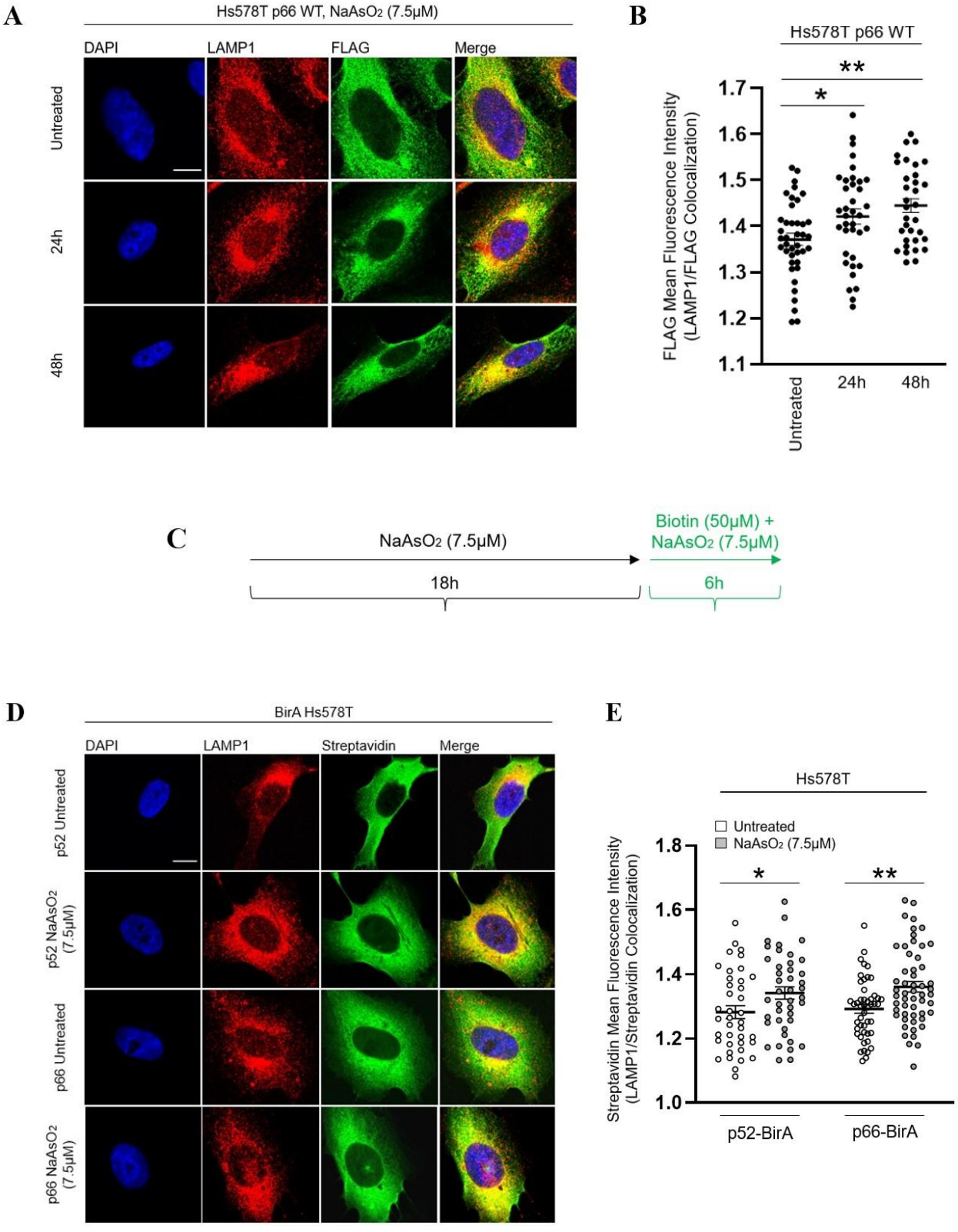
A
Hs578T p66 WT, NaAsO2 (7.5μM)
DAPI
LAMP1
FLAG
Merge
Untreated
24h
48h
B
Hs578T p66 WT
FLAG Mean Fluorescence Intensity (LAMP1/FLAG Colocalization)
1.7
1.6
1.5
1.4
1.3
1.2
1.1
*
**
Untreated
24h
48h
C
NaAsO2 (7.5μM)
18h
Biotin (50μM) + NaAsO2 (7.5μM)
6h
D
BirA Hs578T
DAPI
LAMP1
Streptavidin
Merge
p52 Untreated
p52 NaAsO2 (7.5μM)
p66 Untreated
p66 NaAsO2 (7.5μM)
E
Hs578T
Untreated
NaAsO2 (7.5μM)
Streptavidin Mean Fluorescence Intensity (LAMP1/Streptavidin Colocalization)
1.8
1.6
1.4
1.2
1.0
*
**
p52-BirA
p66-BirA

Figure 3.11: $NaAsO_2$ Treatment Promotes p66ShcA Localization to Lysosomes. (**A**) Representative immunofluorescence images of FLAG (p66ShcA) and LAMP1 (lysosomes) localization in p66ShcA WT expressing Hs578T cells. Breast cancer cells were cultured in the absence (untreated) or presence of $NaAsO_2$ (7.5μM) for the indicated times. Scale bar is 10μM and applies to all images. (**B**) Corresponding quantification of FLAG immunofluorescence intensity in lysosomes normalized to background FLAG immunofluorescence. Each data point represents the normalized mean fluorescence intensity (MFI) of an individual cell, with at least n = 30 cells quantified per condition. Horizontal bars depict the mean values ± SEM in each condition. *, $P < 0.05$; **, $P < 0.01$ by Mann-Whitney *U* test. (**C**) Schematic of the $NaAsO_2$/biotin treatment conditions in p52-BirA and p66-BirA expressing Hs578T cells preceding immunofluorescence staining to visualize biotinylated proteins within lysosomes. (**D**) Representative immunofluorescence images of streptavidin (biotinylated proteins) and LAMP1 (lysosomes) localization in Hs578T cells treated as depicted in (C). Scale bar is 10μM and applies to all images (**E**) Corresponding quantification of streptavidin immunofluorescence intensity in lysosomes normalized to background streptavidin immunofluorescence. Each data point represents the normalized MFI of an individual cell, with at least n = 30 cells quantified per condition. Horizontal bars depict the mean values ± SEM in each condition. *, $P < 0.05$; **, $P < 0.01$ by Mann-Whitney *U* test.

Chapter 4: Discussion

4.1 Discussion and Future Directions

p66ShcA Modulates GPNMB Expression in TNBC

The purpose of this project was to investigate the mechanism of p66ShcA-dependent regulation of GPNMB in TNBC/BLBC under conditions of oxidative stress. Reports from our lab and others show that GPNMB functions as a stress response gene in various disease states [60, 86-92] and is particularly enriched within the TNBC/BLBC subtype where it promotes metastatic phenotypes [63, 66, 72-80, 86]. In this study, we demonstrate that GPNMB expression is upregulated in response to ROS-inducing compounds, and TNBC/BLBC cell lines with high endogenous p66ShcA exhibit strong baseline expression and/or robust induction of GPNMB. Two of these cell lines that display particularly high basal GPNMB expression (MDA-MB-436) and robust stress-induced upregulation (MDA-MB-436/Hs578T) belong to the mesenchymal stem-like TNBC subtype [15]. Intriguingly, we have also observed that the MDA-MB-157 cell line, which expresses low, but detectable levels of p66ShcA, also expresses high endogenous GPNMB and responds to $NaAsO_2$ treatment (data not shown). Intriguingly, MDA-MB-157 also belongs to the mesenchymal stem-like TNBC subtype. This may suggest that tumours expressing even low levels of p66ShcA that have acquired mesenchymal, or stem cell-like characteristics may be predisposed to higher baseline and stress-induced GPNMB expression. We also show that knockout of p66ShcA renders TNBC/BLBC cells unable to upregulate GPNMB expression in response to oxidative stress, and re-expression of p66ShcA WT rescues this phenotype. Combined with TCGA data illustrating a correlation between p66ShcA levels and GPNMB expression, our findings indicate that p66ShcA modulates GPNMB in models of TNBC/BLBC.

ROS-Producing Capabilities of p66ShcA are Dispensable for GPNMB Upregulation

The discovery that the ROS-defective (QQ) and non-mitochondrial (SA) isogenic mutants of p66ShcA were able to induce GPNMB expression was both surprising and compelling, as we had anticipated that the ROS generating capabilities of p66ShcA would need to be intact to modulate GPNMB expression in response to oxidative stress. One possible explanation for p66ShcA QQ and p66ShcA SA-induced GPNMB expression could be that the specific stimulus used throughout this study, $NaAsO_2$, largely generates ROS via non-mitochondrial mechanisms through the plasma-membrane localized NOX enzymes [220-222]. As such, we demonstrate that inhibition of noxROS using the NOX assembly inhibitor apocynin

prior to treatment with $NaAsO_2$ consequently results in significant reduction in GPNMB expression. This may also explain the variable induction of GPNMB following treatment with various ROS-inducers used in this study. For example, actinomycin D has been reported to produce mitochondrial superoxide and inhibit the ETC at complexes I, III, and IV [231]. Likewise, oligomycin and phenformin have been proposed to produce ROS in a mitochondrial-dependent fashion, as oligomycin is an ATP synthase inhibitor [232-233] and phenformin is a known an inhibitor of ETC complex I [234-235]. Additionally, though NOX isoform-specific ROS production has been reported and is somewhat controversial, it is widely agreed that NOX produce large amounts of O_2^- through the transfer of an electron to free oxygen [140-141]. Since $NaAsO_2$ treatment has been demonstrated to result in accumulation of O_2^- derived from NOX [220-222] it is possible that GPNMB upregulation in this context is a result of NOX specifically generating O_2^-. This may explain why H_2O_2, a different oxygen radical, does not appear to induce GPNMB expression, as GPNMB upregulation may be driven by specific oxygen intermediates. Indeed, there is some evidence supporting differential phenotypes of O_2^- and H_2O_2, with varying effects on apoptosis and proliferation [236], oxidative phosphorylation [237], and myogenic signaling [238] previously reported. In each scenario, the lack of NOX engagement by these compounds may explain the moderate or lack of GPNMB induction. Though this has not been experimentally assessed, this could imply that the source of ROS dictates phenotype in response to oxidative stress. In the case of doxorubicin, its pro-oxidant effects have been previously reviewed, with the primary mechanisms of ROS generation involving components of the ETC, mitochondrial enzymes generating semiquinone radicals, and Fenton-like reactions involving iron [239-240]. However, doxorubicin-induced NOX activation in myocytes has also been reported [241]. The contribution of several sources of ROS, as well as ROS-independent mechanisms, may explain why doxorubicin treated cells display a modest increase in GPNMB in this work and others [86]. Furthermore, though phenformin is a complex I inhibitor, the observed induction of GPNMB expression may be due to other actions. Phenformin is a known activator of AMPK [242], and as previously discussed AMPK plays a direct role in the transcriptional activation of TFE3/TFEB [113]. Furthermore, loss of FLCN (a negative regulator of AMPK) results in constitutive AMPK activation. FLCN KO cells exhibit upregulated GPNMB expression, suggesting that the activation of AMPK has an impact on GPNMB levels [86, 104]. This agrees with our own data demonstrating that double KO of the

catalytic subunits of AMPK abolishes basal and stress induced GPNMB expression (data not shown). As such, the increased level of GPNMB in phenformin treated cells can most likely be attributed at least in part to direct effects on AMPK.

Within the cell, mtROS represents a considerable proportion of total cellular ROS, and as previously discussed p66ShcA contributes to overall ROS concentrations through the production of mtROS [178,188]. However, a different mechanism of ROS production by p66ShcA may also exist. In MEFs, p66ShcA was demonstrated to inhibit binding of SOS1 to GRB2 through competitive inhibition via the N-terminal p66ShcA CH2 domain. The decreased SOS1 binding to GRB2 in turn increases SOS1-mediated activation of Rac1 [243]. Members of the Rac family, including Rac1 are known to stimulate noxROS production through activation of various NOX isoforms [244]. The authors expanded their observations in a second study to show that though constitutively active Rac1 can produce ROS upstream of p66ShcA, p66ShcA may enhance Rac1-induced ROS, suggesting that Rac1, p66ShcA, and ROS may function in a feedback loop to promote oxidative stress. Intriguingly, in this context, it was determined that phosphorylation of p66ShcA on S54 and threonine 368 was required for downstream function, and not S36 [245]. It is important to note that these studies were conducted in the absence of stress stimuli and did not differentiate between intracellular sources of ROS production. However when considered with our data, this could provide a compelling explanation as to why p66ShcA QQ and p66ShcA SA mutants still were able to produce some intracellular ROS. Perhaps the slight increase in ROS is attributed to impairment of p66ShcA's main source of ROS production (mtROS) without affecting a secondary source (noxROS). It may be interesting to investigate p66ShcA S54 phosphorylation as well as the expression and activity of Rac1 in p66ShcA KO, WT, QQ, and SA cells in the context of our pro-oxidant stimulus.

Intersection of p66ShcA and the TFE3/TFEB Transcriptional Network

TFE3/TFEB have been described as regulators of GPNMB expression [86, 102-103] that are shuttled to the nucleus and transcriptionally activated in response to various cellular stresses, including ROS [86, 122, 125-133]. Our results reflect these findings, as oxidative stress induced GPNMB expression was shown to be dependent on the expression of TFE3/TFEB. This is in accordance with previous work suggesting that TFE3/TFEB are to some degree functionally redundant but are both required for optimal adaptation to stress [94].

An especially compelling finding was the discovery that p66ShcA regulates the localization, activity, and expression of TFE3. Immunofluorescence experiments show that p66ShcA WT expressing cells display high nuclear intensity of TFE3 at 24 and 48h post-treatment and robust induction of mRNA expression of TFE3 transcriptional targets in addition to GPNMB following exposure to ROS. As the nuclear localization of TFE3 in p66ShcA KO and p66ShcA WT cells is comparable between 2 and 6h, it is possible that these early dynamics are p66ShcA-independent. It is likely that exposure to ROS engages other pathways that promote early nuclear translocation of TFE3, given the extensive reports of TFE3/TFEB activation by oxidative stress [86, 122, 125-133]. As such, p66ShcA may promote or sustain the nuclear accumulation of TFE3 at later time points, surpassing a threshold that ultimately upregulates GPNMB in p66ShcA WT expressing cells. The stark differences in TFE3 nuclear positivity and signal strength between p66ShcA KO and p66ShcA WT cells at 24/48h is seemingly in line with our gene and protein expression data, as parental Hs578T cells begin to upregulate GPNMB mRNA at 24h, with visible differences in protein apparent at 48h. Utilizing TCGA data, it is also clear that p66ShcA influences TFE3 expression, as high p66ShcA correlates with high TFE3 expression in the interrogated tumours. A discrepancy in these findings appears to be that in our hands, p66ShcA WT expressing cells do not significantly upregulate *TFE3* mRNA levels. At first glance, this seems at odds with TCGA results. However, this difference can likely be explained partially because TCGA data set is much larger than our study of two TNBC cell lines. Additionally, since TCGA data is derived from patient tumours and our data is from cell models, the microenvironments are likely drastically different. Though cell models are a useful tool in studying various aspects of cancer progression, the context in which we study p66ShcA-dependent regulation of TFE3 is potentially not entirely representative of the highly stressful microenvironment that tumour cells must endure due to the convergence of numerous different cellular stressors. It would also be interesting to characterize TCGA data of TFE3 target genes, such as those used as transcriptional readouts in this study. Should tumours expressing high levels of p66ShcA also exhibit high gene expression of TFE3 transcriptional targets, this would further support the role of p66ShcA in the regulation of both TFE3 levels and activity.

Since our data suggest that TFE3 makes a larger contribution than TFEB to GPNMB upregulation in response to ROS, we selected TFE3 for further investigation in relation to p66ShcA. Still, it may be worthwhile to similarly analyze the localization of TFEB. Since TFEB

is required, albeit less than TFE3, for increased GPNMB expression following $NaAsO_2$ treatment, one would expect to also see increased nuclear accumulation of TFEB in treated cells. However, it is possible that TFEB does not translocate to the nucleus as rapidly, or to the same degree as TFE3, which may explain why TFE3 predominantly regulates GPNMB in this context. Though not experimentally tested, this hypothesis is seemingly supported by recent work from the lab demonstrating that TFE3 is the MiTF/TFE member that is responsible for GPNMB regulation in TNBC models [86, 104]. Interestingly, one of these studies showed that elevated GPNMB levels are heavily dependent on TFE3 in MDA-MB-436 cells, concomitant with increased nuclear intensity of TFE3 in treated cells. Conversely, TFEB was not significantly shuttled to the nucleus, and TFEB depletion prior to treatment under the same conditions did not inhibit GPNMB upregulation [86].

Nevertheless, modulation of TFE3 by p66ShcA uncovered in this work may further rationalize findings from other publications. For example, several studies in recent years have described the adaptor and ROS-producing functions of p66ShcA in the induction of autophagy and mitophagy [202, 246-247]. The pro-autophagic role of p66ShcA in these studies could be explained by the engagement of TFE3/TFEB, thus resulting in the expression of autophagy and lysosomal associated genes. This same train of thought may in part also be responsible for reports of pro- and anti-tumorigenic functions of p66ShcA described previously [190, 197-216]. Given that the effects of ROS and autophagy on cancer progression are highly dependent on stimulus, context, and in the case of ROS, overall levels, the p66ShcA-dependent regulation of TFE3/TFEB could contribute to the conflicting role of these factors in various cancers. It may be interesting to investigate the relationship between p66ShcA, TFE3/TFEB downstream transcriptional activation, and GPNMB in models where p66ShcA appears to have opposing effects, such as in models of primary lung and breast cancer. Furthermore, since p66ShcA engages the TFE3/TFEB transcriptional program, it may be intriguing to extend these observations beyond cancer. TFE3/TFEB have been implicated in various pathological conditions. Any disease that requires clearance of cellular debris, or is intertwined with lysosomal biogenesis or autophagy, could possibly benefit from leveraging p66ShcA-dependent TFE3/TFEB activation. These include but are not limited to neurological disorders, lysosomal storage and metabolic diseases, pathogen infection, autoimmune disorders, and developmental conditions [95-97].

p66ShcA Localizes to Lysosomes in Response to Oxidative Stress

Lastly, using a BioID approach to identify potential protein interactions with p66ShcA, we discovered an enrichment of lysosomal genes in proximity to p66ShcA following exposure to ROS. Gene ontology analysis revealed that 2/7 (almost 30%) of the resulting genes are localized to lysosomes. Using two different immunofluorescence approaches, we validated that p66ShcA localization to lysosomes is enhanced following oxidative stress, as evidenced by increased co-localization signal of p66ShcA or biotinylated proteins with LAMP1-positive organelles. This is a very exciting finding as a lysosomal pool of p66ShcA has never been previously reported. Our data suggests that other isoforms of ShcA (p52) also have the capacity to localize to lysosomes. Given that p66ShcA KO cells or parental cell models of TNBC/BLBC with low or absent p66ShcA can induce GPNMB to some extent, it is possible that p46/p52ShcA may also promote slight GPNMB upregulation; however, it is clear based on data presented in this work that p66ShcA makes the most significant contribution to elevated GPNMB expression under oxidative stress. The novel discovery of p66ShcA localization to the lysosome may also explain the increased levels of GPNMB in p66ShcA SA cells. Since the SA mutation prevents mitochondrial trafficking, perhaps in these cells there is a larger proportion of p66ShcA localizing to the lysosomal surface compared to p66ShcA WT cells. The increased lysosomal pool could explain why GPNMB upregulation in the p66ShcA SA model exceeds that of p66ShcA WT cells.

These findings could prove to be very compelling based on the regulation of TFE3/TFEB at the lysosomal surface. Interestingly, one study has shown that p66ShcA, but not other ShcA isoforms, can inhibit mTORC1. In this publication, loss of p66ShcA resulted in metabolic characteristics that are consistent with chronic mTORC1 activation. In contrast, p66ShcA expression resulted in mTORC1 inhibition and changes to cellular metabolism [249]. However, the specific mechanism through which p66ShcA inhibits the activity of mTORC1 was not characterized in this work. In the context of our experiments, TFE3/TFEB activation could be a result of direct inhibition of mTORC1, or from p66ShcA-dependent effects on other regulatory elements of mTORC1 and/or TFE3/TFEB at the lysosome. mTORC1 activation under nutrient replete conditions involves a variety of lysosomal associated proteins (Figure 1.2). At the lysosome, amino acids promote vacuolar-H^+-ATPase (v-ATPase) interactions with Ragulator, which in turn stimulates Ragulator's guanine nucleotide exchange factor (GEF) activity towards

the Rag A/B GTPases. Similarly, FLCN exhibits GAP activity towards the Rag C/D GTPases. When Rag A/B are bound with Rag C/D, the active complex can then recruit mTORC1 to the lysosomal membrane, where it is activated by the small GTPase Rheb [226]. As such, the dysregulation of any of these regulatory factors has a direct impact on mTORC1 activity, and in extent, may result in the nuclear accumulation and activation of TFE3/TFEB. Some precedence exists for modulation of these components by adaptor proteins. An interesting study identified the SH3 domain-binding protein 4 (SH3BP4) as a negative regulator of Rag GTPases. It was demonstrated that in response to starvation SH3BP4 binds to inactive Rag complexes and inhibits their activation by preventing GTP loading. This in turn disrupts mTORC1 localization to the lysosomal membrane, blocking its activity. Compellingly, in this same study the mechanism was demonstrated to produce downstream activation of autophagy, which can presumably be attributed to active TFE3/TFEB [250]. Another publication has demonstrated that AXIN, a scaffold protein involved in AMPK activation, binds to the v-ATPase and Ragulator in response to glucose starvation. This interaction inhibits the GEF activity of Ragulator on the Rag GTPases, dissociating mTORC1 from the lysosome and inhibiting its activation [251]. In response to oxidative stress, it is possible that p66ShcA is acting in a similar fashion at the lysosome to disrupt a component of mTORC1 regulation.

Potential p66ShcA Interactors: Avenues for Further Characterization of TFE3/TFEB Regulation

Among the genes identified as potential p66ShcA interactors in our BioID screen, FLCN is a particularly intriguing possibility for further investigation. Should p66ShcA traffic to lysosomes following oxidative stress and bind to FLCN, such an interaction could explain the p66ShcA-dependent effects on TFE3 localization, transcriptional target expression, and GPNMB upregulation seen throughout this study.

Mechanistically, p66ShcA binding to FLCN may result in TFE3/TFEB activation and induction of GPNMB in several ways. As discussed, inactivation/KO of FLCN results in constitutive AMPK activation [86, 104] and phosphorylation of TFE3/TFEB on a series of C-terminal serine residues by AMPK, which is required for engagement of TFE3/TFEB transcriptional activity [113]. Binding of p66ShcA to FLCN may render FLCN unable to exert its effects as a negative regulator of AMPK and result in enhanced AMPK phosphorylation of

TFE3/TFEB. However, a more compelling explanation for TFE3/TFEB activation in the context of oxidative stress may be due to the direct effects of FLCN on mTORC1 signaling. As mentioned, FLCN also acts as a GAP for the Rag C/D GTPases, the activation of which in turn recruits mTORC1 to the lysosome [104, 224-226]. Therefore, the inhibition of Rag GTPase-FLCN binding or attenuated GDP loading onto the Rag GTPases, which could potentially be caused by interactions with p66ShcA, would result in mTORC1 inhibition and enhanced TFE3/TFEB nuclear accumulation. Competitive inhibition by p66ShcA could also render FLCN inactive by preventing the formation of the active FLCN complex, comprised of FLCN and folliculin interacting protein 1/2 (FNIP1/2). It has been previously demonstrated that function of the FLCN complex requires FLCN itself and at least one FNIP binding partner (FNIP1 or FNIP2), and that binding of FLCN to AMPK is mediated by FNIP1/2 [104, 252]. Thus, p66ShcA binding to FLCN may also block assembly of the FLCN complex by preventing its interaction with FNIP1/2. Any one of these possibilities could provide a rationale for GPNMB upregulation in response to elevated ROS.

A potential interaction between p66ShcA and FLCN, and the downstream effects on TFE3/TFEB and GPNMB expression is exciting considering previous work on the relationship between FLCN and TFE3. In renal cancer cells, inactivation of FLCN results in TFE3 nuclear localization and transcriptional activity, in turn upregulating GPNMB expression. Expression of WT FLCN in FLCN-null cells consequently reverses this phenotype [102]. Recent work from members of our laboratory has corroborated these findings in models of breast cancer, with loss of FLCN resulting in nuclear translocation of TFE3 and activation of diverse TFE3-dependendent signaling pathways including autophagy and lysosomal biogenesis, angiogenesis, metabolic reprogramming, and most importantly, significant upregulation of GPNMB [86, 104]. Intriguingly, alterations in cellular metabolism, angiogenesis, and tumour growth in FLCN KO models were shown to be dependent specifically on TFE3 [104]. An interaction between p66ShcA and FLCN, potentially causing the inactivation of FLCN, would be in line with these previous findings, as our results demonstrate that TFE3 makes the largest contribution to increased GPNMB expression in response to oxidative stress.

To further characterize p66ShcA-dependent modulation of TFE3/TFEB signaling, it will first be important to validate the acquisition of a p66ShcA-FLCN interaction by immunoprecipitation in $NaAsO_2$ treated cells. Should p66ShcA-FLCN binding be gained or

enhanced in pro-oxidant conditions, it would be interesting to identify the specific region of p66ShcA required for this function. The natural explanation as to why p66ShcA, but not other ShcA isoforms engages the TFE3/TFEB transcriptional program and elevates GPNMB levels would be that p66ShcA interactions with FLCN are mediated through the N-terminal CH2 domain that is unique to p66ShcA. Additional experiments to determine how exactly p66ShcA affects the function of FLCN, whether it be through hindered GAP activity or impaired FNIP1/2 or Rag GTPase binding could serve as the basis for future investigation.

Prognostic and Therapeutic Value of p66ShcA-Dependent GPNMB Regulation

The prognostic importance of p66ShcA expression in breast cancer has been described previously. p66ShcA has been linked to EMT independent of molecular subtype, and thus may be used to predict if tumours will be particularly invasive through gaining a mesenchymal gene signature [212]. Based on our findings, p66ShcA may serve as a predictive biomarker for GPNMB expression in TNBC. Patients within the TNBC subtype who exhibit tumours with high p66ShcA expression may have an even higher propensity to develop metastases, due to the accompanied pro-metastatic phenotypes that may be present because of high endogenous or stress induced GPNMB in the tumour microenvironment.

The results of this thesis may also represent new potential for TNBC therapeutics. Recent work from the Ursini-Siegel lab has shown that in models of TNBC, p66ShcA expression results in increased sensitivity to combination therapy, specifically doxorubicin and PARPi [217]. p66ShcA thus represents a useful biomarker for this treatment approach in TNBC and modulating p66ShcA expression could enhance the synergy between such drugs. Though in this study the ability of p66ShcA to produce ROS was not dispensable for increased cytotoxicity, it is possible that other avenues of TNBC management may not require this function. CDX-011 is an ADC designed to target GPNMB-expressing tumour cells [82]. CDX-011 has been employed in various clinical trials, however its use in women with metastatic TNBC was ceased after it failed to demonstrate improved impacts on survival and response [84], creating heightened interest in CDX-011 combination therapies. As discussed, recent work from our lab has demonstrated enhanced anti-tumour activity of CDX-011 in models of TNBC when combined with therapies that induce the expression of GPNMB such as MAPKi, mTORi, and HSP90i. HSP90i in particular increased not only the levels of GPNMB, but also its delivery to the plasma membrane

through lysosomal scattering. This paper not only validates that therapy-induced stress when combined with CDX-011 improves the targeted cell death of GPNMB expressing cells, but also illustrates the idea that lysosomes, their regulation/localization, and functional components localized at lysosomes are emerging as important aspects of TNBC.

A similar approach to MAPKi/mTORi/HSP90i combination therapy with CDX-011 could be evaluated with $NaAsO_2$. Based on data presented in this thesis, increased GPNMB expression in p66ShcA expressing TNBC/BLBC due to oxidative stress may enhance CDX-011 anti-tumour activity. A phase I evaluation of KML-001, an orally available form of $NaAsO_2$, demonstrated anti-tumour effects when administered with cisplatin to patients with solid tumours that may be sensitive to platinum-based treatments. More than half of the patients enlisted in the trial showed controlled disease for eight weeks or more, however trials were halted due to prevalent cardiac effects. The toxicity seen in this study was proposed to be because of cisplatin amplifying the known effects of arsenical compounds [253]. Nevertheless, administration of KML-001 as a combination therapy is possible, and if the therapy were symptomatically tolerable alongside CDX-011, could potentially inhibit disease progression in TNBC patients that present high expression of p66ShcA. Additional studies have described anti-cancer effects of KML-001 in other pre-clinical cancer models. For example, in prostate cancer cells, KML-001 was shown to inhibit tumour growth in mice and promote apoptosis and autophagy through the activation of oxidative stress [254]. The engagement of autophagy may imply the activation of TFE3/TFEB, and thus increased GPNMB. Therefore, coupling KML-001 with CDX-011 could have a synergistic inhibitory effect on TNBC tumour burden.

Finally, $NaAsO_2$ is not the only ROS-inducing compound that is capable of inducing GPNMB expression. Though the involvement of p66ShcA-dependent ROS generation has not been investigated in the same detail as $NaAsO_2$ in this study, it is quite possible that p66ShcA can exert similar effects on GPNMB in response to other pro-oxidant compounds that induce noxROS or perhaps other diverse cellular stressors, given the role of p66ShcA, TFE3/TFEB, and GPNMB as genes involved in adaptation to stress. For example, As_2O_3 is a trivalent arsenical compound that is the subject of past and present clinical trials in several cancers. Additionally, As_2O_3 is currently employed as a therapeutic in acute promyelocytic leukemia [255] and like $NaAsO_2$, As_2O_3 has been shown to induce oxidative stress through the production of noxROS [256]. Therefore, it is plausible that As_2O_3 could similarly promote upregulation of GPNMB in

TNBC/BLBC models that express p66ShcA. This may present a particular attractive option for therapy as As_2O_3 is already in use clinically and thus certain aspects of the treatment such as toxicity profile are already known, however studies in combination with CDX-011 would certainly be required. As mentioned, doxorubicin primarily exerts its ROS inducing effects through iron or mitochondrial based mechanisms but can also act on NOX to generate ROS which may account for the modest induction of GPNMB reported in this thesis and other published work [86]. It is possible that doxorubicin could stimulate noxROS in p66ShcA expressing tumours, and thus be synergistic with CDX-011. Several other naturally occurring compounds, as well as ROS producing drugs and existing chemotherapies are also being studied for their pro-oxidant functions in various cancers [161]. Clearly, the effects of oxidative stress on cancer progression warrant further investigation. Many of these ROS-inducing compounds or drugs may offer a unique approach for management of metastasis when combined with CDX-011, especially in TNBC/BLBC patients that express p66ShcA.

4.2 Conclusions

Taken together, these experiments have identified a p66ShcA-dependent oxidative stress response that upregulates expression of GPNMB, a pro-metastatic protein in TNBC. TNBC cells expressing p66ShcA exhibit a propensity for higher baseline and ROS-induced GPNMB upregulation, independently of the ability of p66ShcA to localize to the mitochondria or generate mtROS. Given that the GPNMB-targeting ADC CDX-011 is more effective with increased GPNMB expression and cell surface localization, it is possible that p66ShcA expression in TNBC/BLBC patients may serve as a predictive biomarker for response to combination therapies comprised of CDX-011 and a ROS-inducing compound or chemotherapy. p66ShcA modulates GPNMB by regulating the localization and transcriptional activity of TFE3/TFEB, and may do so by translocating to and interacting with lysosomal proteins. To our knowledge, this is the first report of p66ShcA localization to lysosomes under cellular stress and demonstrates a novel intersection of p66ShcA, cellular adaptation to stress and the TFE3/TFEB lysosomal and autophagy gene expression network.

References

1. C.C.S., *Cancerous tumours of the breast.* Toronto, ON: Canadian Cancer Society.
2. C.C.S.A.C in collaboration with the C.C.S, Statistics Canada and the Public Health Agency of Canada, *Canadian Cancer Statistics 2021*. 2021: Toronto, ON: Canadian Cancer Society.
3. Perou, C.M., et al., *Molecular Portraits of Human Breast Tumours.* Nature, 2000. **406**(6797): p. 747-752.
4. Sørlie, T., et al., *Gene expression patterns of breast carcinomas distinguish tumor subclasses with clinical implications*. Proc Natl Acad Sci USA, 2001. **98**(19): p. 10869-10874.
5. Sorlie, T., et al., Proc Natl Acad Sci USA, 2003. *Repeated observation of breast tumor subtypes in independent gene expression data sets* Acad Sci U S A, 2003. **100**(14): p. 8418- 8423.
6. Eliyatkin, N., et al., *Molecular Classification of Breast Carcinoma: From Traditional, Old-Fashioned Way to A New Age, and A New Way.* J Breast Health, 2015. **11**(2). p. 59-66.
7. Bhushan, A., et al., *Current State of Breast Cancer Diagnosis, Treatment and Theranostics.* Pharmaceutics, 2021. **13**(5). p. 723.
8. Wang, J., and Xu B., *Targeted therapeutic options and future perspectives for HER2-positive breast cancer.* Signal Transduct Target Ther, 2019. **4**(34).
9. Gupta, G.K., Collier, A.L., Lee, D., et al., *Perspectives on Triple-Negative Breast Cancer: Current Treatment Strategies, Unmet Needs, and Potential Targets for Future Therapies.* Cancers (Basel), 2020. **12**(9). p. 2392.
10. Pal, S.K., et al., *Triple negative breast cancer: unmet medical needs.* Breast Cancer Res Treat, 2011. **125**(3). p. 627-636.
11. Zuzana, S., et al., *Genetic Markers in Triple-Negative Breast Cancer.* Clin Breast Cancer, 2018. **18**(5). p. 841-850.
12. Prat, A., et al., *Phenotypic and molecular characterization of the claudin-low intrinsic subtype of breast cancer.* Breast Cancer Res, 2010. **12**(5). R68.

13. Dent, R., et al., *Triple-Negative Breast Cancer: Clinical Features and Patterns of Recurrence.* Clin Cancer Res, 2007. **13**(15). p. 4429-4434.
14. Bianchini, G., et al. *Triple-negative breast cancer: challenges and opportunities of a heterogeneous disease.* Nat Clin Rev Oncol, 2017. **13**(11). p. 674-690.
15. Lehmann B.D., et al., *Identification of human triple-negative breast cancer subtypes and pre-clinical models for selection of targeted therapies.* J Clin Invest, 2011. **121**(7). p. 2750-2767.
16. Chaffer C.L., and Weinberg R.A., *A Perspective on Cancer Cell Metastasis.* Science, 2011. **331**(6024). p. 1559-1564.
17. Majidpoor, J., and Mortezaee, K., *Steps in metastasis: an updated review.* Medical Oncology, 2021. **38**(3).
18. Lambert, A.W., Pattabiraman, D.R., Weinberg R.A., *Emerging Biological Principles of Metastasis.* Cell, 2017. **168**(4). p. 670-691.
19. Thiery J.P., *Epithelial-mesenchymal transitions in tumour progression.* Nat Rev Cancer, 2002. **2**(6). p.442-454
20. Kim, Y.N., et al., *Anoikis resistance: an essential prerequisite for tumor metastasis.* Int J Cell Biol, 2012. 306879.
21. Klein, C.A., *Parallel progression of primary tumours and metastases.* Nature Reviews Cancer, 2009. **9**(4). p.302-312.
22. Ghajar, C.M., Bissell, M.J., *Pathways of parallel progression.* Nature, 2016. **540**(7634). p. 528-529.
23. Peinado, H., Zhang, H., Matei, I., et al., *Pre-metastatic niches: organ-specific homes for metastases.* Nat Rev Cancer, 2017. **17**(5). p. 302-317
24. Paget, S., *The Distribution of Secondary Growths in Cancer of the Breast.* Lancet Oncol, 1889. **133**(3421). p.571-573.
25. A.C.S, *Survival Rates for Breast Cancer.* American Cancer Society.
26. Weigelt, B., Peterse, J.L., van't Veer, L.J., *Breast cancer metastasis: markers and models.* Nat Rev Cancer, 2005. **5**(8). p. 591-602.
27. Liang, Y., et al., *Metastatic heterogeneity of breast cancer: Molecular mechanism and potential therapeutic targets.* Semin Cancer Biol, 2020. **60**. p. 14-27.

28. Gong, Y., et al., *Impact of molecular subtypes on metastatic breast cancer patients: a SEER population-based study.* Sci Rep, 2017. **7.** p.45411.
29. Molnár, I.A., Molnár, B.A., Vízkeleti, L. et al., *Breast carcinoma subtypes show different patterns of metastatic behavior.* Virchows Arch, 2017. **470**(3). p. 275-283.
30. Yao, Y., Chu, Y., et al., *Risk factors for distant metastasis of patients with primary triple-negative breast cancer.* Biosci Rep, 2019. **39**(6). BSR20190288
31. Liedtke, C., et al., *Response to neoadjuvant therapy and long-term survival in patients with triple-negative breast cancer.* J Clin Oncol, 2008. **26**(8). p. 1275-1281. n
32. Dent, R., et al., *Triple-negative breast cancer: clinical features and patterns of recurrence.* Clin Cancer Res, 2007. **13**(15 pt 1). p. 4429-4434.
33. Shen, M., et al., *A review of current progress in triple-negative breast cancer therapy.* Open Med (Wars), 2020. **15**(1). p. 1143-1149.
34. Carey, L.A., et al., *The triple negative paradox: primary tumor chemosensitivity of breast cancer subtypes.* Clin Cancer Res, 2007. **13**(8). p. 2329-2334.
35. O'Reilly, D., Al Sendi, M., and Kelly, C.M., *Overview of recent advances in metastatic triple negative breast cancer.* World J Clin Oncol, 2021. **12**(3). p. 164-182.
36. Schmid, P., et al., IMpassion130 Investigators. *Atezolizumab plus nab-paclitaxel as first-line treatment for unresectable, locally advanced or metastatic triple-negative breast cancer (IMpassion130): updated efficacy results from a randomised, double-blind, placebo-controlled, phase 3 trial.* Lancet Oncol, 2020. **21**(1). p. 44-59
37. Bergin, A.R.T., and Loi, S., *Triple-negative breast cancer: recent treatment advances.* F1000Res, 2019. **8**. F1000 Faculty Rev-1342.
38. Vagia, E., Mahalingam, D., and Cristofanilli, M., *The Landscape of Targeted Therapies in TNBC.* Cancers (Basel), 2020. **12**(4). p. 916.
39. Singh, D.D., Parveen, A., and Yadav, D.K., *Role of PARP in TNBC: Mechanism of Inhibition, Clinical Applications and Resistance.* Biomedicines, 2021. **9**(11). p. 1512.
40. Rose, M., et al., *PARP Inhibitors: Clinical Relevance, Mechanisms of Action and Tumor Resistance.* Front Cell Dev Biol, 2020. **8**. 564601.
41. Robson, M. et al., *Olaparib for Metastatic Breast Cancer in Patients with a Germline BRCA Mutation.* N Engl J Med, 2017. **377**(6). p. 523-533.

42. Khongorzul, P., et al., *Antibody-Drug Conjugates: A Comprehensive Review.* Mol Cancer Res, 2020. **18**(1). p. 3-19.
43. Goldenberg, D.M., Stein, R., and Sharkey, R.M., *The emergence of trophoblast cell-surface antigen 2 (TROP-2) as a novel cancer target.* Oncogene, 2018. **9**(48). p. 28989-29006.
44. Bardia, A., et al., *Sacituzumab Govitecan-hziy in Refractory Metastatic Triple-Negative Breast Cancer.* N Engl J Med, 2019. **380**(8). p. 741-751.
45. Carey, L.A., et al., *TBCRC 001: randomized phase II study of cetuximab in combination with carboplatin in stage IV triple-negative breast cancer.* J Clin Oncol, 2012. **30**(21). p. 2615-2623.
46. Cameron, D., et al., *Adjuvant bevacizumab-containing therapy in triple-negative breast cancer (BEATRICE): primary results of a randomised, phase 3 trial.* Lancet Oncol, 2013. **14**(10). p. 933-942.
47. Schmid, P., et al., *Capivasertib Plus Paclitaxel Versus Placebo Plus Paclitaxel As First-Line Therapy for Metastatic Triple-Negative Breast Cancer: The PAKT Trial.* J Clin Oncol, 2020. **38**(5). p. 423-433.
48. Traina, T.A., et al., *Enzalutamide for the Treatment of Androgen Receptor-Expressing Triple-Negative Breast Cancer.* J Clin Oncol, 2018. **36**(9). p.884-890.
49. Wisinski, K.B., et al., *Targeting Estrogen Receptor Beta in a Phase 2 Study of High-Dose Estradiol in Metastatic Triple-Negative Breast Cancer: A Wisconsin Oncology Network Study.* Clin Breast Cancer, 2016. 1**6**(4). p. 256-261.
50. Weterman, M.A., et al., *nmb, a novel gene, is expressed in low-metasatic human melanoma cell lines and xenografts.* Int J Cancer, 1995. **60**(1). p. 73-81.
51. Safadi, F.F., et al., *Cloning and characterization of osteoactivin, a novel cDNA expressed in osteoblasts.* J Cell Biochem, 2001. **84**(1). p. 12-26.
52. Shikan, S., et al., *Molecular cloning of a dendritic cell-associated transmembrane protein, DC-HIL, that promotes RGD-dependent adhesion of endothelial cells through recognition of heparan sulfate proteoglycans.* J Biol Chem, 2001. **276**(11). p. 8125-34.
53. Bandari, P.S., Qian, J., Yehia, G., et al., *Hematopoietic growth factor inducible neurok inin-1 type: a transmembrane protein that is similar to neurokinin 1 interacts with substance P.* Regul Pept, 2003. **111**(1-3). p. 169-178.

54. Turque, N., et al., *Characterization of a new melanocyte-specific gene (QNR-71) expressed in v-*myc*-transformed quail neuroretina.* EMBO J, 1996. **15**(13). p. 3338-3350
55. Kuan, C-T., et al., *Glycoprotein Nonmetastatic Melanoma Protein B, a Potential Molecular Therapeutic Target in Patients with Glioblastoma Multiforme.* Clin Cancer Res, 2006. **12**(7 pt 1). p. 1970-1982.
56. Onoufriadis, A., et al., *Semidominant GPNMB Mutations in Amyloidosis Cutis Dyschromica.* J Invest Dermatol, 2019. **139**(12). p. 2550-2554.
57. Hoashi, T., Sato, S., et al., *Glycoprotein nonmetastatic protein b, a melanocytic cell marker, is a melanosome-specific and proteolytically released protein.* FASEB L, 2010. **24**(5). p. 1616-1629.
58. Selim, A.A. *Osteoactivin bioinformatic analysis: prediction of novel functions, structural features, and modes of action.* Med Sci Monit, 2009. **15**(2). MT 19-33.
59. Maric, G., et al., *Glycoprotein non-metastatic b (GPNMB): A metastatic mediator and emerging therapeutic target in cancer.* Onco Targets Ther, 2013. **6.** p. 839-852.
60. Tsou, P-S., Sawalha, A.H., *Glycoprotein nonmetastatic melanoma protein B: A key mediator and an emerging therapeutic target in autoimmune diseases.* FASEB J, 2020. **34**(7). p. 8810-8823.
61. Chrystal, P.W., Footz, T., et al., *Functional Domains and Evolutionary History of the PMEL and GPNMB Family Proteins.* Molecules, 2021. **26**(12). 3529.
62. Chung, J-S., et al., *Binding of DC-HIL to dermatophytic fungi induces tyrosine phosphorylation and potentiates antigen presenting cell function.* J Immunol, 2009. **183**(8). p. 5190-5198.
63. Lin, A., Li, C., Xing, Z., et al., *The LINK-A lncRNA Activates Normoxic HIF1α Signaling in Triple-Negative Breast Cancer.* Nat Cell Biol, 2016. **18**(2). p. 213-224.
64. Furochi, H., et al., *Osteoactivin fragments produced by ectodomain shedding induce MMP-3 expression via ERK pathway in mouse NIH-3T3 fibroblasts.* FEBS Lett, 2007. **581**(30). p. 5743-5750.
65. Taya, M., and Hammes, S.R., *Glycoprotein Non-Metastatic Melanoma Protein B (GPNMB) and Cancer: A Novel Potential Therapeutic Target.* Steroids, 2018. **133.** p. 102-107.

66. Huang, Y-H., Chu, P-Y., et al., *Expression pattern and prognostic impact of glycoprotein non-metastatic B (GPNMB) in triple-negative breast cancer.* Sci Rep, 2021. **11.** 12171.
67. Rose, A.A.N., et al., *Targeting GPNMB with glembatumumab vedotin: Current developments and future opportunities for the treatment of cancer.* Pharmacol Ther, 2017. **179.** p. 127-141.
68. Raggi, C., Correnti, M., et al., *Cholangiocarcinoma stem-like subset shapes tumor-initiating niche by educating associated macrophages.* J Hepatol, 2017. **66**(1). p. 102-115.
69. Xu, S., Fan, Y., et al., *Glycoprotein nonmetastatic melanoma protein B accelerate tumorigenesis of cervical cancer* in vitro *by regulating the Wnt/β-catenin pathway.* Braz J Med Biol Res, 2018. **52**(1). e7567.
70. Ma, R-Q., Tang, Z-J., Ye, X., et al., *Overexpression of GPNMB predicts an unfavorable outcome of epithelial ovarian cancer.* Arch Gynecol Obstet, 2018. **297.** p. 1235-1244.
71. Wang, Z., Ran, X., et al., *GPNMB promotes the progression of diffuse large B cell lymphoma via YAP1-mediated activation of the Wnt/β-catenin signaling pathway.* Arch Biochem Biophys, 2021. **710**. 108998.
72. Rose, A.A.N., et al., *Osteoactivin promotes breast cancer metastasis to bone.* Mol Cancer Res, 2007. **5**(10). p. 1001-1014.
73. Rose, A.A., Annis, M.G., et al., *ADAM10 Releases a Soluble Form of the GPNMB/Osteoactivin Extracellular Domain with Angiogenic Properties.* PLoS One, 2010. **5**(8). e12093.
74. Tabariès, S., et al., *Claudin-2 is selectively enriched in and promotes the formation of breast cancer liver metastasis through engagement of integrin complexes.* Oncogene, 2011. **30**(11). p. 1318-1328.
75. Rose, A.A., et al., *Glycoprotein Nonmetastatic B Is an Independent Prognostic Indicator of Recurrence and a Novel Therapeutic Target in Breast Cancer.* Clin Cancer Res, 2010. **16**(7). p. 2147-2156.
76. Yardley, D.A., et al., *EMERGE: A Randomized Phase II Study of the Antibody-Drug Conjugate Glembatumumab Vedotin in Advanced Glycoprotein NMB-Expressing Breast Cancer*. **33**(14). p. 1609-1619.

77. Okita, Y., et al., *The transcription factor MAFK induces EMT and malignant progression of triple-negative breast cancer cells through its target GPNMB.* Sci Signal, 2017. **10**(474). Eaak9397.
78. Maric, G., et al., *GPNMB cooperates with neuropilin-1 to promote mammary tumour growth and engages integrin $\alpha_5\beta_1$ for efficient breast cancer metastasis.* Oncogene, 2015. **34**(43). p. 5494-5504.
79. Maric, G., et al., GPNMB augments Wnt-1 mediated breast tumour initiation by enhancing PI3K/AKT/mTOR pathway signaling and *β-catenin activity.* Oncogene, 2019. **38**(26). p. 5294-5307.
80. Xie, R., Okita, Y., Ichikawa, Y., et al., *Role of the kringle-like domain in glycoprotein NMB for its tumorigenic potential.* Cancer Sci, 2019. **110**(7). p. 2237-2246.
81. Chung, J-S., et al., *Syndecan-4 mediates the co-inhibitory function of DC-HIL on T cell activation.* J Immunol, 2007. **179**(9). p. 5778-5784.
82. Tse, K.F., et al., *CR011, a fully human monoclonal antibody-auristatin E conjugate, for the treatment of melanoma.* Clin Cancer Res, 2006. **12**(4). p. 1373-1382.
83. Bendell, J., et al., *Phase I/II Study of the Antibody-drug Conjugate Glembatumumab Vedotin in Patients with Locally Advanced or Metastatic Breast Cancer.* J Clin Oncol, 2014. **32**(32). p. 3619-3625.
84. Vahdat, L.V., Schmid, P., et al., *Glembatumumab vedotin for patients with metastatic, gpNMB overexpressing, triple-negative breast cancer ("METRIC"): a randomized multicenter study.* NPJ Breast Cancer, 2021. **7**(1). 57.
85. Rose, A.A.N., et al., *MAPK Pathway Inhibitors Sensitize BRAF Mutant Melanoma to an Antibody-Drug Conjugate Targeting GPNMB.* Clin Cancer Res, 2016. **22**(24). p. 6088-6098.
86. Biondini, M., et al., *HSP90 inhibitors induce GPNMB cell-surface expression by modulating lysosomal positioning and sensitize breast cancer cells to glembatumumab vedotin*. Oncogene, 2022.
87. Saade, M., et al., *The Role of GPNMB in Inflammation.* Front Immunol, 2021. **12**. 674739.
88. Hetmańczyk-Sawicka, K., et al., *Changes in global gene expression indicate disordered autophagy, apoptosis and inflammatory processes and downregulation of cytoskeletal*

signalling and neuronal development in patients with Niemann-Pick C disease. Neurogenetics, 2020. **21**(2). p. 105-119.

89. Moloney, E.B., et al., *The glycoprotein GPNMB is selectively elevated in the substantia nigra of Parkinson's disease patients and increases after lysosomal stress.* Neurobiol Dis, 2018. **120**. p.1-11.
90. Gabriel, T.L., et al., *Lysosomal stress in obese adipose tissue macrophages contributes to MITF-dependent Gpnmb induction.* Diabetes, 2014. **63**(10). p. 3310-3323.
91. Noda, Y., Tsuruma, K., Takata, M., et al., *GPNMB Induces BiP Expression by Enhancing Splicing of* BiP *Pre-mRNA during the Endoplasmic Reticulum Stress Response.* Sci Rep, 2017. **7**. 12160.
92. Lu, Y., Zhou, D., et al., *Investigating a downstream gene of Gpnmb using the system genetics method.* Mol Vis, 2019. **25**. p. 222-236.
93. Hemesath, T.J., et al., *microphthalmia, a critical factor in melanocyte development, defines a discrete transcription factor family.* Genes Dev, 1994. **8**(22). p. 2770-2780.
94. Martina, J.A., et al., *The Nutrient-Responsive Transcription Factor TFE3, Promotes Autophagy, Lysosomal Biogenesis, and Clearance of Cellular Debris.* Sci Signal, 2014. **7**(309). ra9.
95. La Spina, M., Contreras, P.S., et al., *MiT/TFE Family of Transcription Factors: An Evolutionary Perspective.* Front Cell Dev Biol, 2021. **8.** 609683.
96. Raben, N., and Puertollano, R. *TFEB and TFE3, Linking Lysosomes to Cellular Adaptation to Stress.* Annu Rev Cell Dev Biol, 2016. **32.** p. 255-278.
97. Ramirez Reyes, J.M.J., Cuesta, R., and Pause, A., *Folliculin: A Regulator of Transcription Through AMPK and mTOR Signaling Pathways.* Front Cell Dev Biol, 2021. **9.** 667311.
98. Sardiello, M., et al., *A Gene Network Regulating Lysosomal Biogenesis and Function.* Science, 2009. **325**(5939). p. 474-477.
99. Yun, C.W., and Lee, S.H., *The Roles of Autophagy in Cancer.* Int J Mol Sci, 2018. **19**(11). 3466.
100. Eichner, L.J., et al., *Genetic analysis reveals AMPK is required to support tumour growth in murine Kras-dependent lung cancer models.* Cell Metab, 2019. **29**(2). p. 285-302.

101. Kundu, S.T., Grzeskowiak, C.L., et al., *TMEM106B drives lung cancer metastasis by inducing TFEB-dependent lysosome synthesis and secretion of cathepsins.* Nat Commun, 2018. **9.** 2731.

102. Hong, S.B., et al., *Inactivation of the FLCN Tumor Suppressor Gene Induces TFE3 Transcriptional Activity by Increasing Its Nuclear Localization.* PLoS One, 2010. **5**(12). e15793

103. Baba, M., et al., *TFE3 Xp11.2 translocation renal cell carcinoma mouse model reveals novel therapeutic targets and identifies GPNMB as a diagnostic marker for human disease.* Mol Cancer Res, 2019. **17**(8). p. 1613-1626.

104. El-Houjeiri, L., Biondini, M., et al., *Folliculin impairs breast tumour growth by repressing TFE3-dependent induction of the Warburg effect and angiogenesis.* J Clin Invest, 2021. **131**(22). e144871.

105. Puertollano, R., et al., *The complex relationship between TFEB transcription factor phosphorylation and subcellular localization.* EMBO J, 2018. **37**(11). e98804.

106. Martina, J.A., Puertollano, R., *Rag GTPases mediate amino acid-dependent recruitment of TFEB and MITF to lysosomes.* J Cell Biol, 2013. **200**(4). p. 475-491.

107. Martina, J.A., et al., *MTORC1 functions as a transcriptional regulator of autophagy by preventing nuclear transport of TFEB.* Autophagy, 2012. **8**(6). p. 903-914.

108. Roczniak-Ferguson, A., et al., *The transcription factor TFEB links mTORC1 signaling to transcriptional control of lysosomes homeostasis.* Sci Signal, 2012. **5**(228). ra42.

109. Settembre, C., Zoncu, R., et al., *Lysosome-to-nucleus signalling mechanism senses and regulates the lysosome via mTOR and TFEB.* EMBO J, 2012. **31**(5). p. 1095-1108.

110. Medina, D.L., et al., *Lysosomal calcium signalling regulates autophagy through calcineurin and TFEB.* Nat Cell Biol, 2015. **17**(3). p. 288-299.

111. Napolitano, G., et al., *mTOR-dependent phosphorylation controls TFEB nuclear* export. Nat Commun, 2018. **9.** 3312.

112. Vega-Rubin-de-Celis, S., et al., *Multistep regulation of TFEB by MTORC1.* Autophagy, 2017. 1**3**(3). p. 464-472.

113. Paquette, M., et al., *AMPK-dependent phosphorylation is required for transcriptional activity of TFEB and TFE3.* Autophagy, 2021. **17**(12). p. 3957-3975.

114. *Settembre, C., TFEB Links Autophagy to Lysosomal Biogenesis.* Science, 2011. **332**(6036). p. 1429-1433.
115. Li Y., et al., *Protein kinase C controls lysosome biogenesis independently of mTORC1.* Nat Cell Biol, 2016. **18**(10). p. 1065-1077.
116. Li, L., Friedrichsen, H.J., et al., *A TFEB nuclear export signal integrates amino acid supply and glucose availability.* Nat Commun, 2018. **9**(1). 2685.
117. Ferron, M., et al., *A RANKL-PKCβ-TFEB signaling cascade is necessary for lysosomal biogenesis in osteoclasts.* Genes Dev, 2013. **27**(8). p. 955-969.
118. Nezich, C.L., et al., *MiT/TFE transcription factors are activated during mitophagy downstream of Parkin and Atg5.* J Cell Biol, 2015. **210**(3). p. 435-450.
119. Pi, H., Li, M., Zou, L., et al., *AKT inhibition-mediated dephosphorylation of TFE3 promotes overactive autophagy independent of MTORC1 in cadmium-exposed bone mesenchymal stem cells.* Autophagy, 2018. **15**(4). p. 565-582.
120. Palmieri, M, et al., *mTORC1-independent TFEB activation via Akt inhibition promotes cellular clearance in neurodegenerative storage disease.* Nat Commun, 2017. **8**. 14338.
121. Martina, J.A., et al., *TFEB and TFE3 are novel components of the integrated stress response.* EMBO J, 2016. **35**(5). p. 479-495.
122. Martina, J.A., et al., and Puertollano, R., *Protein phosphatase 2A stimulates activation of TFEB and TFE3 transcription factors in response to oxidative stress.* J Biol Chem, 2018. **293**(32). p. 12525-12534.
123. Nakamura, H., and Takada, K., *Reactive oxygen species in cancer: Current findings and future directions.* Cancer Sci, 2021. **112**(10). p. 3945-3952.
124. Pham, H.Q., et al., *MTMR4, a phosphoinositide-specific 3'-phosphatase, regulates TFEB activity and the endocytic and autophagic pathways.* Genes Cells, 2018. **23**(8). p. 670-687.
125. Zhang, X., Cheng, X., Yu, L., et al., *MCOLN1 is a ROS Sensor in lysosomes that regulates autophagy.* Nat Commun, 2016. **7.** 12109.
126. La Spina, M., et al., *Multiple Mechanisms Converging on Transcription Factor EB Activation by the Natural Phenol Pterostilbene.* Oxid Med Cell Longev, 2021. **2021.** 7658501.

127. Fang, S., Wan, X., Zou, X., et al., *Arsenic trioxide induces macrophage autophagy and atheroprotection by regulating ROS-dependent TFEB nuclear translocation and AKT/mTOR pathway.* Cell Death Dis, 2021. **12**(1). 88.
128. Leow, S.M., et al., *Sub-lethal stress induces lysosome biogenesis via a lysosomal membrane permeabilization-cathepsin-caspase 3-transcription factor EB-dependent pathway.* Oncotarget, 2017. **8**(10). p. 16170-16189.
129. Wu, B., Tan, M., et al., *Arsenic trioxide induces autophagic cell death in osteosarcoma cells via the ROS-TFEB signaling pathway.* Biochem Biophys Res Commun, 2018. **496**(1). p. 167-175.
130. Zhang, M., et al., *Blockage of Extracellular Signal-Regulated Kinase Exerts an Antitumor Effect via Regulating Energy Metabolism and Enhances the Efficacy of Autophagy Inhibitors by Regulating Transcription Factor EB Nuclear Translocation in Osteosarcoma.* Front Cell Dev Biol, 2021. **9.** 650846.
131. Deng, F., et al., *Suppressing ROS-TFE3-dependent autophagy enhances ivermectin-induced apoptosis in human melanoma cells.* J Cell Biochem, 2018. **120**(2). p. 1702-1715.
132. Tan, M., Wu, A., et al., *Inhibiting ROS-TFE3-dependent autophagy enhances the therapeutic response to metformin in breast cancer.* Free Radic Res, 2018. **52**(8). p. 872-886.
133. Wang, H., Wang, N., Xu, Q., et al., *Oxidation of multiple MiT/TFE transcription factors links oxidative stress to transcriptional control of autophagy and lysosome biogenesis.* Autophagy, 2019. **16**(9). p. 1683-1696.
134. Ray, P.D., Huang, B-W., and Tsuji, Y., *Reactive oxygen species (ROS) homeostasis and redox regulation in cellular signaling.* **24**(5). p. 981-990.
135. Nolfi-Donegan, D., Braganza, A., and Shiva, S., *Mitochondrial electron transport chain: Oxidative phosphorylation, oxidant production, and methods of measurement.* Redox Biol, 2020. **37.** 101674.
136. Fenton, H.J.H., *LXXIII. – Oxidation of Tartaric Acid in presence of Iron.* J Chem Soc, 1894. **65.** p. 899-910.
137. Beyersmann, D., and Hartwig, A., *Carcinogenic metal compounds: recent insight into molecular and cellular mechanisms.* Arch Toxicol, 2008. **82**(8). p. 493-512.

138. Villalpando-Rodriguez, G.E., and Gibson, S.B., *Reactive Oxygen Species (ROS Regulates Different Types of Cell Death by Acting as a Rheostat.* Oxid Med Cell Longev, 2021. **2021.** 9912436.
139. Weinberg, F., Ramnath, N., and Nagrath, D., *Reactive Oxygen Species in the Tumor Microenvironment: An Overview*. Cancers (Basel), 2019. **11**(8). 1191.
140. Magnani, F., and Mattevi, A., *Structure and mechanisms of ROS generation by NADPH oxidases.* Curr Opin Struct Biol, 2019. **59.** p. 91-97.
141. Meitzler, J.L., et al., *NADPH Oxidases: A Perspective on Reactive Oxygen Species Production in Tumour Biology.* Antioxid Redox Signal, 2014. **20**(17). p. 2873-2889.
142. Phaniendra, A., Jestadi, D.B., and Periyasamy, L., *Free Radicals: Properties, Sources, Targets, and Their Implication in Various Diseases.* Indian J Clin Biochem, 2015. **30**(1). p. 11-26.
143. Dikalov, S., *Crosstalk between mitochondria and NADPH oxidases.* Free Radic Biol Med, 2011. **51**(7). p. 1289-1301.
144. Mustapha, N.M., et al., *NADPH Oxidase* versus *Mitochondria-Derived ROS in Glucose-Induced Apoptosis of Pericytes in Early Diabetic Retinopathy.* J Opthalmol, 2010. **2010.** 746978.
145. Lin, N., et al., *Mitochondrial reactive oxygen species (ROS) inhibition ameliorates palmitate-induced INS-1 beta cell death.* Endocrine, 2012. **42**(1). p. 107-117.
146. Weinberg, F., and Chandel, N.S., *Reactive oxygen species-dependent signaling regulates cancer.* Cell Mol Life Sci, 2009. **66**(23). p. 3663-3673.
147. Cerutti, P.A., *Prooxidant states and tumor promotion.* Science, 1985. **227**(4685). p. 375-381.
148. Chandel, N.S., et al., *Reactive oxygen species generated at mitochondrial complex III stabilize hypoxia-inducible factor-1alpha during hypoxia: a mechanism of O2 sensing.* J Biol Chem, 2000. **275**(33). p. 25130-25138.
149. Semenza, G.L., *HIF-1 and tumor progression: pathophysiology and therapeutics.* Trends Mol Med, 2002. **8**(4 Suppl). p. S62-67.
150. Traore, K., et al., *Redox-Regulation of ERK 1/2- Directed Phosphatase by Reactive Oxygen Species.* J Cell Physiol, 2008. **216**(1). p. 276-285.

151. Leslie, N.R., et al., *Redox regulation of PI3-kianse signalling via inactivation of PTEN.* EMBO J, 2003. **22**(20). p. 5501-5510.
152. Yellaturu, C.R., et al., *N-Ethylmaleimide inhibits platelet-derived growth factor BB-stimulated Akt phosphorylation via activation of protein phosphatase 2A.* J Biol Chem, 2002. **277**(42). p. 40148-40155.
153. Lischper, M., et al., *Metalloproteinase mediated occluding cleavage in the cerebral micropillary endothelium under pathological conditions.* Bain Res, 2010. **1326.** p. 114-127.
154. Lee, S.Y., et al., *Reactive oxygen species induce epithelial-mesenchymal transition, glycolytic switch, and mitochondrial repression through the Dlx-2/Snail signaling pathways in MCF-7 cells.* Mol Med Rep, 2019. **20**(3). p. 2339-2346.
155. Su, X., et al., *NOX4-Derived ROS Mediates TGF-β1-Induced Metabolic Reprogramming during Epithelial-Mesenchymal Transition through the PI3K/AKT/HIF-1α Pathway in Glioblastoma.* Oxid Med Cell Longev, 2021. **2021.** 5549047.
156. Liu, R-M., and Desai, L.P., *Reciprocal regulation of TGF-β and reactive oxygen species: A perverse cycle for fibrosis.* Redox Biol, 2015. **6.** p. 565-577.
157. Okon, I.S., and Zou, M-H., *Mitochondrial ROS and cancer drug resistance: Implications for therapy.* Pharmacol Res, 2015. **100.** p. 170-174.
158. Wang, Y., et al., *The double-edged roles of ROS in cancer prevention and therapy.* Theranostics, 2021. **11**(10). p. 4839-4857.
159. Takahashi, A., et al., *Mitogenic signalling and the p16^{INK4a}-Rb pathway cooperate to enforce irreversible cellular senescence.* Nat Cell Biol, 2006. **8**(11). p. 1291-1297.
160. Szatrowski, T.P., and Nathan, C.F., *Production of Large Amounts of Hydrogen Peroxide by Human Tumor Cells.* Cancer Res, 1991. **51**(3). p. 794-798.
161. Venugopal, R., and Jaiswal, A.K., *Nrf1 and Nrf2 positively and c-Fos and Fra1 negatively regulate the human antioxidant response element-mediated expression of NAD(P)H:quinone oxidoreductase1 gene.* Proc Natl Acad Sci USA, 1996. **93**(25). p. 14960-14965.
162. DeNicola, G.M., et al., *Oncogene-induced Nrf2 transcription promotes ROS detoxification and tumorigenesis.* Nature, 2011. **475**(7354). p. 106-109.

163. Fuchs-Tarlovsky, V., *Role of antioxidants in cancer therapy.* Nutrition, 2013. **29**(1). p. 15-21.

164. Poljsak, B., and Milisav, I., *The Role of Antioxidants in Cancer, Friends or Foes?* Curr Pharm Des, 2018. **24**(44). p. 5234-5244

165. Sarmiento-Salinas, F.L., et al., *Breast Cancer Subtypes Present a Differential Production of Reactive Oxygen Species (ROS) and Susceptibility to Antioxidant Treatment*. Front Oncol, 2019. **9.** 480.

166. Pelicci, G., et al., *A novel transformation protein (SHC) with an SH2 domain is implicated in mitogenic signal transduction.* Cell, 1992. **70**(1). p. 93-104.

167. Ursini-Siegel, J., and Muller, W.J., *The ShcA adaptor protein is a critical regulator of breast cancer progression.* Cell Cycle, 2008. **7**(13). p. 1936-1943.

168. Bhat, S.S., Anand, D., and Khanday, F.A., *p66Shca as a switch in bringing about contrasting responses in cell growth: implications on cell proliferation and apoptosis.* Mol Cancer, 2015. **14**(76).

169. Migliaccio, E., et al., *Opposite effects of the p52shc/p46shc and p66shc splicing isoforms on the EGF receptor-MAP kinase-fos signalling pathway*. EMBO J, 1997. **16**(4). p. 706-716.

170. Blaikie, P., et al., *A region in Shc distinct from the SH2 domain can bind tyrosine-phosphorylated growth factor receptors*. J Biol Chem, 1994. **269**(51). p. 32031-32034.

171. van der Geer, P., et al., *The Shc adaptor protein is highly phosphorylated at conserved, twin tyrosine residues (Y239/240) that mediate protein-protein interactions*. Curr Biol, 1996. **6**(11). p. 1435-1444.

172. Rozakis-Adcock, M., et al., *Association of the Shc and Grb2/Sem5 SH2-containing proteins is implicated in activation of the Ras pathway by tyrosine kinases.* Nature, 1992. **360.** p. 689-692.

173. Rozakis-Adcock, M., et al., *The SH2 and SH3 domains of mammalian Grb2 couple the EGF receptor to the Ras activator mSos1.* Nature, 1993. **363**(6424). p. 83-85.

174. Gotoh, N., Toyoda, M., and Shibuya, M., *Tyrosine phosphorylation sites at amino acids 239 and 240 of Shc are involved in epidermal growth factor-induced mitogenic signaling that is distinct from Ra/mitogen-activated protein kinase activation*. Mol Cell Biol, 1997. **17**(4). p. 1824-1831.

175. Ursini-Siegel, J., et al., *ShcA signalling is essential for tumor progression in mouse models of human breast cancer*. EMBO J, 2008. **27**(6). p. 910-920.
176. Pacini, S., et al., *p66SHC Promotes Apoptosis and Antagonizes Mitogenic Signaling in T Cells.* Mol Cell Biol, 2004. **24**(4). p. 1747-1757.
177. Lai, K.M., and Pawson, T., *The ShcA phosphotyrosine docking protein sensitizes cardiovascular signaling in the mouse embryo.* Genes Dev. 2000. **14**(9). p. 1132-1145.
178. Migliaccio, E., et al., *The p66ShcA adaptor protein controls oxidative stress response and life span in mammals.* Nature, 1999. **402**(6759). p. 309-313.
179. Basya, A., et al., *The p66ShcA adaptor protein regulates healing after myocardial infarction.* Basic Res Cardiol, 2015. **110**(2). 13.
180. Liu, B., et al., *Knockdown of p66ShcA activates Nrf2 pathway to protect cardiomyocytes from oxidative stress and inflammation induced by H2O2*. Eur Rev Med Pharmacol Sci, 2020. **24**(12). p. 6994-7001.
181. Vashistha, H., et al., *Aging phenotype(s) in kidneys of diabetic mice are p66ShcA dependent*. Am J Physiol Renal Physiol, 2018. **315**(6). p. 1833-1842.
182. Ranieri, S.C., Fusco, S., and Pani, G., *p66(ShcA): linking mammalian longevity with obesity-induced insulin resistance.* Vitam Horm, 2013. **91.** p. 219-241.
183. Sragovich, S., et al., *Molecular alterations associated with the NMDA preconditioning-induced neuroprotective mechanism against glutamate cytotoxicity*. J Mol Neurosci, 2012. **47**(3). p. 519-532.
184. Su, K., Bourdette, D., and Forte, M., *Genetic inactivation of mitochondria-targeted redox enzyme p66ShcA preserves neuronal viability and mitochondrial integrity in response to oxidative challenges.* Front Physiol, 2012. **3.** 285.
185. Salhan, D., et al., *HIV gene expression deactivates redox-sensitive stress response program in mouse tubular cells both in vitro and in vivo*. Am J Physiol Renal Physiol, 2012. **302**(1). p. 129-140.
186. Koch, O.R., et al., *Role of the life span determinant P66(shcA) in ethanol-induced liver damage.* Lab Invest, 2008. **88**(7). p. 750-760.
187. Orsini, F., et al., *The Life Span Determinant p66Shc Localizes to Mitochondria Where It Associates with Mitochondrial Heat Shock Protein 70 and Regulates Trans-membrane Potential.* J Biol Chem, 2004. **279**(24). p. 25689-25695.

188. Giorgio, M., et al., *Electron transfer between cytochrome c and p66Shc generates reactive oxygen species that trigger mitochondrial apoptosis*. Cell, 2005. **122**(2). p. 221-233.
189. Galimov, E.R., *The Role of p66shc in Oxidative Stress and Apoptosis*. Acta Naturae, 2010. **2**(4). p. 44-51.
190. Lewis, K., Kiepas, A., Hudson, J., et al., *p66ShcA functions as a contextual promoter of breast cancer metastasis.* Breast Cancer Res, 2020. **22.** 7.
191. Gertz, M., et al., *Identification of Peroxiredoxin 1 as a novel interaction partner for the lifespan regulator protein p66Shc*. Aging (Albany NY), 2009. **1**(2). p. 254-265.
192. Le, S., Connors, T.J., and Maroney, A.C., *C-Jun N-terminal kinase specifically phosphorylates p66ShcA at serine 36 in response to ultraviolet irradiation.* J Biol Chem, 2001. **276**(51). p. 48332-48336.
193. Pinton, P., et al., *Protein Kinase C β and Prolyl Isomerase 1 Regulate Mitochondrial Effects of the Life-Span Determinant p66Shc*. Science, 2007. **315**(5812). p. 659-663.
194. Hu, Y., et al., *ERK phosphorylates p66ShcA on ser36 and subsequently regulates p27kip1 expression via the Akt-FOXO3a pathway: implication of p27kip1 in cell response to oxidative stress.* Mol Biol Cell, 2005. **16**(8). p. 3705-3718.
195. Yannoni, Y.M., Gaestel, M., and Lin, L-L., *P66(ShcA) interacts with MAPKAP kinase 2 and regulates its activity*. FEBS Lett, 2004. **564**(1-2). p. 205-211.
196. Ow, Y-L.P., et al., *Cytochrome c: functions beyond respiration*. Nat Rev Mol Cell Biol, 2008. **9**(7). p. 532-542.
197. Li, X., Xu, Z., Du, W., et al., *Aiolos Promotes Anchorage Independence by Silencing p66^{Shc} Transcription in Cancer Cells.* Cancer Cell, 2014. **25**(5). p. 575-589.
198. Ma, Z., et al., *p66(Shc) restrains Ras hyperactivation and suppresses metastatic behaviour*. Oncogene, 2010. **29**(41). p. 5559-5567.
199. Li, X., Gao, D., et al., *Negative feedback loop between p66^{Shc} and ZEB1 regulates fibrotic EMT response in lung cancer cells*. Cell Death Dis, 2015. **6**(4). e1708.
200. Taddei, M.L., et al., *Anoikis: an emerging hallmark in health and diseases*. J Pathol, 2012. **226**(2). p. 380-393.
201. Ma, Z., et al., *p66Shc mediates anoikis through RhoA*. J Cell Biol, 2007. **179**(1). p. 23-31.

202. Zheng, Z., Yang, J., et al., *Downregulated adaptor protein p66^{Shc} mitigates autophagy process by low nutrient and enhances apoptotic resistance in human lung adenocarcinoma A549 cells.* FEBS J, 2013. **280**(18). p. 4522-4530.
203. Kasuno, K., et al., *Antagonism of p66Shc by melanoma inhibitory activity*. Cell Death Differ, 2007. **14**(8). p. 1414-1421.
204. Sakao, K., and Singh, S.V., *D,L-Sulforaphane-Induced Apoptosis in Human Breast Cancer Cells by the Adaptor Protein p66^{Shc}*. J Cell Biochem, 2012. **113**(2). p. 599-610.
205. Davol, P.A., et al., *Shc proteins are strong, independent prognostic markers for both node-negative and node-positive primary breast cancer*. Cancer Res, 2003. **63**(20). p. 6772-6783.
206. Su, K., Bourdette, D., and Forte, M., *Mitochondrial dysfunction and neurodegeneration in multiple sclerosis.* Front Physiol, 2013. **4**(169).
207. Bashir, M., et al., *P66shc and its downstream Eps8 and Rac1 proteins are upregulated in esophageal cancers.* Cell Commun Signal, 2010. **8.** 13.
208. Liu, G., et al., *The expression of p66Shc protein in benign, premalignant, and malignant gastrointestinal lesions*. Pathol Oncol Res, 2014. **20**(3). p. 733-739.
209. Muniyan, S., Chou, Y-W., et al., *p66Shc longevity protein regulates the proliferation of human ovarian cancer cells*. Mol Carcinog, 2015. **54**(8). p. 618-631.
210. Pelicci, G., et al., *The motogenic and mitogenic responses to HGF are amplified by the Shc adaptor protein.* Oncogene, 1995. **10**(8). p. 1631-1638.
211. Lee, M-S., et al., *p66Shc protein is upregulated by steroid hormones in hormone-sensitive cancer cells and in primary prostate carcinomas*. Int J Cancer, 2004. **108**(5). p. 672-678.
212. Hudson, J., et al., *p66ShcA Promote Breast Cancer Plasticity by Inducing an Epithelial-to-Mesenchymal Transition*. Mol Cell Biol, 2014. **34**(19). p. 3689-3701.
213. Jackson, J.G., et al., *Elevated levels of p66 Shc are found in breast cancer cell lines and primary tumors with high metastatic potential*. Clin Cancer Res, 2000. **6**(3). p. 1135-1139.
214. Haines, E., Saucier, C., and Claing, A., *The Adaptor Proteins p66Shc and Grb2 Regulate the Activation of the GTPases ARF1 and ARF6 in Invasive Breast Cancer Cells*. J Biol Chem, 2014. **289**(9). p. 5687-5703.

215. Bhat, H.F., et al., *Role of SNTA1 in Rac1 activation, modulation of ROS generation, and migratory potential of human breast cancer cells*. Br J Cancer, 2014. **110**(3). p. 706-714.
216. Sansone, P., et al., *p66Shc/Notch-3 interplay controls self-renewal and hypoxia survival in human stem/progenitor cells of the mammary gland expanded in vitro as mammospheres*. Stem Cells, 2007. **25**(3). p. 807-815.
217. Cepeda-Cañedo, E., et al., *p66ShcA potentiates the cytotoxic response of triple-negative breast cancers to PARP inhibitors*. JCI Insight, 2021. **6**(4). e.138382.
218. Invitrogen, *Molecular Probes: CM-H2DCFDA (General Oxidative Stress Indicator).* ThermoFisher Scientific.
219. Invitrogen, *Taking a close look at mitochondrial dysfunction: MITOSOX™ RED MITOCHONDRIAL SUPEROXIDE INDICATOR PROVES TO BE A VERSATILE PROBE ACROSS APPLICATIONS.* BioProbes, 2010. **62.** p. 26-28.
220. Smith, K.R., Klei, L.R., and Barchowsky, A., *Arsenite stimulates plasma membrane NADPH oxidase in vascular endothelial cells.* Am J Physiol Lung Cell Mol Physiol, 2001. **280.** p. 442-449.
221. Chou, W-C., et al., *Role of NADPH oxidase in arsenic-induced reactive oxygen species formation and cytotoxicity in myeloid leukemia cells*. Proc Natl Acad Sci USA, 2004. **101**(13). p. 4578-4583.
222. Qian, Y., et al., *Cdc42 regulates arsenic-induced NADPH oxidase activation and cell migration through actin filament reorganization*. J Biol Chem, 2005. **280**(5). p. 3875-3884.
223. Stolk, J., et al., *Characteristics of the inhibition of NADPH oxidase activation in neutrophils by apocynin, a methoxy-substituted catechol*. Am J Respir Cell Mol Biol, 1994. **11**(1). p. 95-102.
224. Ashburner, M., et al., *Gene ontology: tool for the unification of biology.* Nat Genet, 2000. **25**(1). p. 25-29.
225. The Gene Ontology Consortium, *The Gene Ontology resource: enriching a Gold mine.* Nucleic Acids Res, 2021. **49**(D1). D325-334.
226. Shen, K., et al., *Cryo-EM structure of the human FLCN-FNIP2-Rag-ragulator complex.* Cell, 2019. **179**(6). p.1319-1329.

227. Tsun, Z-Y., et al., *The Folliculin tumor suppressor is a GAP for RagC/D GTPases that signal amino acid levels to mTORC1.* Mol Cell, 2013. **52**(4).
228. Bar-Peled, L., and Sabatini, D.M., *Regulation of mTORC1 by amino acids.* Trends Cell Biol, 2014. **24**(7). p. 400-406.
229. Zheng, Z., Deng, W., Bai, Y., Miao, R., et al., *The Lysosomal Rag-Ragulator Complex Licenses RIPK1 and Caspase-8-mediated Pyroptosis by Yersinia.* Science, 2021. **372**(6549).
230. Najafov, A., et al., *RIPK1 Promotes Energy Sensing by the mTORC1 Pathway.* Mol Cell, 2021. **81**(2). p. 370-385.
231. Wu, H-C., et al., *Actinomycin D Targets NPM1c-Primed Mitochondria to Restore PML-Driven Senescence in AML Therapy*. Cancer Discov, 2021. **11**(12). p. 3198-3213.
232. Kirkland, R.A., and Franklin, J.L., Bax Affects Production of Reactive Oxygen by the Mitochondria of Non-apoptotic neurons. Exp Neurol, 2007. **204**(1). p. 458-461.
233. Liu, Y., and Schubert, D.R., *The specificity of neuroprotection by antioxidants*. J Biomed Sci, 2009. **16**(98).
234. Bridges, H.R., et al., *Effects of metformin and other biguanides on oxidative phosphorylation in mitochondria*. Biochem J, 2014. **462**(pt 3). p. 475-487
235. Miskimins, W.K., et al., *Synergistic Anti-Cancer Effect of Phenformin and Oxamate.* PLoS One, 2014. **9**(1). e85576.
236. Li, P.F., et al., *Differential effect of hydrogen peroxide and superoxide anion on apoptosis and proliferation of vascular smooth muscle cells.* Circulation, 1997. **96**(10). p. 3602-3609.
237. Zini, R., et al., *The differential effects of superoxide anion, hydrogen peroxide and hydroxyl radical on cardiac mitochondrial oxidative phosphorylation.* Free Radic Res, 2007. **41**(10). p. 1159-1166.
238. Li, L., Lai, E.Y., et al., *Differential effects of superoxide and hydrogen peroxide on myogenic signaling, membrane potential, and contraction of mouse renal afferent arterioles.* Am J Physiol, 2016. **310**(11). F1197-1205.
239. Deavall, D.G., et al., *Drug-Induced Oxidative Stress and Toxicity.* J Toxicol, 2012. **2012**(645460).

240. Kim, S-Y., Kim, S-J., et al., *Doxorubicin-induced reactive oxygen species generation and intracellular Ca^{2+}increase are reciprocally modulated in rat cardiomyocytes*. Exp Mol Med, 2006. **38**(5). p. 535-545.
241. Gilleron, M., et al., *NADPH oxidases participate to doxorubicin-induced cardiac myocyte apoptosis*. Biochem Biophys Res Commun, 2009. **388**(4). p. 727-731.
242. Hawley, S.A., et al., *Use of cells expressing gamma subunit variants to identify diverse mechanisms of AMPK activation*. Cell Metab, 2010. **11**(6). p. 554-565.
243. Khanday, F.A., et al., *Sos-mediated activation of rac1 by p66shc.* J Cell Biol, 2006. **172**(6). p. 817-822.
244. Hordijk, P.L., *Regulation of NADPH oxidases: the role of Rac proteins.* Circ Res, 2006. **98**(4). p. 453-462.
245. Khanday, F.A., et al., *Rac1 Leads to Phosphorylation-dependent Increase in Stability of the p66shc Adaptor Protein: Role in Rac1-induced Oxidative Stress.* Mol Cell Biol, 2006. **17**(1). p. 122-129.
246. Onnis, A., et al., *Regulation of Selective B Cell Autophagy by the Pro-oxidant Adaptor p66SHC*. Front Cell Dev Biol, 2020. **8**(193).
247. Onnis, A., et a., *The pro-oxidant adaptor p66SHC promotes B cell mitophagy by disrupting mitochondrial integrity and recruiting LC3-II.* Autophagy, 2018. **14**(12). p. 2117-2138.
248. Cai, Z., et al., *Detachment-Based Equilibrium of Anoikic Cell Death and Autophagic Cell Survival Through Adaptor Protein $p66^{Shc}$*. Anat Rec (Hoboken), 2016. **299**(3). p. 325-333.
249. Soliman, M.A., et al., *The Adaptor Protein p66Shc Inhibits mTOR-Dependent Anabolic Metabolism*. Sci Signal, 2014. **7**(313). ra17.
250. Kim, Y-M., et al., *SH3BP4 is a negative regulator of amino acid-Rag GTPase-mTORC1 signaling.* Mol Cell, 2012. **29**(6). p. 844-846.
251. Zhang, C-S., et al., *The lysosomal v-ATPase-Ragulator complex is a common activator for AMPK and mTORC1, acting as a switch between catabolism and anabolism.* Cell Metab, 2014. **20**(3). p. 526-540.

252. Baba, M., et al., *Folliculin encoded by the BHD gene interacts with a binding protein, FNIP1, and AMPK, and is involved in AMPK and mTOR signaling.* Proc Natl Acad Sci USA, 2006. **103**(42). p. 15552-15557.
253. Edelman, M.J., et al., *Phase I and pharmacokinetic evaluation of the anti-telomerase agent KML-011 with cisplatin in advanced solid tumours.* Cancer Chemother Pharmacol, 2016. **78**(5). p. 959-967.
254. You, D., et al., *KML001 Induces Apoptosis and Autophagic Cell Death in Prostate Cancer Cells via Oxidative Stress Pathway*. PLoS One, 2015. 1**0**(9). e0137589.
255. Alimoghaddam, K., *A Review of Arsenic Trioxide and Acute Promyelocytic Leukemia*. Int J Hematol Oncol Stem Cell Res, 2014. **8**(3). p. 44-54.
256. Srivastava, R.K., et al., ATF4 regulates arsenic trioxide-mediated NADPH oxidase, ER-mitochondrial crosstalk and apoptosis. Arch Biochem Biophys, 2016. **609.** p. 39-50.